creative commons
COMMONS DEED

저작자표시-비영리-변경금지 2.0 대한민국

이용자는 아래의 조건을 따르는 경우에 한하여 자유롭게

- 이 저작물을 복제, 배포, 전송, 전시, 공연 및 방송할 수 있습니다.

다음과 같은 조건을 따라야 합니다:

저작자표시. 귀하는 원저작자를 표시하여야 합니다.

비영리. 귀하는 이 저작물을 영리 목적으로 이용할 수 없습니다.

변경금지. 귀하는 이 저작물을 개작, 변형 또는 가공할 수 없습니다.

- 귀하는, 이 저작물의 재이용이나 배포의 경우, 이 저작물에 적용된 이용허락조건을 명확하게 나타내어야 합니다.
- 저작권자로부터 별도의 허가를 받으면 이러한 조건들은 적용되지 않습니다.

저작권법에 따른 이용자의 권리는 위의 내용에 의하여 영향을 받지 않습니다.

이것은 이용허락규약(Legal Code)을 이해하기 쉽게 요약한 것입니다.

Disclaimer

dCollection

공학박사 학위논문

Assessment of Internal Instability of Well-graded Soils through Seepage Tests

침투실험을 통한 입도분포가 좋은 풍화토의 내부불안정성 평가

2022년 8월

서울대학교 대학원

건설환경공학부

이 희 준

Assessment of Internal Instability of Well-graded Soils through Seepage Tests

지도 교수 정 충 기

이 논문을 공학박사 학위논문으로 제출함
2022 년 6월

서울대학교 대학원
건설환경공학부
이 희 준

이희준의 공학박사 학위논문을 인준함
2022 년 8 월

위 원 장 박 준 범 (인)

부위원장 정 충 기 (인)

위 원 김 성 렬 (인)

위 원 정 영 훈 (인)

위 원 김 태 식 (인)

Abstract

Assessment of Internal Instability of Well-graded Soils through Seepage Tests

Lee, Hee-Jun

Department of Civil & Environmental Engineering

The Graduate School

Seoul National University

Internal erosion is an important process that affects the stability of a fill dam. Suffusion and suffosion, also known as internal instability, are forms of internal erosion. Suffusion involves the selective erosion of fine particles from the matrix of coarse particles of an internally unstable soil through seepage flow, thereby removing the fine particles through the voids and leaving behind a soil skeleton formed by coarse particles. Suffosion is a similar process but results in volume changes. The erosion of fine particles increases the soil permeability, resulting in a decrease in shear strength and changes in hydraulic conditions. In turn, this scenario may cause various types of dam failures.

Generally, gap-graded soil with two distinct grain sizes is vulnerable to internal instability. Such soils show clear manifestations of suffusion, such as the erosion of a significant quantity of fine particles and an increase in permeability and void ratio. Therefore, previous studies on seepage erosion problems commonly focused on gap-graded soils as the target. However, no study has shown whether the well-graded soils, used as fill dam materials in South Korea, are susceptible to suffusion. Moreover, the process and cause of internal instability in well-graded soils have not been investigated.

In this dissertation, suffusion tests were performed on gap-graded and well-graded soils with different relative densities by using a newly developed suffusion test apparatus. In short-term tests, hydraulic gradient was increased stepwise, and the occurrence of internal instability were analyzed. In contrast to gap-graded soils, well-graded soils showed a continuous reduction in permeability before the initiation of internal instability. At the onset of internal instability, permeability and soil discharge suddenly increased. Additionally, when the relative density of well-graded soils increased, the hydraulic gradient required to reach an unstable state also increased.

Long-term tests were carried out to analyze the progress and cause of the internal instability of well-graded soils at constant hydraulic gradients. Results revealed that well-graded soils in internally stable conditions had clogging of fine particles in the bottom, which reduces the overall permeability. Similar clogging was identified in internally unstable conditions, and subsequent unclogging resulted in a rapid increase in permeability and erosion rate with the collapse of soil structure. Consequently, the internal instability of well-graded soils developed in the form of suffosion. On this basis, the mechanism of internal instability and its progress in well-graded soils were proposed.

Seepage tests with pore water pressure transducer were used to verify the above mechanism of internal instability in well-graded soils. The erosion of fine particles increased permeability and decrease the pressure, while the clogging of fine particles decreased permeability and increased pressure. Consequently, the test confirmed that the movement path of fine particles and verified the mechanism of internal instability in well-graded soils.

Results indicated that the characteristics and development of the internal instability of well-graded soils differed from those of gap-graded soils. The findings can be used to deepen the understanding of the development of internal instability in well-graded soils.

Keywords: Internal erosion, Internal instability, Suffusion, Suffosion, Clogging, Well-graded soils
Student Number: 2017-34915

Contents

Chapter 1. Introduction 1

1.1 Research Background 1

1.2 Objective and Scope of Research 7

1.3 Organization and Structure 9

Chapter 2. Literature review 11

2.1 Introduction 11

2.2 Conditions governing the internal instability 13

2.2.1 Geometric condition 13

2.2.2 Hydraulic condition 16

2.3 Previous studies on well-graded soil 22

Chapter 3. Research methods 26

3.1 Introduction 26

3.2 Testing materials 27

3.2.1 Particle size distributions and properties of specimens 27

3.2.2 Assessment of the internal instability 29

3.3 Experimental apparatuses 34

3.3.1 Apparatus for the short-term and long-term tests 34

3.3.2 Apparatus with pore pressure transducer 38

3.4 Experimental procedure and program 42

3.4.1 Short-term tests 42

3.4.2 Long-term tests 45

3.4.3 Tests with pore pressure transducer 46

Chapter 4. Short-term test results and analyses 48

4.1 Introduction 48

4.2 Short-term test results and analyses 49

4.2.1 Gap soil with a relative density of 78% 49

4.2.2 WG soil with a relative density of 50% 51

4.2.3 WG soil with a relative density of 65% 53

4.2.4 WG soil with a relative density of 80% 56

4.3 Assessment of internal instability 59

4.4 Summary 63

Chapter 5. Long-term test results and analyses 65

5.1 Introduction 65

5.2 Amount of eroded soil and erosion rate 68

5.3 Hydraulic conductivity 73

5.3.1 Gap soil 75

5.3.2 Internally stable WG soil 79

5.3.3 Internally unstable WG soil 84

5.4 Settlement 92

5.5 Mechanism of internal instability 98

5.6 Summary 103

Chapter 6. Test results with pore pressure transducer 106

6.1 Introduction 106

6.2 Hydraulic conductivity and pore water pressure 108

6.2.1 Internally unstable result 109

6.2.2 Internally stable result 114

6.3 Verification of mechanism of internal instability in WG soil 118

6.4 Summary 121

Chapter 7. Conclusions and Recommendations 122

7.1 Conclusions 122

7.2 Recommendations for further researches 130

List of References 131

List of Tables

Table 2-1 Criteria for suffusion 15

Table 2-2 Summary of previous studies on the hydraulic condition 21

Table 2-3 Summary of previous studies on well-graded soil 24

Table 3-1 Properties of specimens..... 28

Table 3-2 Criteria for suffusion and assessment results 31

Table 3-3 Experimental program for short-term tests 44

Table 3-4 Experimental program for long-term tests 46

Table 3-5 Experimental program for tests with pore pressure transducer..... 47

Table 4-1 Summary of the short-term test results 62

Table 5-1 Summary of the long-term test results 67

Table 5-2 Internal instability of test results 74

Table 5-3 Test results of WG soil (Dr= 50%) at a hydraulic gradient of 15 .. 82

List of Figures

Figure 1-1 Schematic diagram of internal instability 2

Figure 1-2 Schematic diagram of gap-graded soils 3

Figure 1-3 Particle size distribution of fill dam materials in South Korea and schematic diagram of well-graded soils 4

Figure 2-1 Schematic drawing of testing apparatus in USACE (1953) 12

Figure 2-2 The coefficient of permeability calculated by the seepage velocity and hydraulic gradients in the test results of Liu et al. (2021) 25

Figure 3-1 Particle size distributions of specimens and fill dam materials in South Korea 28

Figure 3-2 Internal stability of the Gap and WG soils based on Kenney & Lau (1986) 32

Figure 3-3 Internal stability of the Gap and WG soils based on Burenkova (1993) 32

Figure 3-4 Internal stability of the Gap and WG soils based on Wan & Fell (2008) 33

Figure 3-5 Schematic design of experimental apparatus 36

Figure 3-6 Experimental apparatus 37

Figure 3-7 Constriction size of loose and dense particles 38

Figure 3-8 Schematic design of experimental apparatus with pore pressure transducer 40

Figure 3-9 Experimental apparatus with pore pressure transducer 41

Figure 3-10 Experimental procedure..... 44

Figure 4-1 Accumulative eroded soil and k of Gap soil according to the hydraulic gradients 50

Figure 4-2 Particle size distribution of Gap soil..... 50

Figure 4-3 Accumulative eroded soil and k of WG soil (Dr = 50%) according to the hydraulic gradients 52

Figure 4-4 Particle size distribution of WG soil (Dr = 50%) 53

Figure 4-5 Accumulative eroded soil and k of WG soil (Dr = 65%) according to the hydraulic gradients 55

Figure 4-6 Particle size distribution of WG soil (Dr = 65%) 55

Figure 4-7 Accumulative eroded soil and k of WG soil (Dr = 80%) according to the hydraulic gradients 57

Figure 4-8 Particle size distribution of WG soil (Dr = 80%) 57

Figure 4-9 Settlement according to hydraulic gradients 58

Figure 4-10 The assessment results of internal instability according to the hydraulic gradient..... 61

Figure 5-1 Accumulative eroded soil of all test results over time..... 71

Figure 5-2 Particle size distributions of tested and eroded soil..... 71

Figure 5-3 SEM images: (a) Gap soil; and (b) WG soil..... 72

Figure 5-4 Erosion rate of all test results with hydraulic gradients..... 72

Figure 5-5 Accumulative eroded soil and k of Gap soil at a hydraulic gradient of 3 76
Figure 5-6 Particle size distribution of Gap soil at a hydraulic gradient of 3 77
Figure 5-7 Accumulative eroded soil and k of Gap soil at a hydraulic gradient of 5 78
Figure 5-8 Particle size distribution of Gap soil at a hydraulic gradient of 5 78
Figure 5-9 Accumulative eroded soil and normalized k of WG soil (Dr= 50%) at hydraulic gradients of 5 and 15 81
Figure 5-10 Particle size distribution of WG soil (Dr= 50%) at a hydraulic gradient of 15 82
Figure 5-11 Accumulative eroded soil and normalized k of WG soil (Dr= 65%) at a hydraulic gradient of 30 and WG soil (Dr= 80%) at a hydraulic gradient of 60 83
Figure 5-12 Particle size distribution of WG soil (Dr= 65%) at a hydraulic gradient of 30 84
Figure 5-13 Accumulative eroded soil and k of WG soil (Dr= 50%) at a hydraulic gradient of 17 86
Figure 5-14 Accumulative eroded soil and k of WG soil (Dr= 50%) at a hydraulic gradient of 25 86
Figure 5-15 Particle size distribution of WG soil (Dr= 50%) at a hydraulic gradient of 17 87

Figure 5-16 Accumulative eroded soil and k of WG soil (Dr= 65%) at a hydraulic gradient of 60 88
Figure 5-17 Particle size distribution of WG soil (Dr= 65%) at a hydraulic gradient of 60 89
Figure 5-18 Accumulative eroded soil and k of WG soil (Dr= 80%) at a hydraulic gradient of 120 90
Figure 5-19 Particle size distribution of WG soil (Dr= 80%) at a hydraulic gradient of 120 91
Figure 5-20 Accumulative eroded soil and settlement of test results 93
Figure 5-21 Accumulative eroded soil and settlement of WG soil (Dr= 50%) at a hydraulic gradient of 17 93
Figure 5-22 Accumulative eroded soil and settlement of WG soil (Dr= 65%) at a hydraulic gradient of 60 and WG soil (Dr= 80%) at a hydraulic gradient of 120 94
Figure 5-23 k and e of WG soil (Dr= 50%) at a hydraulic gradient of 17 96
Figure 5-24 k and e of WG soil (Dr= 65%) at a hydraulic gradient of 60 96
Figure 5-25 k and e of WG soil (Dr= 80%) at a hydraulic gradient of 120 ... 97
Figure 5-26 Schematic diagram of the progression of internal instability in Gap soil 100
Figure 5-27 Schematic diagram of the progression of internal instability in WG soil 101

Figure 5-28 Schematic of internal instability behavior in WG soil..... 102

Figure 6-1 Schematic design of specimen and pore pressure transducer..... 109

Figure 6-2 Overall *k* and differential pore water pressure in each part.....111

Figure 6-3 The distributions of total head (hT), elevation head (he), and pressure head (hp).....111

Figure 6-4 The distribution of pressure head 112

Figure 6-5 Overall *k* and *k* at each part 112

Figure 6-6 Normalized *k* and settlement 113

Figure 6-7 Particle size distribution of internally unstable result.....114

Figure 6-8 Overall *k* and differential pore water pressure in each part.....115

Figure 6-9 Overall *k* and *k* at each part 116

Figure 6-10 Normalized *k* and settlement 116

Figure 6-11 Particle size distribution of internally stable result.....117

Figure 6-12 Schematic diagram of the progression of internal instability in WG soil..... 120

Chapter 1. Introduction

1.1 Research Background

Hydraulic earth structures, such as levees and dams, can undergo various kinds of damage. Among these, internal erosion, overtopping, and slope instability are the major possible failure modes. Foster et al. (2000) reported that 57 of the 126 cases of dam failure abroad were caused by internal erosion, accounting for 45% of the total number of failures. The other major failure modes (overtopping and slope instability) account for approximately 44% and 4%, respectively. Hence, internal erosion can be regarded as one of the main causes of damage in hydraulic earth structures.

The survey carried out by the National Disaster Management Research Institute (NDMR, 2013) in South Korea shows that 17,611 of the 17,702 hydraulic earth structures are earth-fill dams. Most of the fill dams are made up of well-graded silty sand decomposed from granite and gneiss, and those with well-graded soils suffer from internal erosion.

Suffusion and suffosion, also known as internal instability, are two forms of internal erosion (Figure 1-1). Suffusion involves the selective erosion of fine particles from the matrix of coarse ones of an internally unstable soil. Seepage flow removes the fine particles that pass through the voids, leaving behind a soil skeleton formed by the coarse particles. Suffosion is a similar process but results in volume change (Fell et al., 2015; Reclamation and USACE, 2019).

Once the fine particles are removed, the permeability of the soil increases, which can induce a reduction of shear strength and changes in hydraulic condition (Chang and Zhang, 2013a). Furthermore, suffusion can cause various types of dam breaches, such as the following: increase in seepage, leading to the initiation of backward erosion piping; formation of voids in the foundation, leading to the settlement of the crest and overtopping; and increase in pore pressure and loss of strength in the embankment or foundation, leading to a downstream slide (Chang and Zhang, 2013a; ICOLD, 2017).

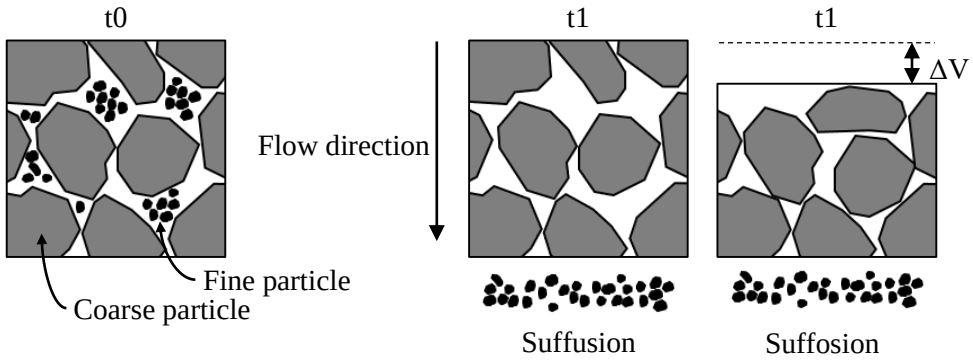

Figure 1-1 Schematic diagram of internal instability

Gap-graded soils are a binary mixture of two distinct particle sizes, missing mid-sized particles (Figure 1-2). For gap-graded soils, the size of voids in coarse particles that is sufficiently larger than the fine particles can be called ‘underfilled’, where fine material is insufficient to fill the voids between coarse particles. In this situation, given that the fine particles can easily move between the coarse particles, which form a soil structure that supports external loads,

then suffusion can easily occur wherein only the fine particles selectively move without changing the overall volume. At very high fine contents, the coarse particles simply become inclusions within a matrix of fine particles, which comprise the majority of the material; this structure is commonly referred to as 'overfilled' (Vaughan, 1994; Taylor, 2016). In this situation, when the fine particles move by seepage force, internal instability occurs in the form of suffosion with a change in volume.

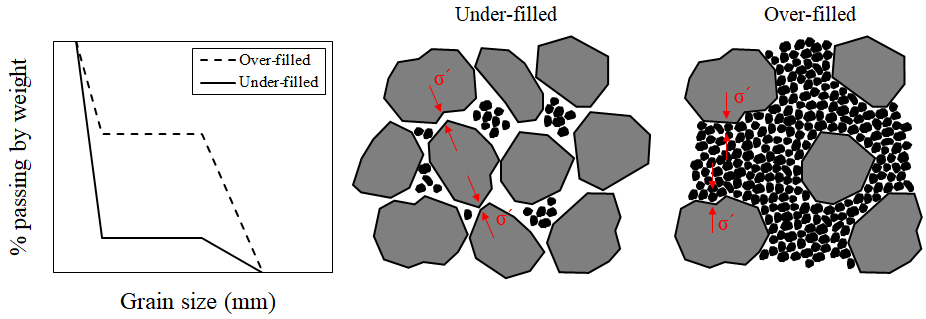

Figure 1-2 Schematic diagram of gap-graded soils

However, in South Korea, most of the dams are made up of well-graded soils, which exhibit successive particle size distribution. Whereas well-graded soils generally have linear particle size distribution with the uniformity coefficient (C_u) values lager than 4, the well-graded soils which are the fill dam materials in South Korea have a wide range of particle size with C_u values lager than 20 (Figure 1-3). Therefore, the fine particles are unlikely to be loose and may transfer effective stress. Nevertheless, as only a limited research examines well-graded soils (Sterpi, 2003; Moffat et al., 2011; Li, 2008; Israr and Indraratna,

2019, Liu et al., 2021), whether internal instability occurs and its types remain unclear.

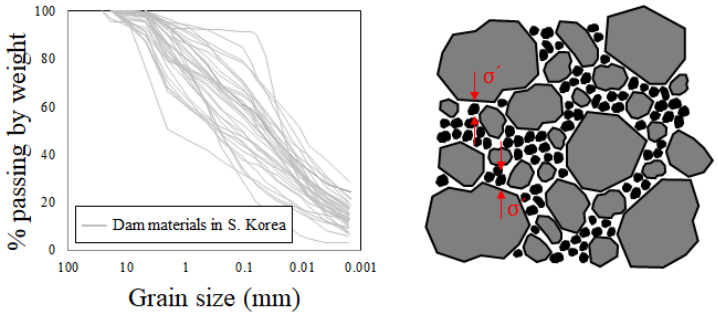

Figure 1-3 Particle size distribution of fill dam materials in South Korea and schematic diagram of well-graded soils

Generally, suffusion can occur when three distinct criteria are satisfied, as follows: 1) fine particles must be under low effective stress and thus free to move ("mechanical criterion"); 2) fine particles must fit within the constrictions between coarse particles ("geometric criterion"); and 3) seepage force must be sufficient to move the fine particles through the voids ("hydraulic criterion") (Kenney and Lau, 1985; Taylor, 2016).

The vulnerability of soils to suffusion has been extensively evaluated. Given that the particle size distribution of soils plays a key role in terms of the first two criteria, many suffusion tests have used various particle size distributions, and on the basis of results, have suggested criteria for particle size distribution for internally unstable soils (Istomina, 1957; Kezdi, 1979; Kenney and Lau, 1985; Burenkova, 1993; Wan and Fell, 2008). In terms of hydraulic criteria, a

critical hydraulic gradient that triggers suffusion has been suggested based on seepage test results (Skempton and Brogan, 1994; Reddi et al., 2000b; Moffat and Fannin, 2006). Post-phenomenon of internal instability and effects of various factors, such as hydraulic gradient and confining stress, has also been examined (Bendahmane et al., 2008; Li, 2008; Moffat et al., 2011; Chang and Zhang, 2013b; Luo et al., 2013; Ke and Takahashi, 2014; Liu et al., 2021).

Previous studies on seepage erosion problems mainly use gap-graded soils as the target, which is relatively easy to evaluate whether the geometrical and mechanical criteria are met according to the particle size distribution. Moreover, such soils show clear manifestations of suffusion, such as a significant quantity of fine particles discharged and an increase in permeability and void ratio. Thus, evaluation of the internal stability can be readily carried out based on the direct seepage test results. Kim (2019), however, showed that the internal stability of fill dam materials in South Korea was evaluated using the geometrical criteria suggested by Kenney and Lau (1985) and Wan and Fell (2008), resulting in poor predictions. Accordingly, improvements of the existing criteria have been proposed (Chang and Zhang, 2013b; Israr and Zhang, 2021).

The causes and progress of internal instability in gap-graded soils have been well explored (Skempton and Brogan, 1994; Moffat and Fannin, 2006; Bendahmane et al., 2008; Chang and Zhang, 2013b; Luo et al., 2013; Ke and Takahashi, 2014). Luo et al. (2013) carried out a short-term suffusion test with stepwise increasing of hydraulic gradient and a long-term test at a constant hydraulic gradient using gap-graded sandy gravel, then compared the characteristics of internal instability progress. However, although internal

instability develops slowly (Fell et al, 2003) and 8,611 reservoirs in South Korea are aged over 60 years (constructed before 1951), accounting for approximately 60% (NDMR, 2013), well-graded soils have not been examined for long-term stability.

Additionally, previous studies of well-graded soils focus on post-occurrence of internal instability rather than its process and cause analysis (Sterpi, 2003; Moffat et al., 2011; Li, 2008; Israr and Indraratna, 2019, Liu et al., 2021). In the test results performed by Li (2008) and Liu et al. (2021), a sudden increase in permeability and amount of eroded soil were observed only after a progressive reduction in permeability, exhibiting a different internal instability process from that of gap-graded soils. In addition, in gap-graded soils, relative density does not significantly affect internal instability (Wan, 2006), but well-graded soils showed higher resistance to internal instability when compacted to a greater relative density (Israr and Indraratna, 2019; Liu et al., 2021). Therefore, the characteristics and development of internal instability of well-graded soils are expected to differ from those of gap-graded soils, but its causes have not been clearly determined.

1.2 Objective and Scope of Research

This study aims to assess the internal instability of fill dam materials in South Korea and to investigate the mechanism and progress of internal instability in well-graded soils, which have a particle size distribution that represents fill dam materials in South Korea. Short- and long-term experiments are carried out to evaluate the internal instability of the well-graded soil at various relative densities and hydraulic gradients. Subsequently, the progress and causes of internal instability are analyzed by comparison with gap-graded soils.

The uncertainty in applying the geometrical criteria and limited studies on well-graded soils necessitate a direct suffusion test for better evaluation and prediction. Therefore, short-term suffusion tests are carried out on both gap-graded and well-graded soil with various hydraulic gradients and relative densities. The ‘‘short-term’’ suffusion tests are the experiments with stepwise increasing of hydraulic gradient until failure, and each step lasts 1 hour. For the experiment, a new suffusion test apparatus is designed and can measure the amount of eroded soil and water without disassembly during the test. This apparatus enables the application of a multistage hydraulic gradient in one test. Based on the test results, a comparative analysis was carried out on the internal erosions of well-graded soils and gap-graded soils.

Previous short-term tests are carried out to easily evaluate the characteristics of internal instability while increasing the hydraulic gradient stepwise. This method has the advantage of observing internal instability in a relatively short time and roughly specifying the hydraulic gradient at the onset of internal

instability. Through the short-term test, however, it is difficult to evaluate the progress of internal instability because the hydraulic gradients are increased in a stepwise manner for a short period and the effect of the hydraulic gradient applied during the previous stage may alter the internal erosion resistance of the soil. Furthermore, as 60% of reservoirs in South Korea are aged over 60 years, and internal instability of well-graded soils is expected to develop slowly, and its long-term stability needs to be evaluated. Therefore, long-term suffusion tests are conducted on the same specimen as that of the short-term test to assess the internal instability and analyze its progress and causes. The “Long-term” is a relative concept for the “short-term” tests, hydraulic gradient remains constant until internal instability occurs, at least 39 hours. The long-term tests are often used to study the evolution mechanism of suffusion (Luo et al., 2013). The amount of eroded soil, flow rate, and settlement are measured over time for the test conditions of various relative densities and hydraulic gradients. Based on the test results, the influence and cause of hydraulic gradient and relative density on the internal instability of well-graded soils, cause of the decrease and increase of permeability, and the cause of settlement are analyzed. The mechanism of the progress of internal instability in well-graded soils are also investigated.

The mechanism of the progress of internal instability in well-graded soils is examined with a series of seepage tests with pore pressure transducer. The specimen is divided into four parts, then pore pressure transducers are installed to measure the overall permeability and the pore pressure of each part. These measures are used to calculate and analyze the movement path of fine particles.

1.3 Organization and Structure

This dissertation comprises five chapters that are briefly introduced as follows:

Chapter 1 introduces the research background, objective, scope of work, and structure.

Chapter 2 describes the literature review on soil internal instability, which is explained by geometric conditions and hydraulic conditions. Subsequently, the internal instability of well-graded soils and its characteristics can be inferred. The weaknesses and limitations of previous research can also be analyzed.

Chapter 3 describes the testing materials, experimental apparatus, and test methods used in this study, including the experimental procedure and program. The specimens in the tests include gap-graded soils for comparative purposes and well-graded soils with a particle size distribution that represents the fill dam materials in South Korea. Previous test devices for internal instability are also explained, and new experimental apparatus and test methods developed to combine their advantages are introduced.

Chapter 4 presents and discusses the short-term test results with stepwise increases of hydraulic gradient. The internal instability of soils is assessed based on the two identification methods (fraction loss of soils and change in permeability). The occurrence and characteristics of internal instability of well-graded soils are comparatively analyzed with those of gap-graded soils. The manuscript in Chapter 4 is published in the KSCE Journal of Civil Engineering.

Chapter 5 presents and discusses the long-term test results. The

characteristics and cause of internal instability of the well-graded soils is analyzed. The mechanism of the progress of internal instability in well-graded soil is also investigated. The manuscript in Chapter 5 was submitted to the Acta Geotechnica, and is under review at the time of submission for this dissertation.

In Chapter 6, the tests with pore pressure transducer are presented. The movement path of fine particles is analyzed by using the pore pressure and permeability of each part. The mechanism of the progress of internal instability in well-graded soil is verified.

Finally, in Chapter 7, the main conclusion of the present study and recommendations for further research are presented.

Chapter 2. Literature review

2.1 Introduction

US Army Corps of Engineers (USACE) has firstly used the term ‘inherent stability’ and ‘internal stability’ in order to address the problem of internal erosion in the filter system of the dams. In their recent research, internal instability (suffusion and suffosion) is defined as follows. Suffusion involves selective erosion of finer particles from the matrix of coarser particles of an internally unstable soil, in such a manner that the finer particles are removed through the voids between the larger particles by seepage flow, leaving behind a soil skeleton formed by the coarser particles. Suffosion is a similar process but results in volume change (Reclamation and USACE, 2019).

The occurrence of internal instability in hydraulic earth structures is difficult to predict, because it readily develops into other failure mechanism types. Therefore, the vulnerability of soils to internal instability is often assessed based on the laboratory seepage tests. The U.S Army Corps of Engineers (1953) conducted constant head permeameter tests on four sand-gravel mixtures to evaluate inherent stability and permeability characteristics (Figure 2-1). The tests were performed with vibration, and water was flowed down while increasing the hydraulic gradient from 5 to 16. Inherent stability was determined by comparing particle size distribution before and after testing. Based on this test, several researchers developed and modified the test method

to evaluate the internal instability.

In evaluating the internal stability through the seepage tests, there are two important conditions governing the internal instability: the geometric and hydraulic conditions. In this chapter, previous studies on the internal instability of soils are presented. In terms of the geometric conditions, the criteria for internal instability suggested based on the grain size distribution is described. And, the previous researches focused on the hydraulic gradient, which triggers suffusion are introduced. Furthermore, the previous studies of well-graded soil are presented, and the weaknesses of previous investigations are analyzed.

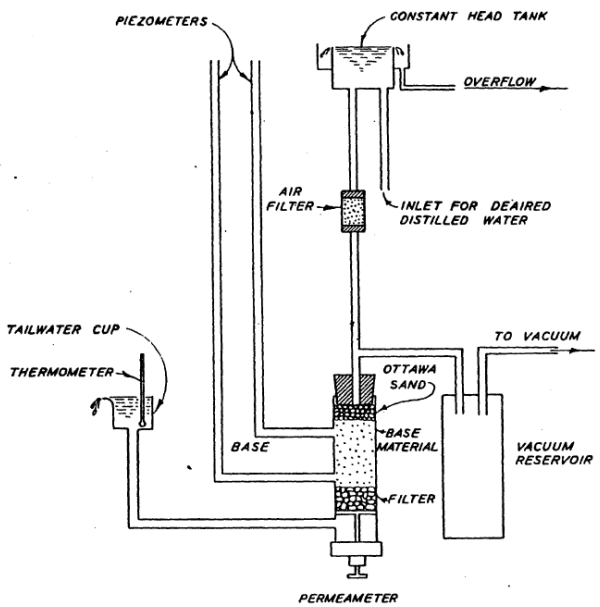

Figure 2-1 Schematic drawing of testing apparatus in USACE (1953)

2.2 Conditions governing the internal instability

2.2.1 Geometric condition

According to the previous studies on the geometric conditions, criteria for internal instability have been suggested based on the grain size distribution (Table 2-1), because the large constriction size formed by the coarse particles allows fine particles to be washed away (Istomina 1957; Kezdi 1979; Kenney and Lau 1985; Burenkova 1993; Wan and Fell 2008).

Istomina (1957) evaluated internal stability using the coefficient of uniformity (C_u). When C_u is less than 10, the soil is internally stable, and when C_u is 20 or more, the soil is internally unstable. Also, the soil is considered transitional when C_u is between 10 and 20.

Kezdi (1979) reported that suffusion occurs when coarse particles are unable to act as a filter which retains the fine particles. In Terzaghi's classic filter criterion, when D15/d85 are less than 4 to 5, the filter (coarser material) will be able to retain the finer (base) material (Terzaghi et al., 1996), where D15 represents the finer fraction of the filter materials and d85 represents the larger fraction of the base materials. The values of 4 to 5 were determined empirically from filter tests by Terzaghi (1922). Accordingly, the particle size curve is divided into its fine and coarse parts, and when both components satisfy the filter criterion, the soils are considered internally stable.

Kenney and Lau (1985) suggested that the constriction size of the filter material is approximately equal to one-quarter of the size of the small particles

making up the filter. This indicates that particles smaller than particle size D can pass through the constrictions formed by the particles of size 4×D and larger, thus being internally unstable.

In the method of Burenkova (1993), conditional factors of uniformity, d90/d60 and d90/d15, were used in analyzing the grain size distribution of the soils. Here, d90, d60 and d15 denotes particle diameter at 90, 60 and 15% passing by weight. The d90/d60 ratio represents the slope of the coarse side of the grain size distribution curve and d90/d15 ratio represents the filter action between the coarse and the finer fraction of the soils.

Wan and Fell (2008) extended the Burenkova's criterion using logistic regression and suggested that the boundary of internal instability can be represented by d90/d60 versus d20/d5, based on the fact that soils with a steep slope on the coarse fraction and flat slope on the finer fraction were likely to be internally unstable.

In a study by Kim (2019), however, the internal stability of fill dam materials in South Korea was evaluated using the geometrical criterion suggested by Kenney and Lau (1985) and Wan and Fell (2008), resulting in poor predictions. And, several attempts have been made to improve the existing criteria (Chang and Zhang, 2013b; Israr and Zhang, 2021).

Table 2-1 Criteria for suffusion

References	Criteria
Istomina (1957)	$C_u \leq 10$: internally stable $10 \leq C_u \leq 20$: transitional $C_u \geq 20$: internally unstable
Kezdi (1969)	$(d_{15c}/d_{85f})_{max} \leq 4$: internally stable d_{15c} : diameter of the 15% mass passing in the coarse part d_{85f} : diameter of the 85% mass passing in the fine part
Kenny and Lau (1985)	$(H/F)_{min} \geq 1.0$: internally stable F : mass fraction at a grain size D H : mass fraction between grain size D and 4D
Burenkova (1993)	$0.76 \log\left(\frac{d_{50}}{d_{15}}\right) + 1 < \frac{d_{90}}{d_{60}} < 1.68\left(\frac{d_{90}}{d_{15}}\right) + 1$: internally stable
Wan and Fell (2008)	$30/\log(d_{90}/d_{60}) < 80$ or $30/\log(d_{90}/d_{60}) > 80$ and $15/\log(d_{20}/d_5) > 22$: internally stable

2.2.2 Hydraulic condition

In terms of the hydraulic condition, the previous researches focused on the hydraulic gradient, which triggers suffusion (Skempton and Brogan, 1994; Reddi et al., 2000b; Sterpi, 2003; Moffat and Fannin, 2006; Bendahmane et al., 2008; Li, 2008; Moffat et al., 2011; Chang and Zhang, 2013b; Luo et al., 2013; Ke and Takahashi, 2014; Liu et al., 2021).

The study of hydraulic gradient affecting internal instability was started in earnest by Skempton and Brogan (1994). Skempton and Brogan (1994) performed upward flow permeameter tests to confirm the potential for internal instability by increasing hydraulic gradient. In the stable materials, internal instability occurred at approximately the critical gradient given by Terzaghi's piping theory (Terzaghi, 1939). But in the unstable materials, migration and strong piping of fines took place at hydraulic gradients of about one fifth to one third of the theoretical value. The lower critical hydraulic gradient was associated with the lower effective stress on the fine particles. According to the test results, Skempton and Brogan (1994) proposed the relationship between the Kenney and Lau (1985) criterion and the hydraulic gradient at which piping occurred.

Reddi et al. (2000b) assess the difference between surface and internal erosion processes on a sand-kaolinite mixture. Internal erosion experiments were performed while increasing the flow rate and measuring pressure and the amount of eroded kaolinite using a turbidimeter. Based on the test results, the applicability of the assessment method in surface erosion test to internal erosion

was evaluated. And, it was noted that internal erosion process may be governed by pore clogging and redeposition of eroded particles.

Sterpi (2003) conducted the seepage tests under various constant hydraulic gradient to investigate the erosion of fine particles from well-graded sand gravel. The erosion and transport of fine particles was modeled considering the tests results. Then, a finite-element analysis estimated the effects of the erosion of fines on the stress–strain distribution within the soil. The settlements due to the water pumping from a drainage trench was evaluated adopting the proposed model.

Moffat and Fannin (2006) introduced a large rigid-walled permeameter to examine hydromechanical conditions at the onset of internal instability. The permeameter had two rows of pressure transducers to establish the change of hydraulic gradient along the specimen. Three tests on specimens of glass beads used to commission the device were reported. The onset of internal instability could be detected by measuring water pressure along the length of the specimen.

Bendahmane et al. (2008) carried out suffusion tests to examine the influence of the hydraulic gradient, clay contents within the soils, and confining pressure on the internal erosion mechanism. The flexible wall permeameter using a modified triaxial cell was developed to control over stresses that act on the soil specimen and to minimize side wall leakage. The erosion rate of clay increased according to the increase of hydraulic gradient and decrease of confining pressure and clay content. When the hydraulic gradient was low, the clay was eroded due to suffusion, and when the hydraulic gradient increased, sand fraction was eroded due to backward erosion.

Li (2008) experimentally investigated internal instability of widely graded cohesionless soils. The hydraulic gradient of the specimen was increased until the onset of internal instability was observed, or the specimen exhibited a heave failure. Particle size distribution of a soil, effective stress and hydraulic gradient governed onset of internal instability. Commonly used criteria for internal instability were reviewed and a new geometric criterion based on capillary tube model was proposed.

Moffat et al. (2011) conducted permeameter tests on four widely graded cohesionless soil to study internal instability. The tests were conducted while increasing hydraulic gradient, and the change in water pressure was measured through a pressure transducer installed along the length of the test specimen. Suffusion and suffosion were detected from visual observations together with changes in local hydraulic gradient, axial displacement.

Chang and Zhang (2013a) carried out internal erosion tests, using a modified triaxial testing apparatus, to investigate the initiation and development of internal erosion and the effect of stress state on critical hydraulic gradients. Based on the test results, the internal erosion stage was divided into four stages according to the erosion of fine particles, the change in the permeability, and the deformation of specimen. Corresponding to the stages of internal erosion, critical hydraulic gradients were defined. Then, the effect of various stress conditions on the defined hydraulic gradient was evaluated.

Luo et al. (2013) performed a short-term suffusion test with stepwise increasing of hydraulic gradient and a long-term test at a constant hydraulic gradient, using gap-graded sandy gravel, and compared the characteristics of

internal instability progress in the short-term and long-term tests. The short-term suffusion tests under various confining pressures were conducted to determine the hydraulic gradient at which the fine particles start to migrate. The long-term suffusion tests were carried out to investigate the influences of the hydraulic gradient and the confining pressures on the evolution of suffusion. Consequently, it was concluded that the suffusion failure in the long-term test is more likely to happen and much more serious than that in the short-term experiment. And, the long-term test was able to reduce the hydraulic gradient initiated the suffusion failure significantly and increase the eroded mass dramatically.

Ke and Takahashi (2014) conducted a series of seepage tests measuring the pore water pressure under the constant flow rate and the isotropic confining pressure. The characteristics of suffusion and its mechanical consequences on gap-graded cohesionless soil with various fines contents and stress was investigated. In the test results, the permeability increased with the progress of suffusion. And, when large amounts of fines were eroded, contractive volumetric strain occurred and the strength of soil decreased.

Liu et al. (2021) carried out suffusion tests on well-graded gravels used in high speed railway roadbed to investigate the effect of degree of compaction and initial fines content on the critical hydraulic gradient and the characteristics of suffusion. The suffusion of well-graded gravels progressed with three different erosion stages according to the change of permeability, the erosion of fine particles. The critical hydraulic gradient increased with the degree of compaction and the initial fines content. Based on the test results, an empirical

equation is proposed to predict the eroded mass of fine particles.

Several researches have studied on the hydraulic gradient at which initiates the internal instability and the influence factors (Table 2-2). Test methods can be divided into two methods to evaluate internal instability while increasing a hydraulic gradient or flow rate, and while maintaining various hydraulic gradient. From the previous test results, when fine particles are eroded due to internal instability, generally, void ratio increases, resulting in increase of permeability and decrease of strength of soil, and settlement occurs infrequently. Additionally, internal instability occurred at a lower hydraulic gradient in the long-term suffusion test than in the short-term test. However, in previous studies, gap-graded soil, which shows clear manifestations of suffusion, was mostly utilized as a target soil because it is relatively easy to evaluate factors affecting internal instability.

Table 2-2 Summary of previous studies on the hydraulic condition

References	Specimen	Hydraulic condition	Elapsed time	Influence factors	Results
Skempton and Brogan (1994)	gap-graded sand gravel	stepwise increment of i (0 ~ 1)	not mentioned	hydraulic gradient (i)	mass of eroded soil (w) coefficient of permeability (k)
Reddi et al. (2000b)	gap-graded sand-kaolinite	increment of flow rate	~ 0.5 h	flow rate	w, i
Sterpi (2003)	well-graded silt-sand (% passing by #200 ≒ 23%)	constant i (0.18 ~ 0.75)	50 h	i, time	w
Moffat and Fannin (2006)	gap-graded sand	stepwise increment of i (0 ~ 15)	1 h	i	pore pressure
Bendahmane et al. (2008)	gap-graded clay sand	constant i (5 ~ 140)	~ 0.5 h	i, σ_3, clay content	w
Li (2008)	gap-graded sand well-graded silt-sand	stepwise increment of i (0 ~ 15)	5 h	i	w, k, pore pressure
Moffat et al. (2011)	well-graded silt sand gravel (% passing by #200 ≒ 30%)	stepwise increment of i (1 ~ 29)	193 h	i	pore pressure
Chang and Zhang (2013a)	gap-graded sand	stepwise increment of i (0 ~ 9)	7 h	i, σ_3, stress path	w, k, strain
Luo et al. (2013)	gap-graded sand gravel	stepwise increment of i and constant i (0 ~ 5)	14 ~ 188 h	i, σ_3, time	w, k
Ke and Takahashi (2014)	gap-graded sand	increment of flow rate	3 h	flow rate, σ_3, fine content	i, w, k, strain
Liu et al. (2021)	well-graded silt sand gravel (% passing by #200 ≒ 10%)	stepwise increment of i and constant i (0 ~ 9)	2~4 h	i, time, compaction	w, k

2.3 Previous studies on well-graded soil

Studies on well-graded soil with a particle size distribution similar to that of a fill dam material in South Korea have been conducted by a few of researchers (Table 2-3). However, rather than a study on the process and cause analysis of internal instability, the post-occurrence phenomenon was mainly studied (Sterpi, 2003; Moffat et al., 2011; Li, 2008; Israr and Indraratna, 2019; Liu et al., 2021). Sterpi (2003) studied focusing on the erosion of fine particles from well-graded sand gravel and modeled the weight of eroded fine particles considering hydraulic gradient and time. Then, the proposed model was applied to evaluate the settlements owing to the water pumping from a drainage trench. Li (2008) experimentally investigated internal instability of widely graded soil and applied the test results to establish a new geometric criterion. Moffat et al. (2011) conducted permeameter tests on widely graded soil to study internal instability and investigated the change in water pressure when internal instability occurred. Israr and Indraratna (2019) carried out hydraulic tests to examine the potential of internal erosion of gap-graded and broadly graded soils compacted at various relative densities. Based on the test results, the critical hydraulic gradient was modeled considering the effects of inter-particle and boundary frictions, and stress reduction in the soil. Liu et al. (2021) carried out suffusion tests on well-graded gravels to investigate the effect of degree of compaction and initial fines content on the critical hydraulic gradient and proposed an empirical equation to predict the eroded mass of fine particles.

In the test results of Li (2008) and Liu et al. (2021), when the coefficient of

permeability was calculated with the seepage velocity and hydraulic gradients, well-graded soil showed a sudden increase in permeability and amount of eroded soil after a progressive reduction in coefficient of permeability, exhibiting an internal instability process different from that of the gap-graded soils (Figure 2-2). And, well-graded soils showed higher resistance to internal instability when compacted to a greater relative density (Israr and Indraratna, 2019; Liu et al., 2021). Therefore, the characteristics of internal instability and the development process of well-graded soil is expected to be different from those of the gap-graded soil, but there is no clear cause analysis for this.

Table 2-3 Summary of previous studies on well-graded soil

References	Specimen	Hydraulic condition	Results
Sterpi (2003)	well-graded silt-sand (% passing by #200 ≒ 23%)	constant i 0.18 ~ 0.75	empirical equation to predict loss of fines $i \uparrow \rightarrow w \uparrow$
Li (2008)	well-graded silt-sand (% passing by #200 ≒ 20%)	stepwise increment of i 0 ~ 15	characterization of failure mode $i \uparrow \rightarrow k \downarrow$, suffosion
Moffat et al. (2011)	well-graded silt sand gravel (% passing by #200 ≒ 30%)	stepwise increment of i 1 ~ 29	observation of internal instability At i = 29, internal instability was observed
Israr and Indraratna (2019)	broadly graded silt sand gravel (% passing by #200 ≒ 25%)	stepwise increment of i 0 ~ 1.3	the development of model for estimating the critical hydraulic gradients relative densities ↑ → critical $i \downarrow$
Liu et al. (2021)	well-graded silt sand gravel (% passing by #200 ≒ 10%)	stepwise increment of i and constant i (0 ~ 9)	empirical equation to predict loss of fines $i \uparrow \rightarrow$ w ↑; compaction ↑ → critical $i \uparrow$, $w \downarrow$ $i \uparrow \rightarrow k \downarrow$ (marginally unstable) → $k \uparrow$ (fully unstable)

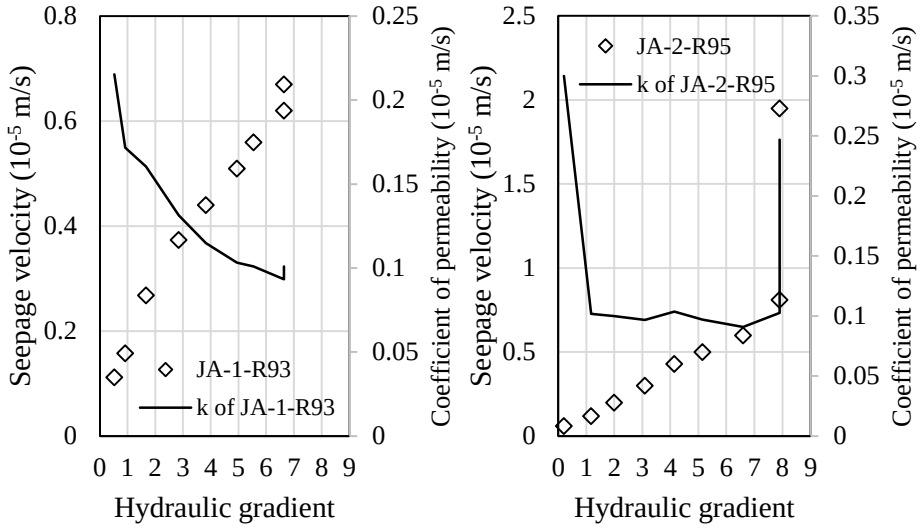

Figure 2-2 The coefficient of permeability calculated by the seepage velocity and hydraulic gradients in the test results of Liu et al. (2021)

Chapter 3. Research methods

3.1 Introduction

This chapter described material, apparatus, and test program used in the laboratory test in this study. Gap-graded soils for comparative purposes and well-graded soils which has a particle size distribution that is representative of the fill dam materials in South Korea were used as specimens. Short-term and long-term experiments were conducted to evaluate the internal instability of well-graded soil, and the progress and causes of internal instability were analyzed comparing with gap-graded soil. For the experiment, a newly designed suffusion test apparatus was developed and registered at the Korean Patent Office (Chung et al., 2018), which can measure the amount of eroded soil and water without disassembling it during the test. The amount of eroded soil, flow rate, and settlement were measured for the test conditions of various relative densities and hydraulic gradient. Based on the test results, the occurrence and cause of internal instability of the well-graded soils were comparatively analyzed with those of the gap-graded soils. And, the mechanism of the progress of internal instability in well-graded soil was investigated. Then, a series of seepage tests with pore pressure transducer was conducted to verify the mechanism of the progress of internal instability in well-graded soil.

3.2 Testing materials

3.2.1 Particle size distributions and properties of specimens

The specimens used in the suffusion tests included artificially constituted gap-graded soil (Gap soil) and well-graded soil (WG soil), a material commonly available in South Korea. Gap soil consists of fine soil (< 0.15 mm) and coarse soil (2–4.75 mm), collected from WG soil by mechanical sieving, comprising 15% and 85%, respectively. WG soil is a natural silty sand decomposed from granite and has a particle size distribution that represents fill dam materials in South Korea. Figure 3-1 shows that particle size distribution of WG soil is included in the range of that obtained from 6 different domestic fill dams (24 particle size distributions from 6 fill dams in operation, investigated by Korea Rural Community Corporation). WG soil is classified as clayey silty sand (SC-SM) in Unified Soil Classification System (USCS), 40% of which is finer than sieve No. 200, after eliminating a diameter larger than that of sieve No. 4. The properties of the soil samples are listed in Table 3-1.

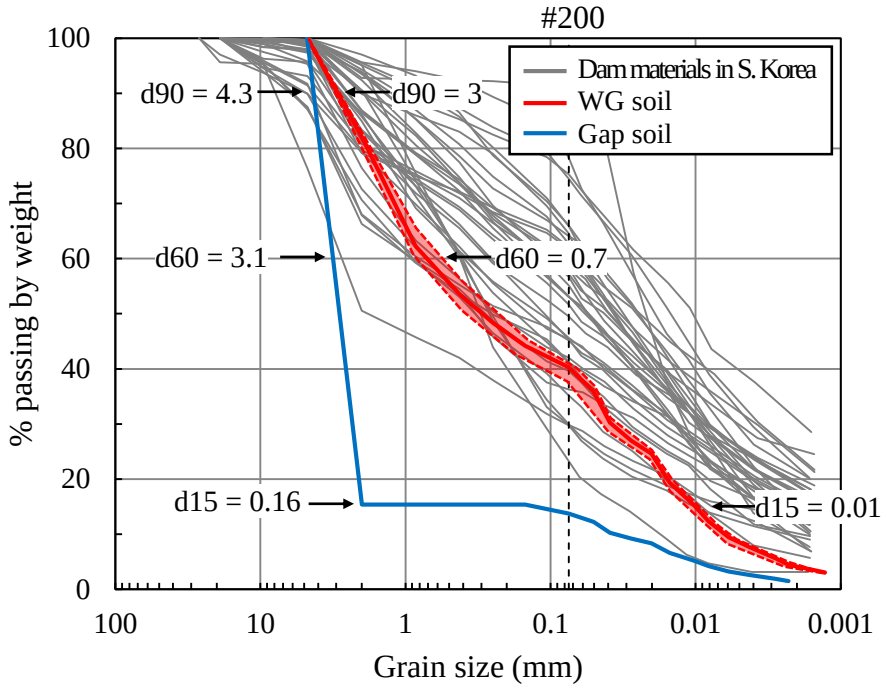

Figure 3-1 Particle size distributions of specimens and fill dam materials in South Korea

Table 3-1 Properties of specimens

Material	Gap soil	WG soil
USCS	SM	SC-SM
Average % passing through sieve no. 200	13.7	40.3
Specific gravity (G_s)	2.65	2.59
Max. dry unit weight (g/cm3)	1.76	1.86
Min. dry unit weight (g/cm3)	1.47	1.25
Uniformity coefficient (C_u)	28	112

Liquid limit (%)	27.5
Plastic limit (%)	21.6
Plasticity index (%)	5.9

3.2.2 Assessment of the internal instability

Prior to the experimental tests, widely used criteria for evaluating the internal instability of soils (Istomina, 1957; Kezdi, 1969; Kenney and Lau, 1985; Burenkova, 1993; Wan and Fell, 2008) were applied to the soils used in this study (Table 3-2). Istomina (1957) evaluated internal stability using C_u. Kezdi (1979) divided the particle size distribution into its fine and coarse parts, and checking Terzaghi's filter criterion is satisfied. However, this method could not be applied to WG soil without a distinct boundary between coarse and fine fractions. Kenney and Lau (1985) proposed an index ratio, H/F, based on the suffusion test results, where F is the mass fraction at particle size D, and H is the mass fraction between particle sizes D and 4D. A limit value of H/F = 1 was suggested at F < 0.2 in widely graded soils and F < 0.3 in narrowly graded soils. Burenkova (1993) used conditional factors of uniformity, d90/d60 and d90/d15, to analyze the particle size distribution of the soils. Wan and Fell (2008) suggested that the boundary of internal instability can be represented by d90/d60 versus d20/d5, using logistic regression, based on the fact that soils with a steep slope on the coarse fraction and flat slope on the finer fraction were

likely to be internally unstable. The d90, d60, d20 and d5 are particle diameter at 90%, 60%, 20% and 5% mass passing, respectively. The assessment results for WG soils were inconsistent with the suggested criteria. The assessment results based on the methods proposed by Istomina (1957) and Kenney and Lau (1985) evaluated both the Gap and WG soils as internally unstable (Figure 3-2). Meanwhile, the methods proposed by Burenkova (1993) and Wan and Fell (2008) assessed the Gap soils as internally unstable and the WG soils as internally stable (Figure 3-3 and Figure 3-4).

Table 3-2 Criteria for suffusion and assessment results

References	Criteria	Results of assessment	
		Gap soils	WG soils
Istomina (1957)	$C_u \leq 10$: internally stable $10 \leq C_u \leq 20$: transitional $C_u \geq 20$: internally unstable	Unstable	Unstable
Kezdi (1969)	$(d_{15c}/d_{85f})_{max} \leq 4$: internally stable d_{15c} : diameter of the 15% mass passing in the coarse part d_{85f} : diameter of the 85% mass passing in the fine part	Unstable	-
Kenny and Lau (1985)	$(H/F)_{min} \geq 1.0$: internally stable F : mass fraction at a grain size D H : mass fraction between grain size D and 4D	Unstable	Unstable
Burenkova (1993)	$0.76 \log\left(\frac{d_{50}}{d_{15}}\right) + 1 < \frac{d_{90}}{d_{60}} < 1.68\left(\frac{d_{90}}{d_{15}}\right) + 1$: internally stable	Unstable	Stable
Wan and Fell (2008)	$30/\log(d_{90}/d_{60}) < 80$ or $30/\log(d_{90}/d_{60}) > 80$ and $15/\log(d_{20}/d_5) > 22$: internally stable	Unstable	Stable

* d90, d60, d20 and d5 = particle diameter at 90%, 60%, 20% and 5% passing, respectively.

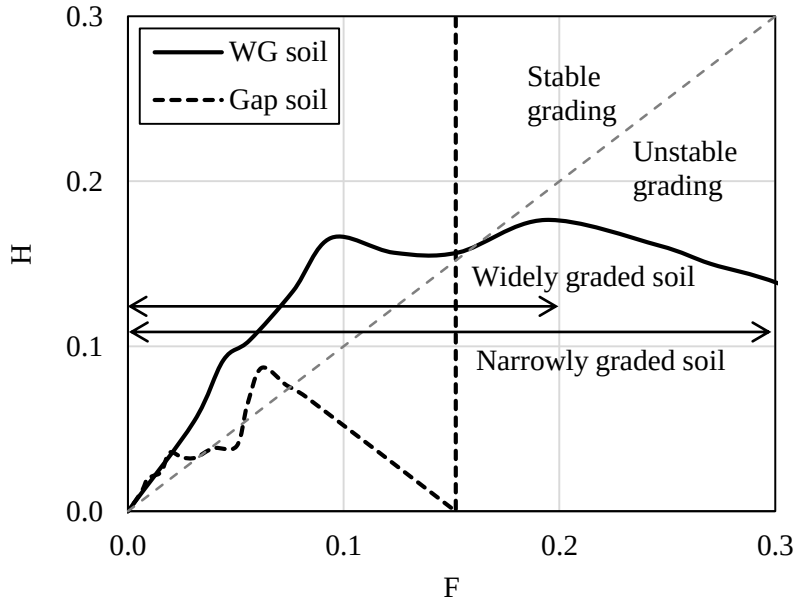

Figure 3-2 Internal stability of the Gap and WG soils based on Kenney & Lau (1986)

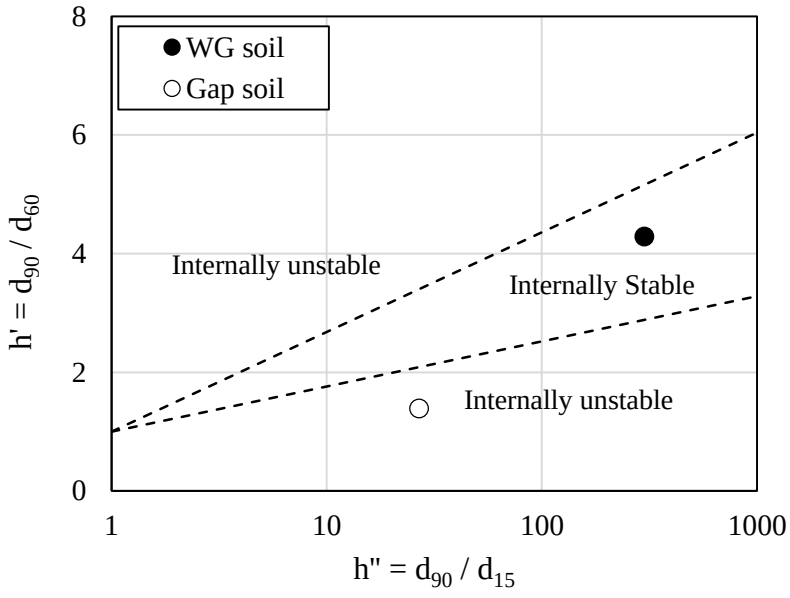

Figure 3-3 Internal stability of the Gap and WG soils based on Burenkova (1993)

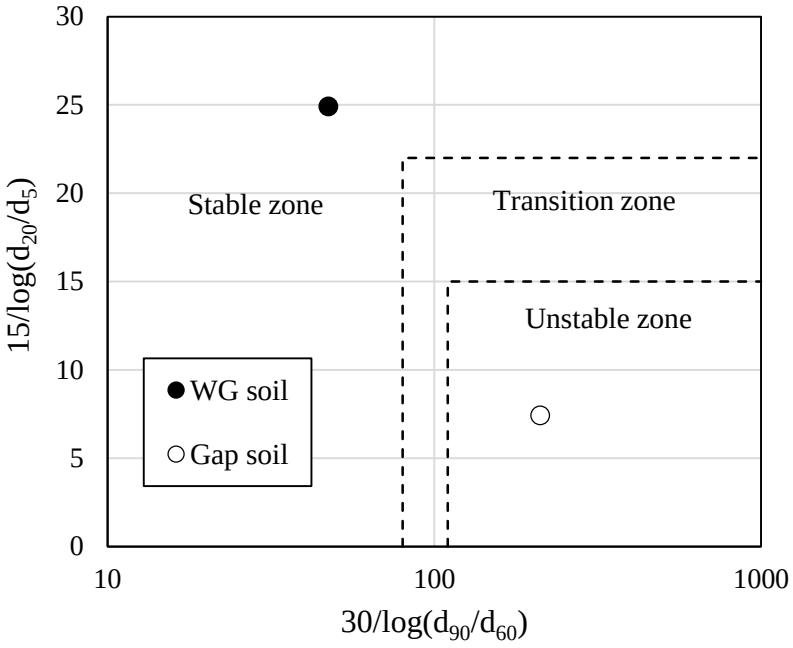

Figure 3-4 Internal stability of the Gap and WG soils based on Wan & Fell (2008)

3.3 Experimental apparatuses

3.3.1 Apparatus for the short-term and long-term tests

Generally, suffusion tests are performed based on the experimental program adopted in the study of the U.S. Army Corps of Engineers (USACE, 1953). The apparatus used in the USACE study was later developed and modified by several researchers (Kenney and Lau, 1985; Wan and Fell, 2008; Bendahmane et al., 2008; Chang and Zhang, 2013b). Kenney and Lau (1985) conducted a downward suffusion test with a perforated plate installed at the lower part of the seepage cell. The plate served as the outflow; therefore, the amount of soil discharged can be easily estimated by simply collecting the outflowing water-soil mixtures from underneath the seepage cell. However, because the plate was exposed to the atmosphere, air was likely to be entrapped in the specimen during the removal of soil particles, resulting in unsaturation of the specimen and inconsistent soil and hydraulic conditions. Wan and Fell (2008) assessed the internal instability of soils with an actual filter layer composed of gravel. The bottom part of the specimen was submerged in water, allowing the saturation of the specimen and a constant outflow water head. However, such an experimental setup makes it difficult to measure the amount of soil discharged during the test. In contrast, Chang and Zhang (2013a) developed a stress-controlled erosion apparatus composed of a triaxial system, a pressurized water supply system, a soil collection system, and a water collection system. The apparatus, which was developed to investigate internal erosion subjected

to complex stress states, is complex and inconvenient.

In this study, a simplified experimental apparatus was developed to combine the advantages of the experimental setup mentioned above. It consists of an inflow water tank, an inner cell, an outer cell, and a replaceable collector (Figure 3-5 and Figure 3-6). The inflow water tank provides a constant water level at the inlet and can be raised to control the hydraulic gradient. The outer cell can maintain the degree of saturation of the specimen and the constant water level of the outflow during the test or while replacing the collector to measure the amount of soil discharged. In the inner cell, submerged inside the outer cell, a cylindrical specimen (10 cm in diameter and 10 cm in height) was installed over a perforated plate. The plate has 80 holes with a size corresponding to the filter criteria (particle diameter at 15% mass passing in of filter material should be smaller than four times of that at 85% mass passing in base material) suggested by USACE (1953). Because D85 of WG soil is 2.5 mm, D15 of filter material should be less than 10 mm. As shown in Figure 3-7, the constriction sizes of 10 mm particles are 1.55 and 4.14 mm in dense and loose, respectively (Kezdi, 1979; Locke, 2001). Therefore, the perforated plate has 80 holes with a size of 4 mm. When the water flows through the specimen toward the outlet tube, eroded soil can quickly settle in the replaceable collector by means of a funnel connector. During the experiment, the amount of water was measured directly from the outlet tube, and the amount of eroded soil was obtained by drying the soil collected in the replaceable collector.

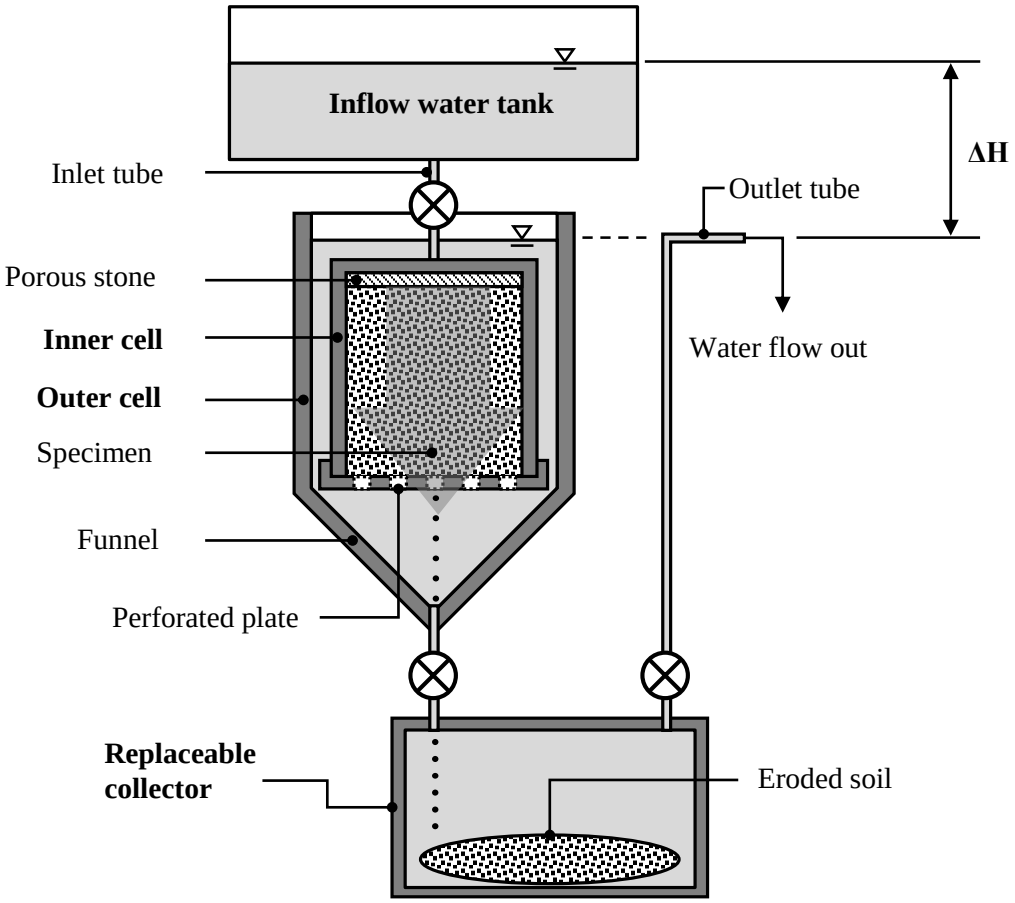

Figure 3-5 Schematic design of experimental apparatus

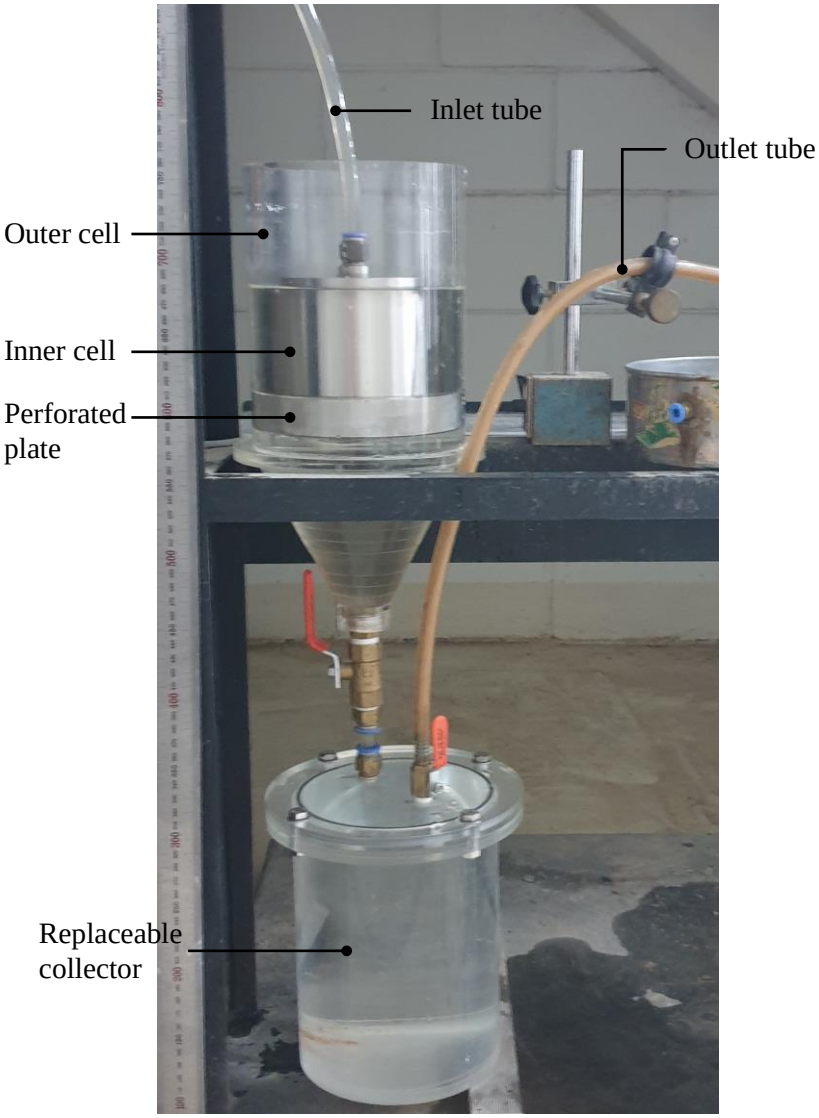

Figure 3-6 Experimental apparatus

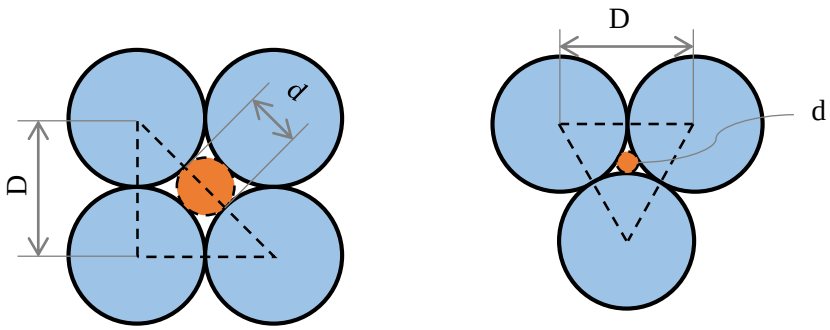

Loose

$d = D\sqrt{2} - D \cong 0.414D$

Dense

$d = \frac{2D\sqrt{3} - 3D}{3} \cong 0.155D$

Figure 3-7 Constriction size of loose and dense particles

3.3.2 Apparatus with pore pressure transducer

Moffat and Fannin (2006) and Moffat et al. (2011) conducted the seepage tests while increasing hydraulic gradient, and the change in water pressure was measured installed along the length of the test specimen. The onset of internal instability was able to be detected by measuring water pressure along the length of the specimen. According to the previous studies, a suffusion test apparatus with pore pressure transducer was developed to verify the mechanism of the progress of internal instability in well-graded soil.

The device consists of an inflow water tank, an acrylic cylinder cell, and a collector (Figure 3-8 and Figure 3-9). The inflow water tank and the collector are the same as the previous test device, and are connected to the acrylic cylinder cell. The acrylic cylinder has a 100 mm internal diameter and 300 mm

height containing the soil sample to be tested. A perforated plate with holes corresponding to the filter criteria was fixed to the lower part of the cylinder cell, and a soil sample was placed on it. The soil sample was divided into four parts and three pore pressure transducers were installed to measure the pore pressures in each part. The pore pressure was recorded with a static data logger. During the experiment, the amount of water was measured directly from the outlet tube, and the coefficient of permeability at each part was calculated using the pore pressure and overall permeability. After the tests, the eroded soil remains in the lower part of the cylinder cell and in the collector.

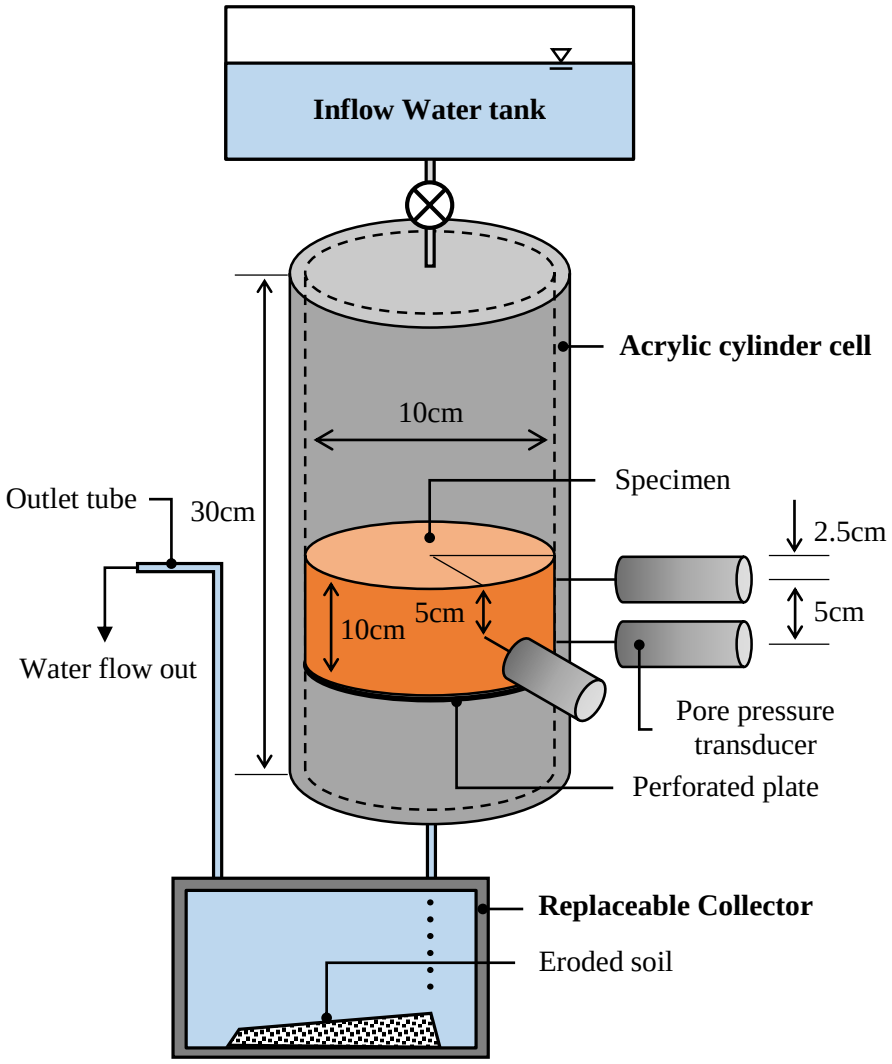

Figure 3-8 Schematic design of experimental apparatus with pore pressure transducer

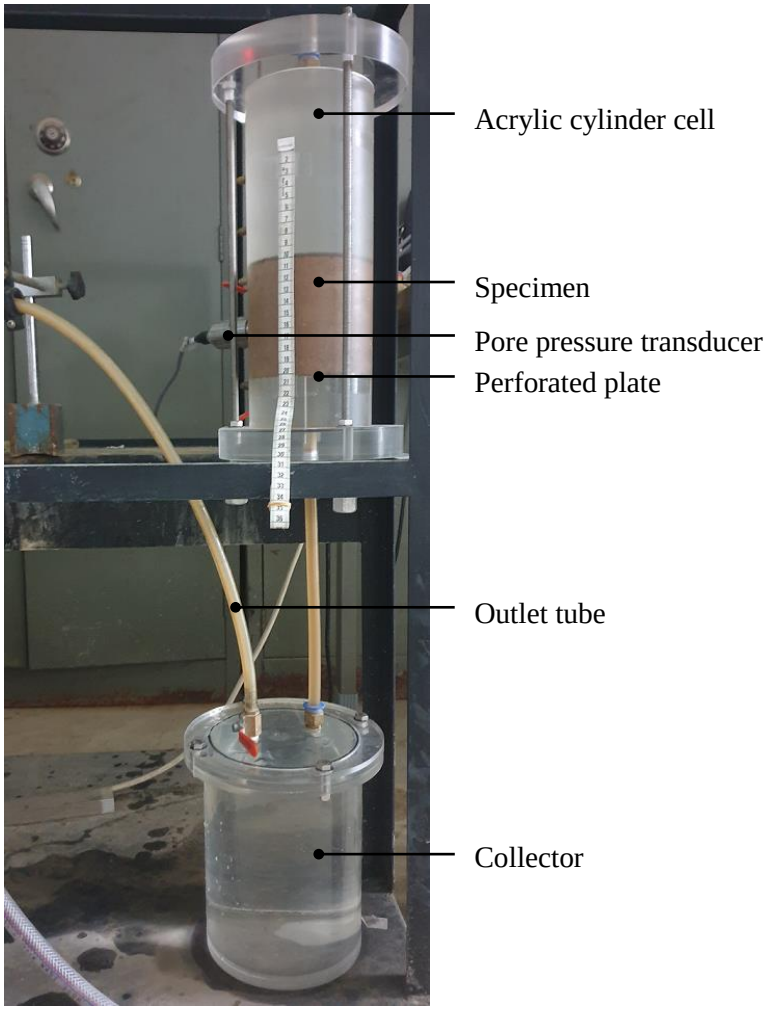

Figure 3-9 Experimental apparatus with pore pressure transducer

3.4 Experimental procedure and program

3.4.1 Short-term tests

For the preparation of the soil sample, the inner cell was flipped upside down to prevent segregation and any loss of soil particles during compaction (Figure 3-10(a)). Initially, the porous stone was placed underneath the sample to protect the soils from scouring and to distribute the influent water evenly across the specimen. Then, the soil sample was compacted to a predetermined relative density (D_r) (Figure 3-10(b)). The WG soils were compacted to reach 50%, 65%, and 80% relative density. The Gap soils were tested for comparative purposes, and because they are relatively vulnerable to suffusion, the experiment was only performed with a sample with a relative density of 78%. After preparing the specimen, the perforated plate was fitted into the inner cell (Figure 3-10(c)) and the cell was rotated back to its position so that the porous stone and the perforated plate could be located on top of and underneath the specimen, respectively. To saturate the specimen, the inner cell was plunged in the outer cell for 24 hours (Figure 3-10(d)). After placing the water tank in accordance with the target hydraulic gradient, the water tank was connected to the inner cell, allowing the water to flow down through the specimen toward the outlet tube (Figure 3-10(e)).

The hydraulic head acting on the specimen is the height difference (ΔH) between the height of the water tank and the outlet tube. The range of the hydraulic gradient was determined based on preliminary test results for each

soil type and relative density. Because well-graded soils show higher resistance to suffusion, the initial hydraulic gradient applied was higher than that of gap-graded soils. Additionally, a greater hydraulic gradient was necessary for soils with a higher relative density. Thus, the tests on WG soils were conducted under hydraulic gradients from 2 to 40, 10 to 80, and 2 to 150 for 50%, 65%, and 80% relative density, respectively. The test on gap-graded soils was conducted under a hydraulic gradient from 0.5 to 12. Although the hydraulic gradient usually experienced in dams and their foundations is less than 5 (Fell et al., 2015), higher hydraulic gradients were applied to observe internal instability in this study.

The amount of water flowing out through the outlet tube was measured at regular intervals to estimate the coefficient of permeability. The weight of the eroded soil was measured by collecting the soils accumulated in the replaceable collector at each step of the hydraulic gradient. At each hydraulic gradient, the test was conducted for 1 hour according to previous studies (Skempton and Brogan, 1994; Moffat and Fannin, 2006; Moffat et al., 2011; Luo et al., 2013), and the amount of eroded soil and the coefficient of permeability were measured for each step (Table 3-3). The particle size distributions of eroded soil and post-test specimens were analyzed.

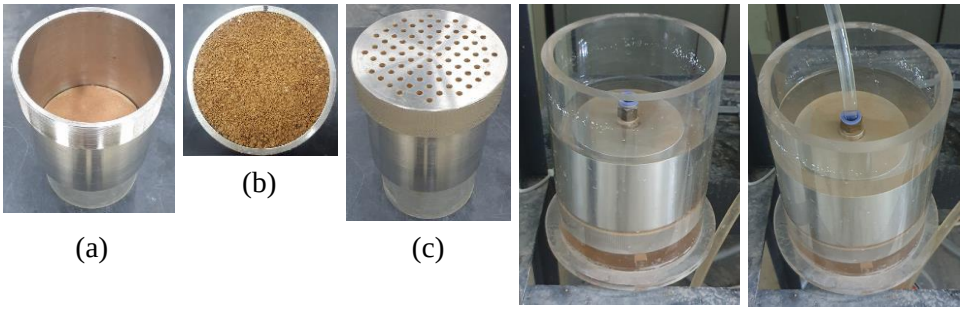

(a) (b) (c) (d) (e)

Figure 3-10 Experimental procedure

Table 3-3 Experimental program for short-term tests

Test No.	Specimen	D_r(%)	Hydraulic gradient
G78	Gap soils	78	0.5, 1, 2, 3, 4, 5, 6, 7, 8, 9, 10, 12
WG50	WG soils	50	2, 5, 10, 15, 20, 25, 30, 35, 40
WG65		65	10, 20, 30, 40, 50, 60, 70, 80
WG80		80	2, 5, 10, 15, 20, 25, 30, 35, 40, 50, 60, … , 150

* The hydraulic gradient was increased stepwise. Each step was maintained for 1 hour.

3.4.2 Long-term tests

The long-term suffusion tests were conducted on the same specimen as that of short-term test to assess the internal instability and analyze the progress and causes of that. The experimental procedure of long-term test was the same as that of short-term tests. The soil samples were compacted to reach predefined relative densities of 78% for Gap soil and 50, 65, and 80% for WG soils. After sample preparation, water was introduced across the specimen by adjusting the height of the water tank according to the desired hydraulic gradient and by connecting the water tank to the inner cell. The hydraulic gradient was established based on the short-term test results to confirm both the internally unstable state and stable state of the soils. Hydraulic gradients of 3 and 5 were applied to Gap soil. For the WG soil prepared at 50% relative density, hydraulic gradients of 5, 15, and 17 were applied, followed by 30 and 60 for 65%, and 60 and 120 for 80% relative density, respectively. The amount of eroded soil, flow rate, and settlement were measured (up to 576 h) under a constant hydraulic gradient (Table 3-4). The weights of the eroded soil and settlement were measured at regular intervals (1, 2, 4, 8, 12, 24, and 48 h). To calculate the coefficient of permeability, the amount of water discharged from the outlet tube was measured at regular intervals three to four times between each measurement on eroded soil. After the tests, a particle size analysis was conducted on the eroded soil and post-test specimens.

Table 3-4 Experimental program for long-term tests

Test No.	Specimen	D_r(%)	Hydraulic gradient
G78	Gap soils	78	3, 5
WG50	WG soil	50	5, 15, 17, 25
WG65		65	30, 60
WG80		80	60, 120

3.4.3 Tests with pore pressure transducer

To verify the mechanism of the progress of internal instability in well-graded soil, the seepage tests with pore pressure transducer were carried out. The acrylic cylinder cell was inverted upside down upon preparation of the sample to prevent segregation and to go through the same preparation process as in the previous tests. A perforated plate was initially placed beneath the sample to protect the soil from scouring and distribute the water evenly over the specimen. The soil sample with a diameter and height of 100 mm was then compacted to reach predefined relative densities of 50%. After sample preparation, the lower part of the acrylic cylinder cell where the perforated plate is fixed was assembled to the cell and the cell was rotated back to its original position. Then, the collector was connected to the cell and, and water was injected into the collector to saturate the soil for 24 h. Water was introduced across the specimen

by adjusting the height of the water tank according to the desired hydraulic gradient and by connecting the water tank to the cylinder cell. The hydraulic gradient of 20 was applied based on the long-term test results. The tests were performed for 30 and 60 minutes to obtain internally stable result and internally unstable result, respectively (Table 3-5). During the tests, the pore pressure was recorded automatically, and the flow rate and settlement were measured under a constant hydraulic gradient. After the tests, weight of eroded soil was measured, and a particle size analysis was conducted on the eroded soil and post-test specimens.

Table 3-5 Experimental program for tests with pore pressure transducer

Test No.	Specimen	D_r(%)	Hydraulic gradient	Testing time (m)
WG50-20PT-a	WG soil	50	20	60
WG50-20PT-b				30

Chapter 4. Short-term test results and analyses

4.1 Introduction

Owing to the uncertainty in applying the geometrical criteria and limited studies on well-graded soils, the short-term suffusion tests were performed on both gap-graded and well-graded soil with various hydraulic gradients and relative densities to assess the internal instability. The test on gap-graded soils was conducted under a hydraulic gradient from 0.5 to 12 for relative density of 78%. The tests on WG soils were carried out under hydraulic gradients from 2 to 40, 10 to 80, and 2 to 150 for 50%, 65%, and 80% relative density, respectively. The hydraulic gradient was increased stepwise. The test was conducted for 1 hour at each hydraulic gradient, and the amount of eroded soil and the coefficient of permeability were measured for each step. The particle size distributions of eroded soil and post-test specimens were analyzed.

In this chapter, the results of short-term suffusion tests and assessment of internal instability were presented. In section 2 of this chapter, the amount of eroded soil, coefficient of permeability and particle size distribution were demonstrated. In section 3, the internal stability of the soils was evaluated based on the seepage test results of this study and indicators of previous studies. And, the occurrence and characteristic of internal instability of the well-graded soils were comparatively analyzed with those of the gap-graded soils.

4.2 Short-term test results and analyses

4.2.1 Gap soil with a relative density of 78%

In the case of the Gap soils (D_r = 78%), the amount of soil discharged and coefficient of permeability (k) increased progressively even in the early stage of the tests at low levels of hydraulic gradient (Figure 4-1). Consequently, the accumulative eroded soil reached 4.1% of the total weight of the specimen at a hydraulic gradient of 12. The "accumulative eroded soil" refers to the percentage of the total eroded soil mass based on the total weight of the specimen. At the completion of the test, k increased almost three times the initial coefficient of permeability (k_0). Based on the post-test particle size distribution analysis, 97% of the eroded soil was fine soil (< 0.15 mm), resulting in a shift in the particle size distribution curve (Figure 4-2). And, the percentage of fines, particles smaller than 0.075 mm denoted herein as FS, was 53.7% (8.3% in the original specimen). During the test, 0.4 mm of settlement was developed (Figure 4-9); nevertheless, the void ratio (e) increased from 0.57 to 0.62, signifying the selective erosion of fines. The results of Gap soils showed clear manifestations of suffusion, such as a significant quantity of fine particles discharged and increases in k and e. Gap soils are a binary mixture of coarse and fine particles with large differences in size. As a result, it was expected that fine particles would be easily moved by the lower seepage force, which was confirmed by the test results.

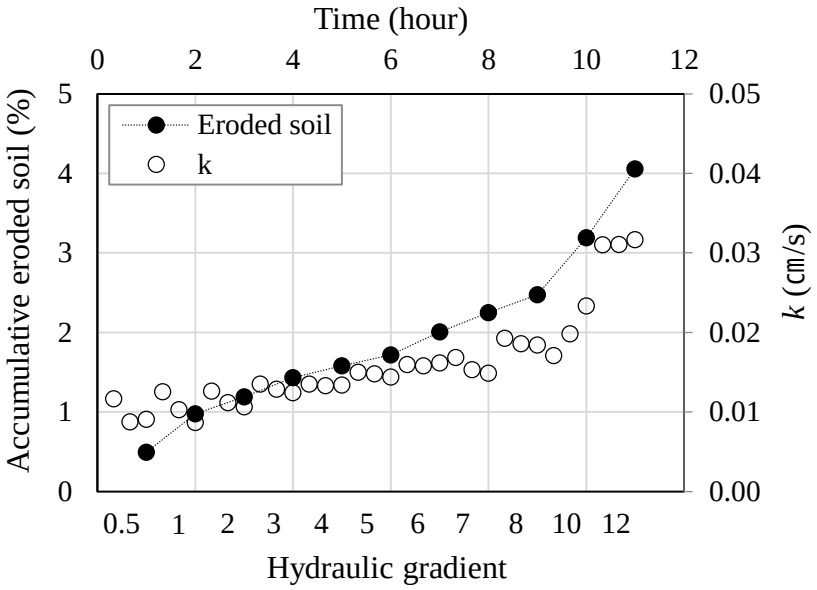

Figure 4-1 Accumulative eroded soil and *k* of Gap soil according to the hydraulic gradients

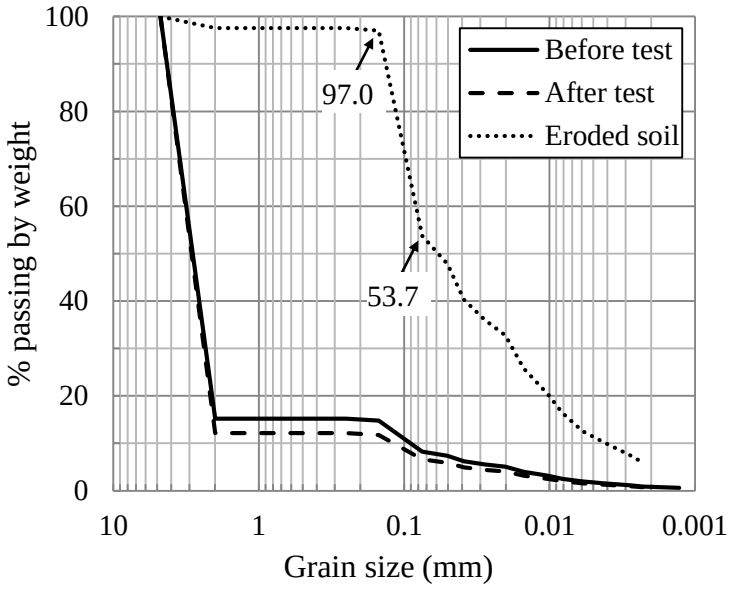

Figure 4-2 Particle size distribution of Gap soil

4.2.2 WG soil with a relative density of 50%

When the test was conducted on the WG soils at a relative density of 50% under a hydraulic gradient of 30 or less, continuous reduction in *k* was observed despite the removal of the soils (1.2% of the total weight of the specimen) (Figure 4-3). When the test was conducted to reach a hydraulic gradient of 35, however, *k* increased significantly, and a considerable amount of soil was eroded. Hence, at a hydraulic gradient of 40, the accumulative eroded soil reached 5.1%, and the estimated *k* reached approximately 1.2 times k_0. A progressive reduction in *k* under a hydraulic gradient of 30 or less can be explained by particulate clogging, which reduces the permeability of the soil. Clogging behavior is generally known to be less likely at higher flow rates and larger constriction sizes (Reddi et al., 2000a). The constriction size and permeability of WG soils are smaller than those of the Gap soils; thus, the WG soils have a higher probability of clogging. Accordingly, this phenomenon was not observed during the test on the Gap soils.

The variation in *k* during the seepage test observed in this study is analogous to the previous experimental studies. Reddi et al. (2000b) reported that, in sand and kaolinite mixture, the effect of clogging and the washout of fine particles caused a decrease and a sudden subsequent increase in *k* with rapid soil erosion. According to the test results of Liu et al. (2021), who conducted a seepage test on well-graded soil, a reduction in *k* was followed by a sudden increase in *k*.

The particle size distribution of the eroded soil showed that the FS content was 66% (40% in the original specimen), resulting in a reduction in FS content

in the post-test specimen. (Figure 4-4). After the experiment, 0.4 mm settlement was observed (Figure 4-9); however, *e* increased from 0.74 to 0.83. Thus, suffusion phenomena, such as selective erosion of fine particles, causing increases in *k* and *e*, were observed to be similar to the results of the Gap soils. However, sudden increases in *k* and soil discharged occurred at a hydraulic gradient of 35 in the WG soils subsequent to the reduction in *k*, exhibiting a different behavior of internal erosion process to that of the Gap soils.

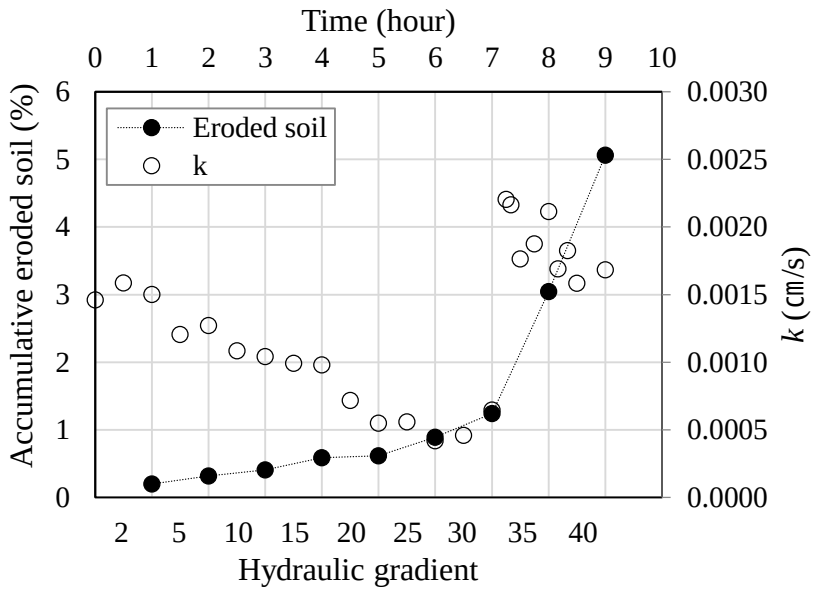

Figure 4-3 Accumulative eroded soil and *k* of WG soil (D_r = 50%) according to the hydraulic gradients

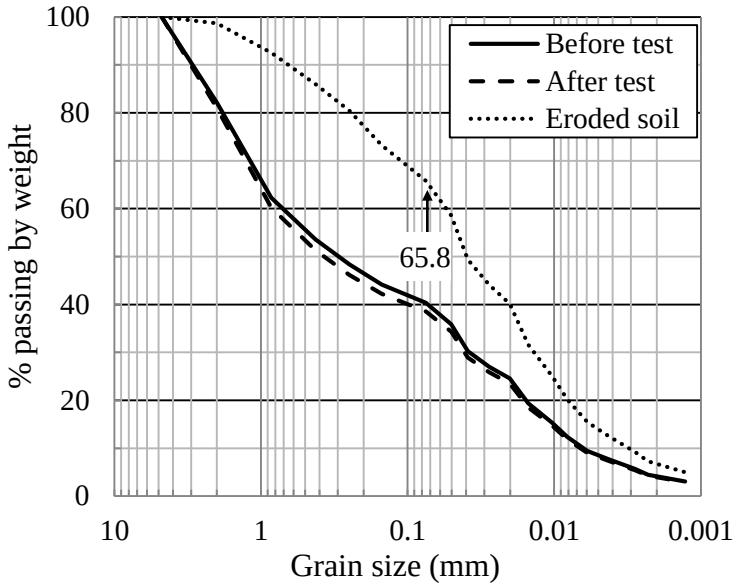

Figure 4-4 Particle size distribution of WG soil (D_r = 50%)

4.2.3 WG soil with a relative density of 65%

In the case of the WG soils at a relative density of 65%, *k* decreased to half of k_0 until the hydraulic gradient reached nearly 20. However, *k* gradually started to increase from a hydraulic gradient of 30 to 50 (Figure 4-5). Subsequently, a large amount of soil (11.6% of the total weight of the specimen) flowed out at a hydraulic gradient of 60, together with an abrupt increase in *k*, reaching 1.6 times k_0. However, after a significant amount of soil was discharged, *k* decreased to approximately 0.6 times k_0 even though the soils were continuously discharged (1.2–1.5%/hour).

The FS content of the eroded soil was 75%; thus, the FS content of the post-

test specimen decreased from 40% to 35% (Figure 4-6). In the Gap soils, only 3% of the discharged particles had a size larger than 0.15 mm, whereas in the WG soils, 20% of the discharged particles had a size larger than 0.15 mm. The results showed that in the WG soils, a relatively large quantity of coarse particles flowed out compared with the test results of the Gap soils.

A 1.4 mm settlement occurred up to the hydraulic gradient of 60, and subsequently a large settlement occurred after the hydraulic gradient reached 70, resulting in a final settlement of 7.3 mm (Figure 4-9). Despite the development of large settlements, the value of e calculated based on the amount of soil discharged and settlement increased from 0.63 to 0.74.

As mentioned above, as the probability of clogging was higher in WG soils, a reduction in k was observed at the beginning of the test, and k gradually increased as the soils were discharged. When a seepage force was sufficient to move the clogged particles into the effluent, a sudden outflow of soil and an increase in k were identified. Then, as the soil with coarse particles flowed out, the soil structure and settlement occurred, and settlement and particle rearrangement reduced k again.

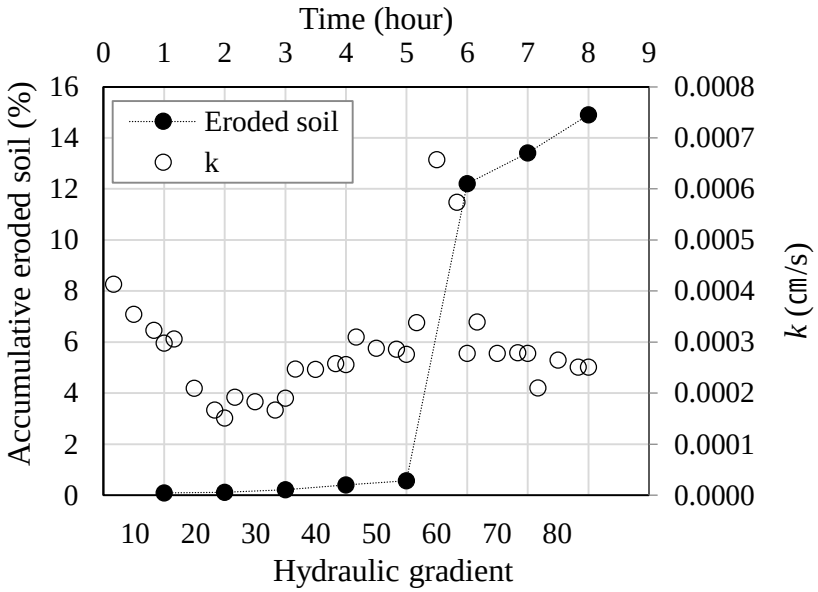

Figure 4-5 Accumulative eroded soil and k of WG soil (D_r = 65%) according to the hydraulic gradients

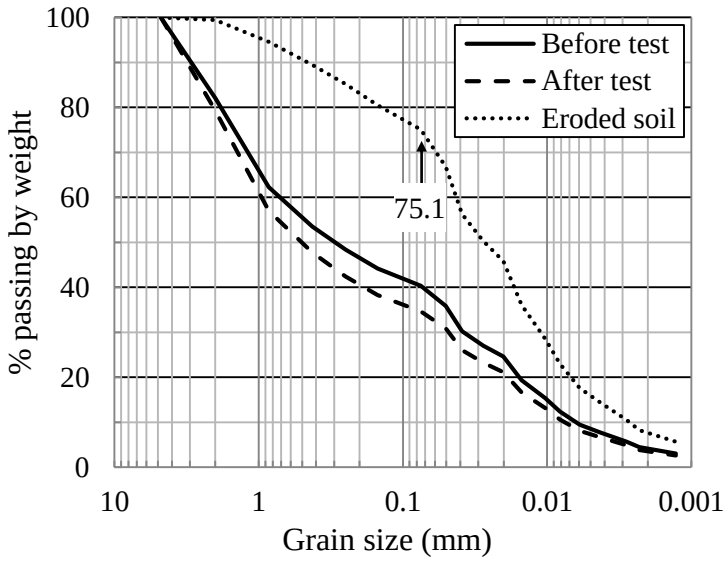

Figure 4-6 Particle size distribution of WG soil (D_r = 65%)

4.2.4 WG soil with a relative density of 80%

For the WG soils at 80% relative density, 0.7% of the soil specimen was discharged up to a hydraulic gradient of 120 (Figure 4-7). k decreased to approximately half of k_0 at a hydraulic gradient of 15. Under a hydraulic gradient of 20, however, k started to increase and reached approximately 1.4 times the value of k_0 at a hydraulic gradient of 50. From a hydraulic gradient of 50 to 120, k decreased to a value close to k_0. When the test was continued to reach a hydraulic gradient of 130, 9.5% of the soil was discharged, and a slight increase in k occurred. At a hydraulic gradient of 150, the accumulative eroded soil reached 10.8%. The particle size distribution of the eroded soil indicated that the percentage of FS was 73% (40% in the original specimen), producing a post-test soil with a smaller fine fraction (Figure 4-8). After the experiment, 5.3 mm settlement was developed (Figure 4-9); however, e increased from 0.52 to 0.61. In the final state, suffusion phenomena such as a significant amount of soil discharge and increases in k and e were observed.

Based on the test results of WG soils (D_r = 65% and 80%), it was confirmed that a relatively large amount of settlement was developed compared with the Gap soils (Figure 4-9). In WG soils, not only fine particles but also coarse particles flow out, resulting in the collapse of the soil structure. This phenomenon in WG soils can be described by the term suffosion, an internal instability resulting in the volume change of the soils (Reclamation and USACE, 2019).

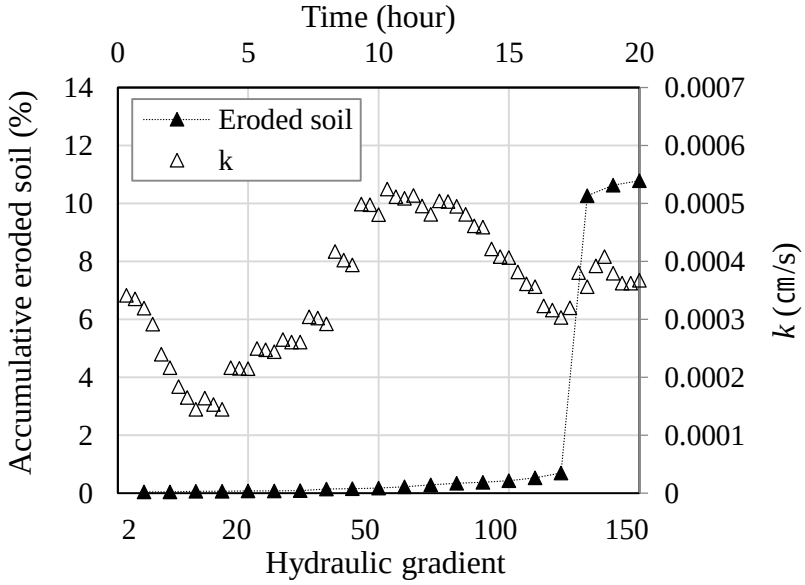

Figure 4-7 Accumulative eroded soil and k of WG soil (D_r = 80%) according to the hydraulic gradients

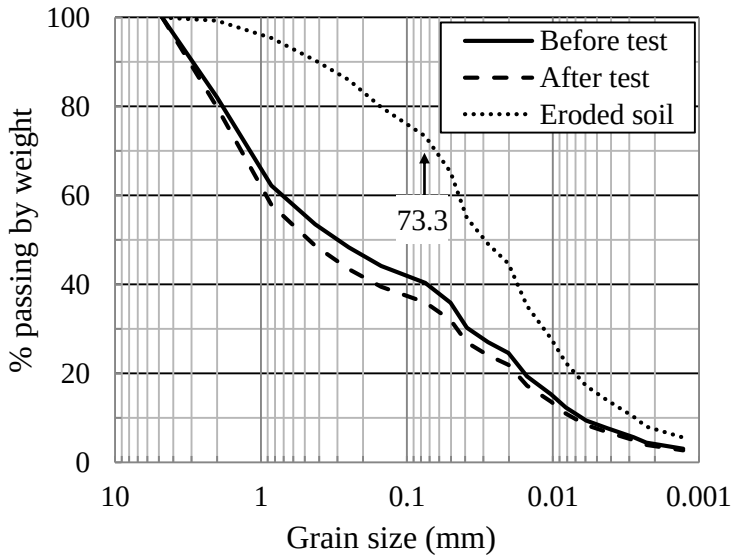

Figure 4-8 Particle size distribution of WG soil (D_r = 80%)

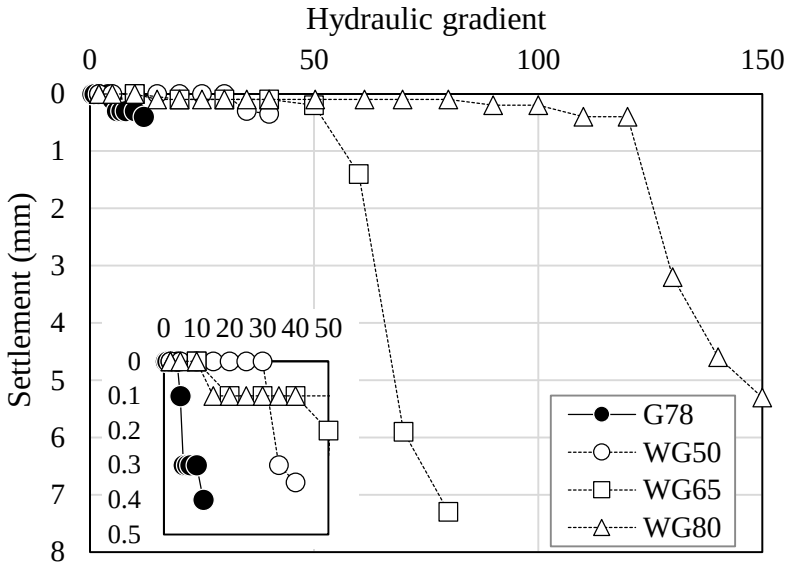

Figure 4-9 Settlement according to hydraulic gradients

4.3 Assessment of internal instability

The internal stability of the soils was evaluated through the seepage test results based on three indicators: 1) the fraction loss of soils, 2) the variation in permeability, and 3) the occurrence of piping failure (Chang and Zhang, 2013a). In terms of the fraction loss of soils, Kenney and Lau (1985) and Wan and Fell (2008) regarded the soils as unstable if the fraction loss of fine particles relative to the total mass of the soils was over 7% and 4%, respectively. Regarding the second indicator, sample was regarded as unstable if a progressive or sudden increase in soil permeability was observed during the test, which can be acknowledged from the time-permeability relationship (Sun, 1989; Liu, 2005; and Kaoser et al, 2006). Lastly, Skempton and Brogan (1994) regarded the soils as internally unstable when piping failure occurred at one-third to one-fifth of the theoretical critical hydraulic gradient. In this study, to determine whether the occurrence of internal erosion was induced by suffusion, the first two indicators were adopted.

The minimum limit of the discharged fine fraction on unstable soils was defined as 4% (Kenney and Lau, 1985) and the results are summarized in Table 4-1. In this study, because the actual soil erosion was measured for each hydraulic gradient, the point where the amount of soil eroded reached more than 4% could be identified. Gap soils, WG soils (D_r = 50%), WG soils (D_r = 65%), and WG soils (D_r = 80%) showed 4% soil erosion at hydraulic gradients of 12, 40, 60, and 130, respectively.

In the test results of Gap soils, k increased progressively from a hydraulic

gradient of 2 (Figure 4-1). In contrast, k for WG soils (D_r = 50%) increased suddenly at a hydraulic gradient of 35 (Figure 4-3). In addition, k for WG soils (D_r = 65%) increased slightly from a hydraulic gradient of 40 and increased suddenly at a hydraulic gradient of 60 (Figure 4-5). In the test results for WG soils (D_r = 80%), a sudden increase in k was pronounced at a hydraulic gradient of 130 after a major fluctuation (Figure 4-7).

It should be noted that when the two identification methods (fraction loss of soils and change in k) are applied individually, the analyses of the test results might be inconsistent with each other. When the standard of minimum fraction loss (4%) is applied solely, gap-graded soils, WG soils with relative densities of 50%, 65%, and 80% can be evaluated as internally unstable at hydraulic gradients of 12, 40, 60, and 130, respectively (Figure 4-10). In contrast, when considering only the variation in k, the hydraulic gradient assessed as internally unstable was lower than the above evaluation results (Figure 4-10). In particular, WG soils (D_r = 80%) show an additional point of unstable behavior at a hydraulic gradient of approximately 20, whereas the amount of eroded soil is negligible. Hence, the internal stability of the well-graded soils evaluated based on the hydraulic standard may exhibit conservative or misleading results. Therefore, in this study, a more rational method to evaluate the internal instability of well-graded soils is proposed regarding both the increase in the fraction loss of soils and k.

Based on the test results of WG soils, when the fraction loss to the total mass of the specimen was more than 4% and k suddenly increased, it was recommended to regard the soil as internally unstable. According to this method,

the hydraulic gradients at which the initiation of internal instability was observed were 10, 40, 60, and 130 in the Gap soil, WG soils at relative densities of 50%, 65%, and 80%, respectively.

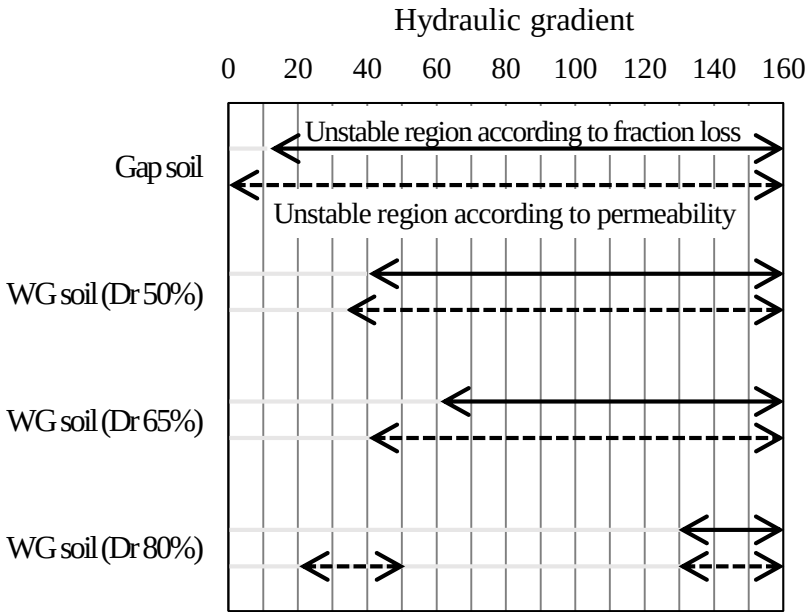

Figure 4-10 The assessment results of internal instability according to the hydraulic gradient

Table 4-1 Summary of the short-term test results

Test No.	Specimen	D_r (%)	Applied maximum hydraulic gradient	Amount of eroded soil (%)	Size of the largest particles eroded (mm)	Permeability
G-80	Gap soils	78	12	4.1	2.0	Progressive increase
WG-50	WG soils	50	40	5.1	2.0	Sudden increase
WG-65		65	80	14.9	2.0	Sudden increase
WG-80		80	150	10.8	2.0	Sudden increase

4.4 Summary

In this chapter, the results of short-term suffusion tests, which were conducted on both gap-graded and well-graded soil with various hydraulic gradients and relative density, were presented. The internal instability of the soils was evaluated according to indicators of previous studies. Additionally, the occurrence and characteristic of internal instability of the well-graded soils were investigated. The specific findings in this chapter can be summarized as follows:

1) The result of Gap soil showed clear manifestations of suffusion. WG soil exhibited a similar suffusion process to Gap soil, such as erosion of fine particles and increases in k and e. However, sudden increases in k and soil discharged occurred at the onset of internal instability, which followed the reduction in k, exhibiting an internal erosion process different from that of Gap soil. Additionally, fine particles and coarse particles flowed out, resulting in settlement.
2) The hydraulic gradient at which internal instability occurs is higher for WG soil than for Gap soil. Additionally, the WG soil showed higher resistance to internal erosion when compacted to a greater relative density. An increase in the degree of compaction not only increases the critical hydraulic gradient, but also reduces the amount of erodible fine particles under the same hydraulic gradient.
3) The test results based on each identification method (fraction loss of

soils and change in k) are inconsistent with each other. Therefore, it is concluded that considering both the fraction loss of soils and the changes in k is more appropriate for evaluating the internal stability of well-graded soils.

Chapter 5. Long-term test results and analyses

5.1 Introduction

In previous short-term test results, the internal instability of WG soil showed a similar suffusion process to Gap soil, such as erosion of fine particles and increases in k and e. However, a sudden increase in k and the amount of soil discharge were observed only after a progressive reduction in k, exhibiting an internal erosion process different from that of Gap soil. This phenomenon can also be observed in the experimental studies performed by Li (2008) and Liu et al. (2021), who conducted a series of seepage tests using well-graded soil. Additionally, well-graded soils signify higher resistance to internal instability when compacted to a greater relative density, whereas the internal instability of gap-graded soil is not significantly affected by relative density (Wan, 2006; Liu et al., 2021).

The previous short-term tests were performed to easily evaluate the characteristics of internal instability while increasing the hydraulic gradient stepwise. This method has the advantage of observing internal instability in a relatively short time and roughly specifying the hydraulic gradient at the onset of internal instability. Through the short-term test, however, it is difficult to evaluate the progress of internal instability because the hydraulic gradients are increased in a stepwise manner for a short period and the effect of the hydraulic gradient applied during the previous stage may alter the internal erosion

resistance of the soil. Furthermore, as 60% of reservoirs in South Korea are aged over 60 years, and internal instability of well-graded soil is expected to develops slowly, long-term stability of well-graded soil needs to be evaluated.

Therefore, long-term suffusion tests were conducted on the same specimen as that of short-term test to assess the internal instability and analyze the progress and causes of that. The amount of eroded soil, flow rate, and settlement were measured during the tests, and k and e were calculated over time for the test conditions of various relative densities and hydraulic gradient. Additionally, the particle size distributions of the eroded soil and the post-test specimen were estimated based on the particle size distribution analysis. A summary of the test results is listed in Table 5-1. Detailed test results and analyses are described in the following section. In section 2, amount of eroded soil and erosion rate were analyzed. In section 3 and 4, hydraulic conductivity and settlement were studied, respectively. In section 5, based on the test results and analysis, the mechanism of internal instability and its progress in well-graded soil was proposed and compared with those in gap-graded soil.

Table 5-1 Summary of the long-term test results

Test	Specimen	% of fines before test (%)	*Dr* (%)	*e* before test	Hydraulic gradient	Testing time (h)	Percentage of eroded soil (%)	% of fines of eroded soil (%)	Settlement (mm)	*e* after test
G78-3	Gap	15 (< 0.15 mm)	78	0.57	3	103	1.3	98.2 (< 0.15 mm)	0.0	0.59
G78-5					5	72	14.0	95.4 (< 0.15 mm)	0.4	0.82
WG50-5	WG	40 (< 0.075 mm)	50	0.74	5	360	2.3	49.8	0.35	0.78
WG50-15					15	576	4.1	70.4	0.25	0.81
WG50-17					17	552	11.3	69.0	7.6	0.79
WG50-25					25	72	11.1	64.8	9.2	0.76
WG65-30			65	0.63	30	243	0.9	48.7	0.2	0.64
WG65-60					60	39	15.6	69.8	9.1	0.74
WG80-60			80	0.52	60	339	1.6	68.3	1.8	0.51
WG80-120					120	63	6.7	77.8	5.5	0.53

5.2 Amount of eroded soil and erosion rate

The amount of eroded soil over time is shown in Figure 5-1. Based on the post-test particle size distribution analysis, the FS content of the eroded soil of WG soil ranged from 48 to 78% and the percentage of fines, particles smaller than 0.15 mm, was from 58 to 83%. Whereas, the percentage of fines, particles smaller than 0.15 mm, in the eroded soil of Gap soil was from 95 to 98% (Figure 5-2). In the case of the WG soil at D_r = 50%, 2.3, 4.1, 11.3, and 11.1% of the soil flowed out at hydraulic gradients of 5, 15, 17, and 25 for 600, 576, 552, and 72 h, respectively. For the WG soil at D_r = 65%, 0.9% of the soil flowed out during 243 h, and 15.6% during 39 hours of testing time under hydraulic gradients of 30 and 60, respectively. For the WG soil at D_r = 80%, 1.6% of the soil was discharged over 339 hours at a hydraulic gradient of 60, and 6.7% of soil flowed out for over 63 hours at a hydraulic gradient of 120. In the Gap soil, 1.3 and 14.0% of the soil eroded at hydraulic gradients of 3 and 5 for 103 and 72 h, respectively.

Figure 5-1 show that the soil erosion rate increased as the hydraulic gradient increased at the same relative density. This is because a higher hydraulic gradient results in a higher seepage force and flow rate acting on the soil. Consequently, the soil erosion rate accelerated with an increase in the hydraulic gradient.

The test results indicated that the behavior of internal instability largely depended on the particle size distribution and relative density of the soils. Comparing the amount of eroded soil at the same hydraulic gradient for each

test result, the amount of soil discharged in the Gap soils was larger than that in the WG soils. The Gap soils in this study are a binary mixture in which the coarse particles are 10 times larger than the finer particles (Figure 5-3(a)). Therefore, fine particles are likely to be located between the constrictions formed by the coarse particles. As a result, fine particles are under low effective stress and can be readily moved by the seepage force (Kenney and Lau, 1985; Taylor, 2016). The method proposed by Kenney and Lau (1985) can estimate whether the fine particles fill the voids in the coarse particles. At the dense state, the volume of voids in the coarse particles can be expressed as $f_c \times e_c$, where f_c is the fraction of the total mass comprising the coarse particles and e_c stands for the minimum void ratio of the coarse particles. The volume of the fine particles is expressed as $f_f \times (e_f + 1)$, where f_f and e_f represent the fraction of fine particles and the maximum void ratio of the fine particles, respectively (Eq. 5-1).

$$f_c \times e_c > f_f \times (e_f + 1) \tag{5-1}$$

The values of e_c = 0.77 and e_f = 2.01 for Gap soils in this study were determined based on the standard described in ASTM D4253 and ASTM D4254 (ASTM, 2016a; ASTM, 2016b), respectively. Using values of f_c = 0.85, f_f = 0.15, e_c = 0.77 and e_f = 2.01, values of $f_c \times e_c$ = 0.65 and $f_f \times (e_f + 1)$ = 0.45 were obtained. Because the size of the constrictions and the volume of voids in coarse particles are greater than that of the fine particles are free to move and can easily flow out.

In contrast, because WG soils have successive particle size distributions, the fine particles are unlikely to be in the loose state and may transfer inter-particle effective stress (Figure 5-3(b)). Accordingly, at the same hydraulic gradient, the amount of eroded soil in WG soils was smaller than that in Gap soils. The hydraulic gradient of WG soils at which internal instability was initiated is higher than that of Gap soils.

When comparing the erosion rates of the WG soil (up to approximately 40 hours of testing time) based on the relative density, the higher the relative density, the lower the soil erosion rate at similar hydraulic gradients (Figure 5-4). In the case of gap-graded soil, which is vulnerable to internal instability, the relative density does not significantly affect the resistance to internal instability because the fine particles are under low effective stress. However, because the fine particles in WG soils are likely to participate in transferring the inter-particle effective stress, the relative density of WG soils will have a greater effect on the resistance toward internal erosion. Thus, the higher the relative density in the WG soils, the higher the effective stress that can be applied to the fine particles, resulting in improved resistance to internal erosion. As demonstrated in Table 5-1, it is estimated that finer particles are unlikely to move, leading to a smaller amount of eroded soil upon increasing the relative density under a similar hydraulic gradient condition.

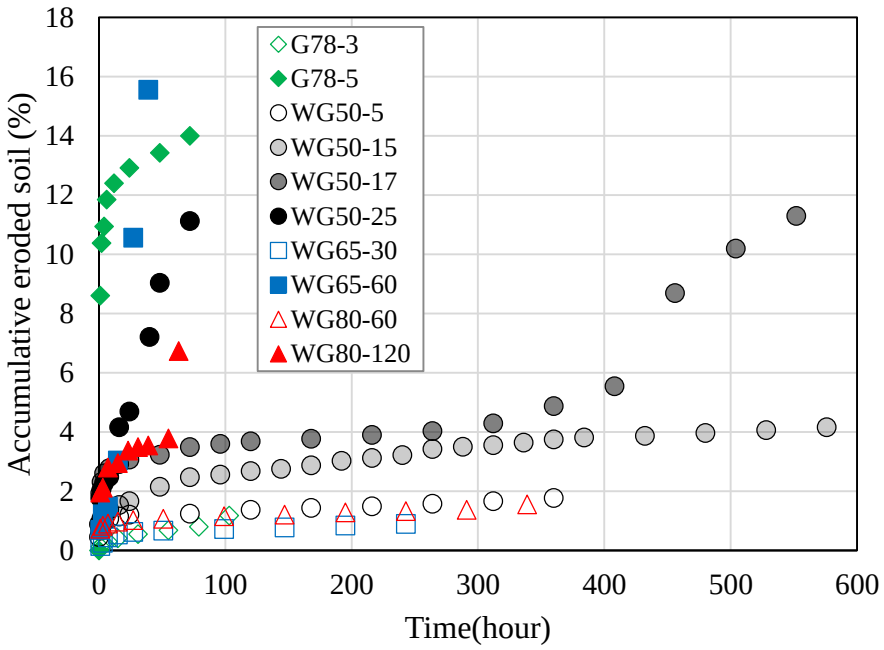

Figure 5-1 Accumulative eroded soil of all test results over time

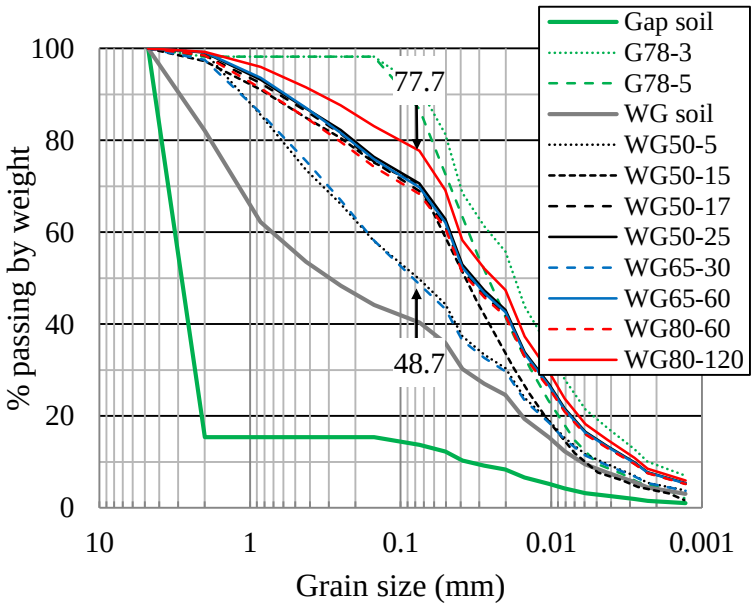

Figure 5-2 Particle size distributions of tested and eroded soil

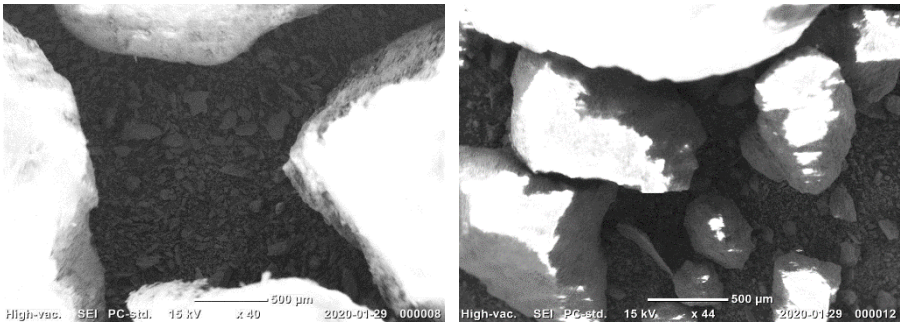

(a) (b)

Figure 5-3 SEM images: (a) Gap soil; and (b) WG soil

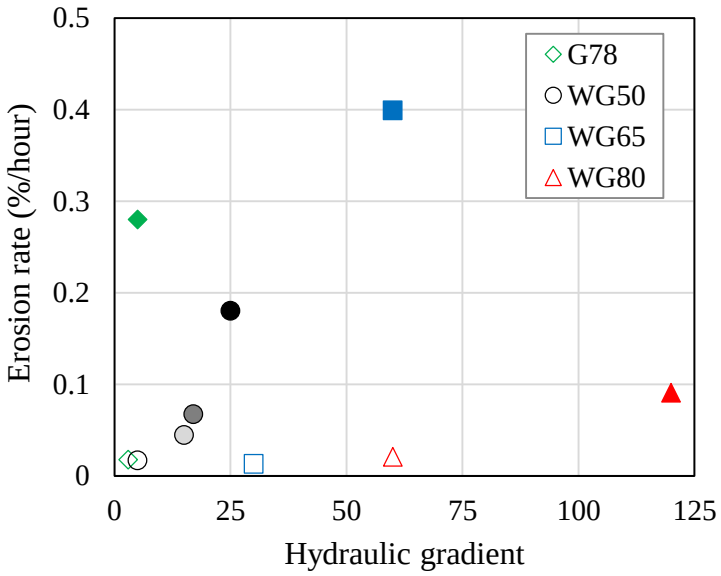

Figure 5-4 Erosion rate of all test results with hydraulic gradients

5.3 Hydraulic conductivity

In order to analyze the permeability change during the tests, the results were classified into internally unstable and stable results according to the amount of accumulative eroded soil. The minimum limit of eroded soil on unstable soils is defined as 4%, as discussed in chapter 4. Based on the predefined soil loss (4%), Gap soil at hydraulic gradient of 3 was assessed as stable, and Gap soil at hydraulic gradient of 5 was assessed as unstable. In case of WG soil at a relative density of 50%, the test results at hydraulic gradients of 5 and 15 were evaluated as stable, and those at hydraulic gradients of 17 and 25 were evaluated as unstable. WG soil (D_r = 65%) at a hydraulic gradient of 30 was stable, and WG soil (D_r = 65%) at a hydraulic gradient of 60 was unstable. Additionally, WG soil (D_r = 80%) was classified as stable at a hydraulic gradient of 60 and unstable at a hydraulic gradient of 120 (Table 5-2).

Table 5-2 Internal instability of test results

Test	Specimen	D_r (%)	Hydraulic gradient	% of eroded soil to the total mass of the specimen	Internal instability
G78-3	Gap soil	78	3	1.3	Stable
G78-5			5	14.0	Unstable
WG50-5	WG soil	50	5	2.3	Stable
WG50-15			15	4.1	Stable
WG50-17			17	11.3	Unstable
WG50-25			25	11.1	Unstable
WG65-30		65	30	0.9	Stable
WG65-60			60	15.6	Unstable
WG80-60		80	60	1.6	Stable
WG80-120			120	6.7	Unstable

5.3.1 Gap soil

The Gap soil at hydraulic gradient of 3, assessed as internally stable, showed progressively increase in k with soil erosion. As the result, the accumulative eroded soil reached 1.3% of the total weight of the specimen and k reached approximately 2.5 times k_0 at the end of the test (Figure 5-5). After the test, the particle size distribution analysis was conducted by dividing the sample into top, middle, and bottom parts. The FS content in the top, middle, and bottom parts was 12.4 %, 13.6 %, and 12.3 %, respectively (Figure 5-6). While the FS content in the middle part was similar to the initial that of the soil (13.7%), that in the top and middle parts decreased. The particle size distribution analysis indicates that the fine particles in the top part moved into the middle part and the fine particles in the middle and bottom parts flowed out. In the case of Gap soil, even in an internally stable state, the washing out of the fine particles within the soil increases the D10 (particle diameter corresponding to 10% passing by weight) and e, resulting in an increase of k.

When the test of Gap soil was continued for 11 hours under the hydraulic gradient of 5, accumulative eroded soil reached 12.4%, and at the end of the test, the total eroded soil reached 14% for 72 h. During the first hour of the experiment, a significant amount of soil was discharged, and then the erosion rate of the soil gradually decreased (Figure 5-7). Accordingly, a rapid increase in k was observed, and a level twice k_0 was maintained. After the test, a 0.4 mm settlement was observed, and e significantly increased from 0.54 to 0.78. Based on the grain size distribution analysis, 98% of the eroded soil turned out

to be the fine particles passing sieve no. 100 (Figure 5-8). As a result, the results of Gap soils showed clear manifestations of suffusion, such as a significant quantity of fine particles discharged and increases in *e* and *k*.

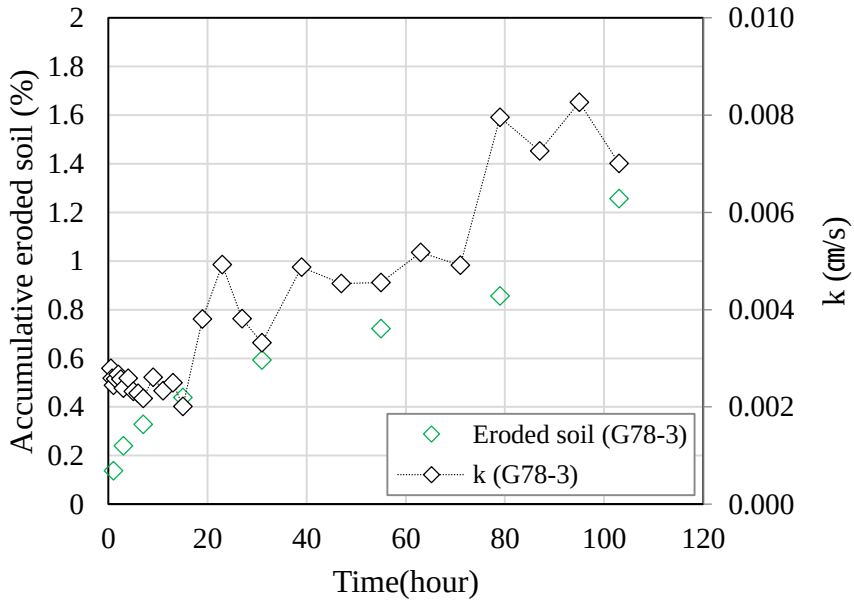

Figure 5-5 Accumulative eroded soil and *k* of Gap soil at a hydraulic gradient of 3

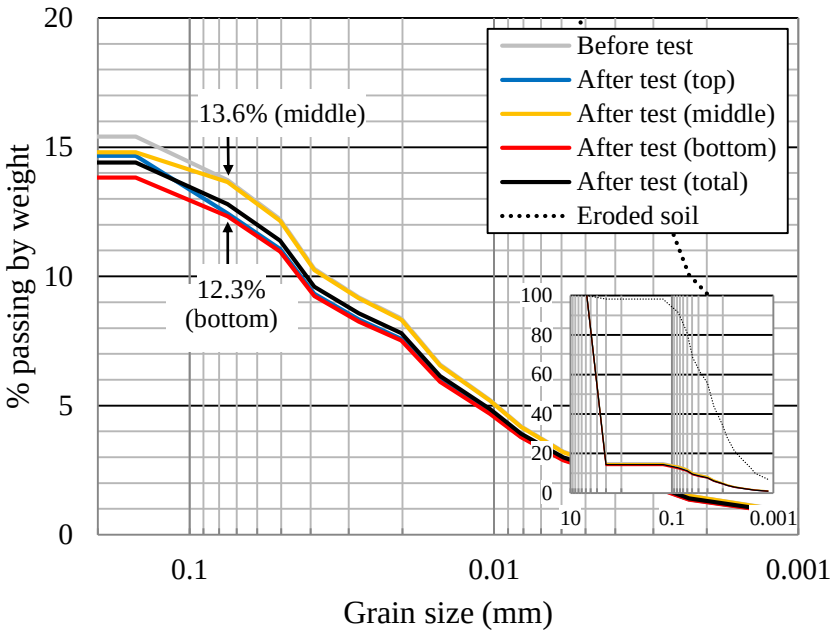

Figure 5-6 Particle size distribution of Gap soil at a hydraulic gradient of 3

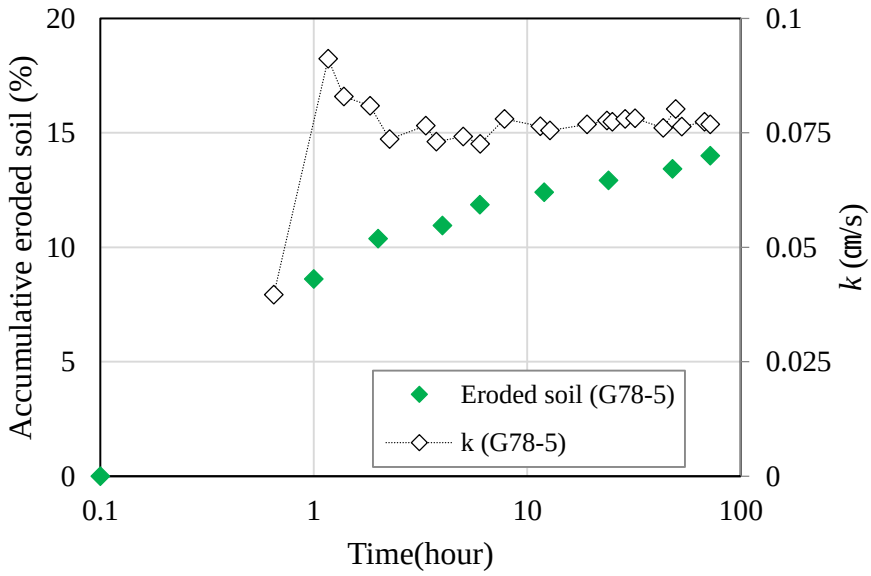

Figure 5-7 Accumulative eroded soil and *k* of Gap soil at a hydraulic gradient of 5

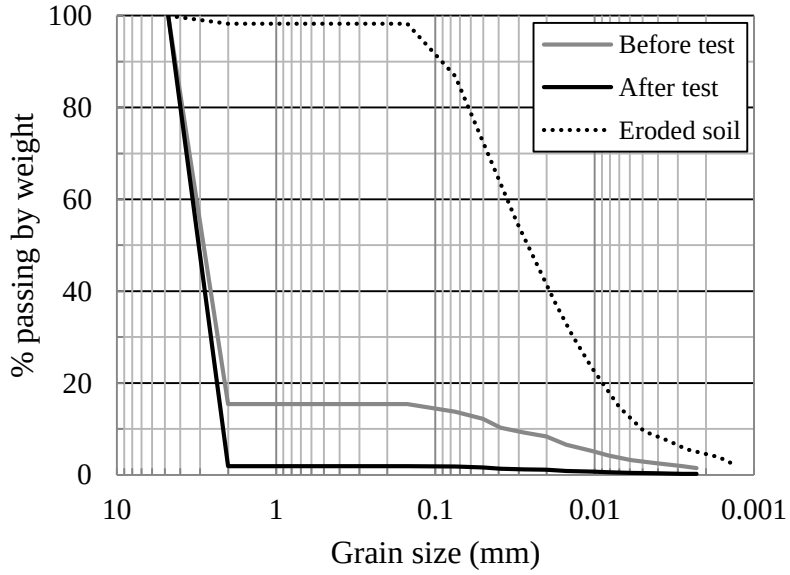

Figure 5-8 Particle size distribution of Gap soil at a hydraulic gradient of 5

5.3.2 Internally stable WG soil

The WG soil classified as internally stable showed a reduction in k and convergence to a constant value despite soil erosion. Figure 5-9 shows the relationship between the accumulative eroded soil and k normalized by the initial k (k_0) at hydraulic gradients of 5 and 15 for WG soil with a 50% relative density. The results show that after the rapid reduction in k, it tends to converge to a lower level while exhibiting small fluctuations within the range of less than k_0. The change in k was caused by the movement of fine particles, clogging, and breakage of the soil structure. The particle size distribution analysis was performed by dividing the sample into top, middle, and bottom parts after the experiment under a hydraulic gradient of 15 to confirm the movement of fine particles and clogging. The FS content of the top, middle, and bottom parts was 42.0 %, 42.3 %, and 44.6 %, respectively (Figure 5-10). In contrast to the initial FS content (42.8%) of the soil, the FS content of the top and middle parts decreased, while that of the bottom part increased, indicating that the fine particles in the top and middle parts moved downward and clogged in the bottom part.

To evaluate the effect of FS migration on the change in permeability, particle size distribution analysis and the graphical technique proposed by Kenney and Lau (1985) were adopted to obtain D10 and e, respectively. As demonstrated in Table 5-3, once the fine particles were clogged in the bottom part, D10 and e decreased, resulting in a reduction in local permeability, whereas it increased in the top and middle parts owing to the selective erosion of FS contents. It should

be noted that the decrease in local permeability can lead to a reduction in the overall permeability.

To validate the reduction in the overall permeability due to the decrease in local permeability, the k of each part was calculated through the predictive method (Eq. 5-2; Chapuis, 2015) and the overall k was calculated using Darcy's Law for continuous flow in saturated media (Eq. 5-3), where k = coefficient of permeability; D10 = diameter of the 10% mass passing; e = void ratio; v = velocity of flow; i = hydraulic gradient.

$$k(cm/s) = 4.236\ (\frac{D10^2 e^3}{1+e})^{0.925} \tag{5-2}$$

$$v = k \times i \tag{5-3}$$

As shown in the results (Table 5-3), D10 and e increased at the top and middle parts due to the migration of the fine particles, leading to a higher k. Meanwhile, in the bottom part, a reduction in k was shown because the clogging of the fine particles reduced D10 and e. Although the D10 and e of the entire specimen increased, the total k decreased. Further, the hydraulic gradient of the bottom part increased to 1.8 times the overall hydraulic gradient. Therefore, it can be concluded that when the overall hydraulic gradient is constant and the fine particles are clogged locally within the soil, the decrease in local permeability can reduce the overall permeability, resulting in a greater local hydraulic gradient.

When k in the bottom part decreases, the pore water pressure in the bottom part increases, and the clogging can be partly released, resulting in a temporary increase in k. However, the clogging cannot be completely broken, and k decreases again because of the repeated migration and clogging of the fine particles. Consequently, k decreases gradually after a series of fluctuations. The flow rate decreases owing to the reduction in k; consequently, the amount of migration of fine particles and the amount of clogging are reduced, leading to the convergence of k.

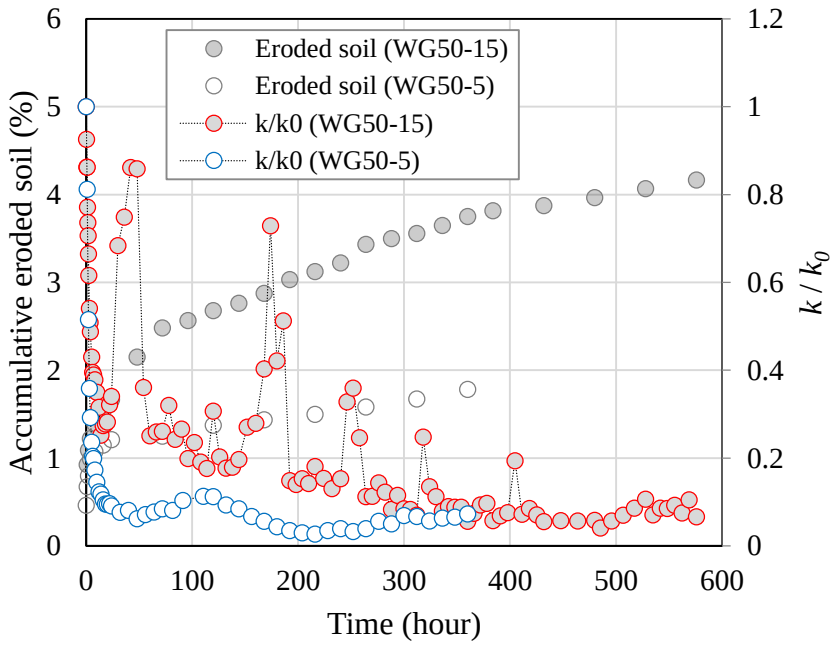

Figure 5-9 Accumulative eroded soil and normalized k of WG soil (D_r= 50%) at hydraulic gradients of 5 and 15

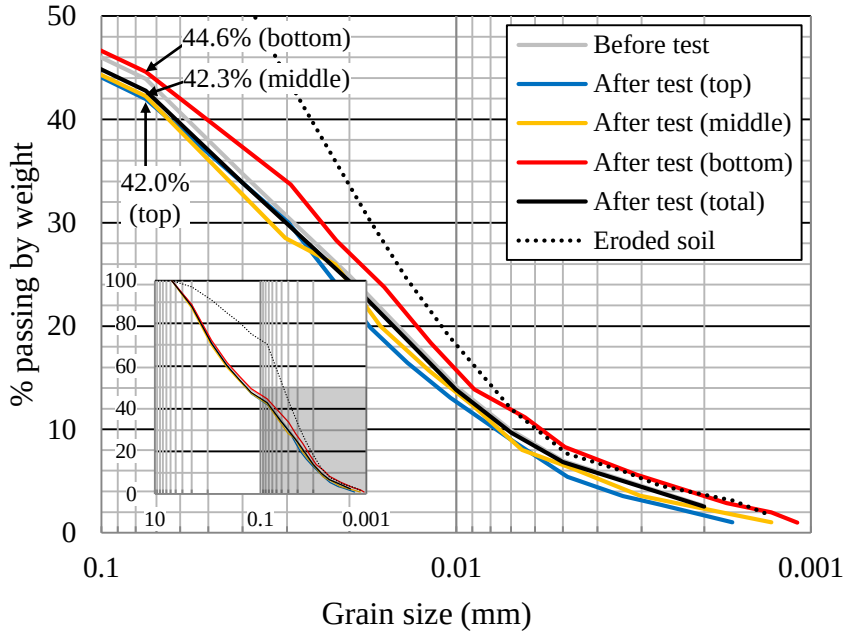

Figure 5-10 Particle size distribution of WG soil (D_r= 50%) at a hydraulic gradient of 15

Table 5-3 Test results of WG soil (D_r= 50%) at a hydraulic gradient of 15

Test results	Initial state	After test			
		Top	Middle	Bottom	Total
% passing sieve no. 200	43.9	42.0	42.3	44.6	42.8
D10(mm)	0.0071	0.0077	0.0075	0.0057	0.0072
Eroded soil mass (%)		2.5	2.3	-0.8	4.0
e	0.74	0.87	0.87	0.70	0.81
Calculated k (10^{-4} cm/s)	1.19	1.98	1.89	0.68	1.18
Hydraulic gradient		9	9	27	15

Even in the test results of WG soil at a hydraulic gradient of 30 (D_r= 65%), and 60 (D_r= 80%), the convergence of k toward a lower level was accompanied by the fluctuations in k (Figure 5-11). The FS content of the top and middle parts decreased, and that of the bottom part increased when it is compared to the initial FS content of the soil specimen (Figure 5-12).

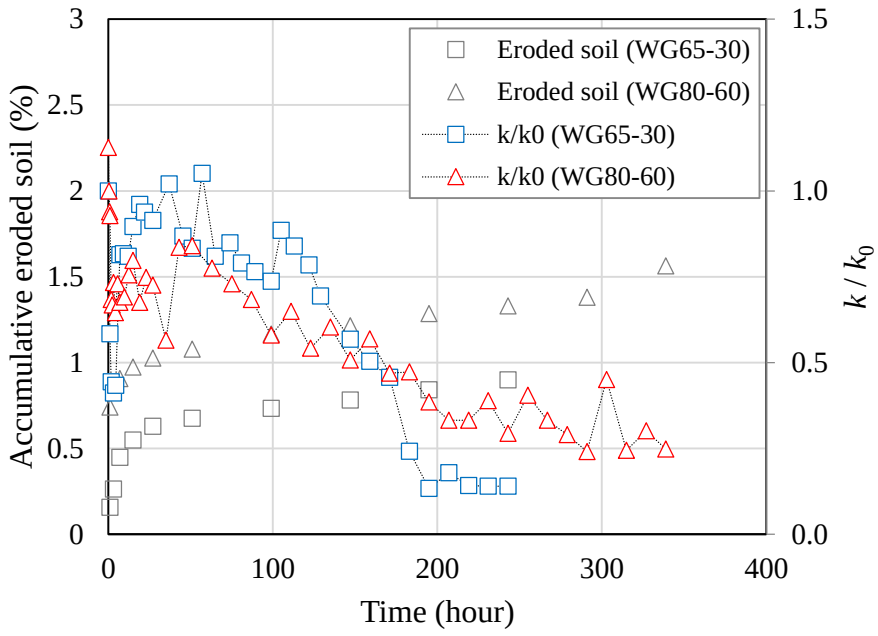

Figure 5-11 Accumulative eroded soil and normalized k of WG soil (D_r= 65%) at a hydraulic gradient of 30 and WG soil (D_r= 80%) at a hydraulic gradient of 60

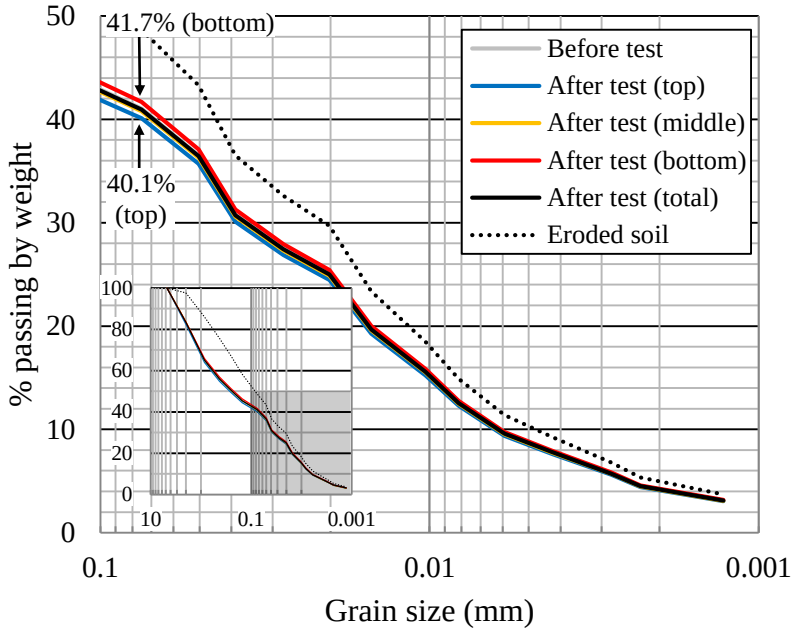

Figure 5-12 Particle size distribution of WG soil (D_r= 65%) at a hydraulic gradient of 30

5.3.3 Internally unstable WG soil

WG soil (D_r= 50%) at hydraulic gradients of 17 and 25, which was evaluated to be internally unstable, showed a reduction in k and a gradual decrease in erosion rate until the accumulative eroded soil reached approximately 4% of the total mass of the specimen (Figure 5-13 and Figure 5-14). At 4% or more, however, k and the erosion rate of the soil increased rapidly. Particle size distribution analysis after the seepage experiment at a hydraulic gradient of 17

showed that the FS content of each part was 36.4, 34.8, and 29.1% in the top, middle, and bottom parts, respectively (Figure 5-15), indicating that fine particles were reduced in all parts when compared to the initial FS content (42.3%). It should be noted that, unlike the particle size distribution analysis result of internally stable soil at a hydraulic gradient of 15, the FS content in the bottom part was the lowest. Therefore, it can be deduced that the decrease in k before the onset of internal instability can be attributed to clogging, and a subsequent abrupt increase in k is resulted from the breakage of clogging and erosion of fine particles.

The variation in k during the seepage test observed in this study is analogous to the previous experimental studies. Reddi et al. (2000b) reported that, in gap-graded soil (sand and kaolinite mixture), the effect of clogging and the washout of fine particles caused a decrease and a sudden subsequent increase in k with rapid soil erosion. According to the test results of Liu et al. (2021), who conducted a seepage test on well-graded soil, a reduction in k was followed by a sudden increase in k.

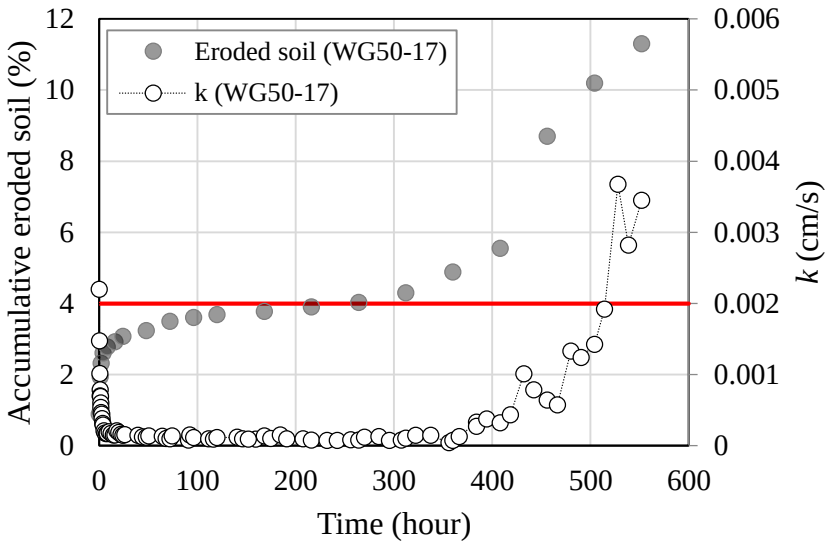

Figure 5-13 Accumulative eroded soil and k of WG soil (D_r= 50%) at a hydraulic gradient of 17

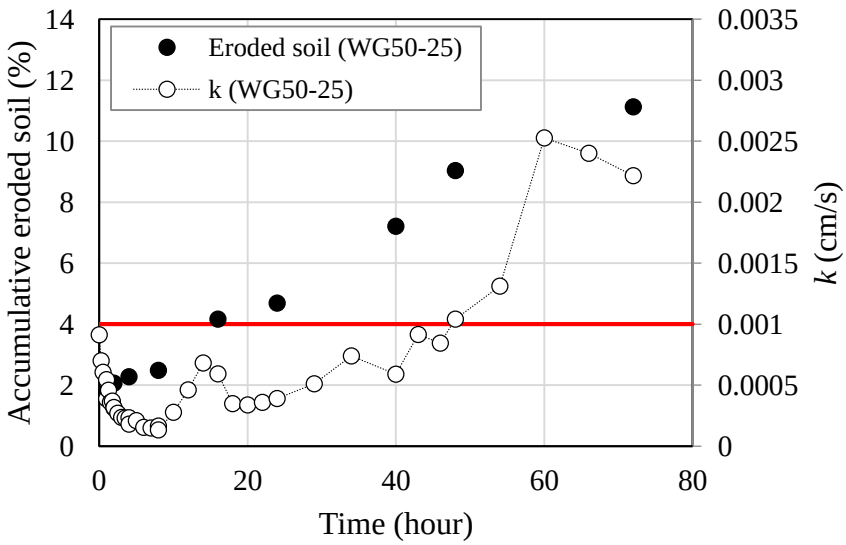

Figure 5-14 Accumulative eroded soil and k of WG soil (D_r= 50%) at a hydraulic gradient of 25

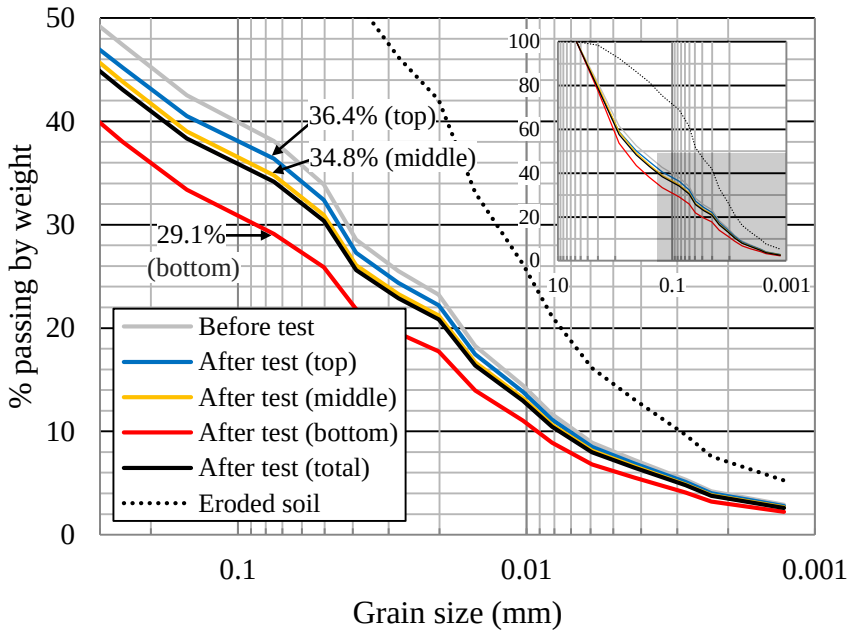

Figure 5-15 Particle size distribution of WG soil (D_r= 50%) at a hydraulic gradient of 17

Similar results were obtained from the test on WG soil (D_r= 65%) at a hydraulic gradient of 60 (Figure 5-16). Initially, k demonstrated an unsteady pattern, but over time, k and the rate of soil erosion decreased to approximately 4% of the total eroded soil. Afterwards, k and the erosion rate exhibited a sudden increase, similar to the internally unstable test result of WG soil (D_r= 50%). Additionally, The FS content of all parts decreased, and that of the bottom part was the lowest (Figure 5-17).

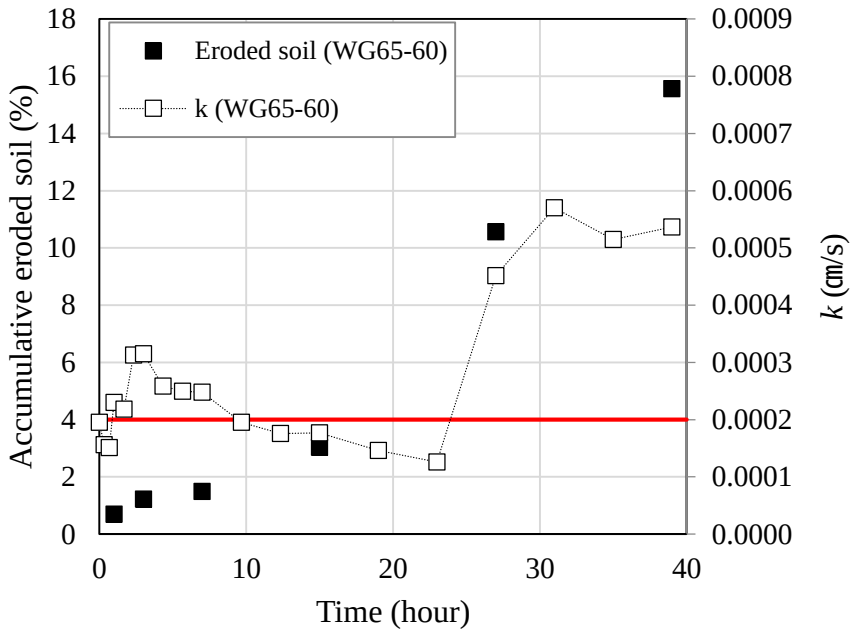

Figure 5-16 Accumulative eroded soil and k of WG soil (D_r= 65%) at a hydraulic gradient of 60

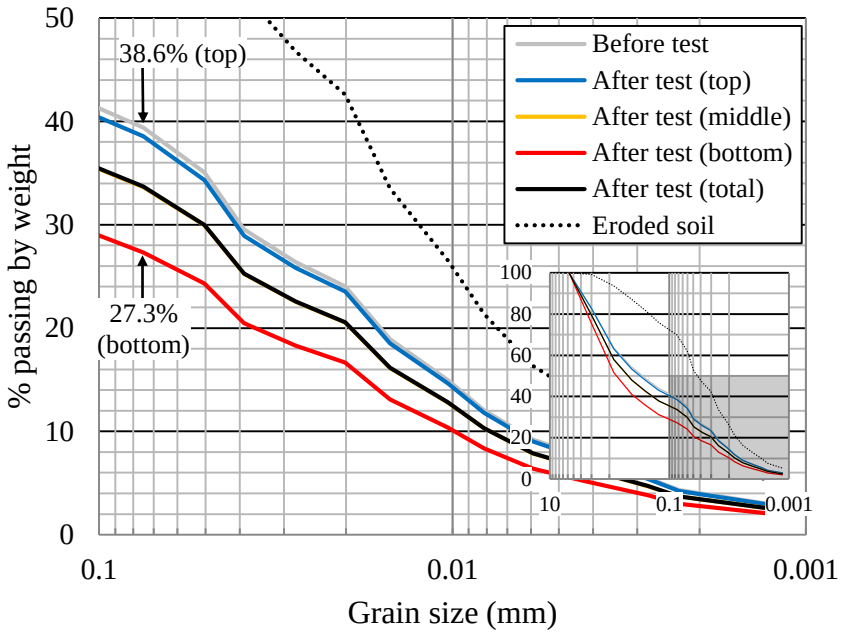

Figure 5-17 Particle size distribution of WG soil (D_r= 65%) at a hydraulic gradient of 60

In WG soil (D_r= 80%) at a hydraulic gradient of 120, up to approximately 4% of accumulative eroded soil, k and the erosion rate of the soil decreased over time. When the percentage of eroded soil reached 4% or higher, the erosion rate increased rapidly (Figure 5-18). The distribution trend of the FS content of each parts was similar to that of the previous tests (Figure 5-19). Contrary to the test results at low relative densities, k did not demonstrate any significant changes. This difference was due to the settlement of the specimen, resulting in a decrease in e. A detailed discussion of this discrepancy is provided in the next section.

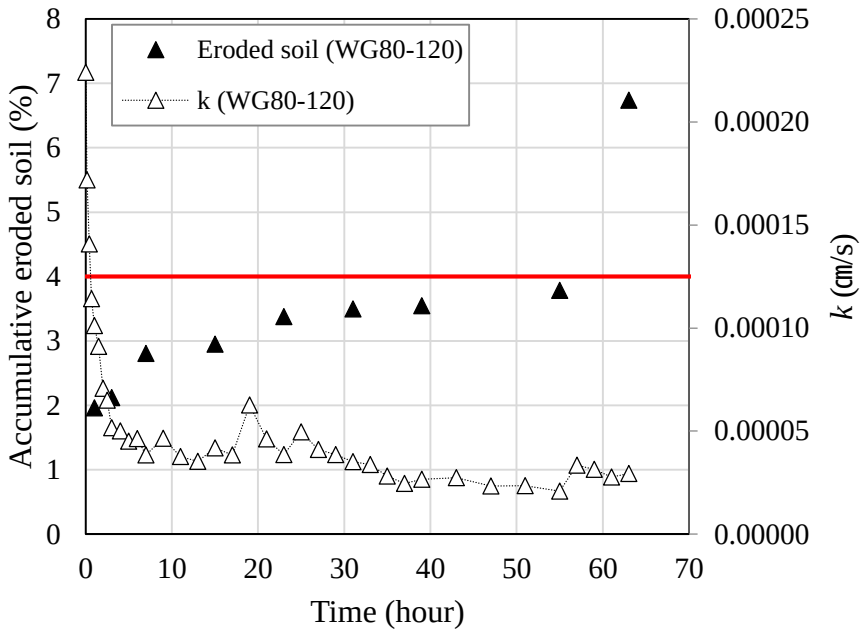

Figure 5-18 Accumulative eroded soil and k of WG soil (D_r= 80%) at a hydraulic gradient of 120

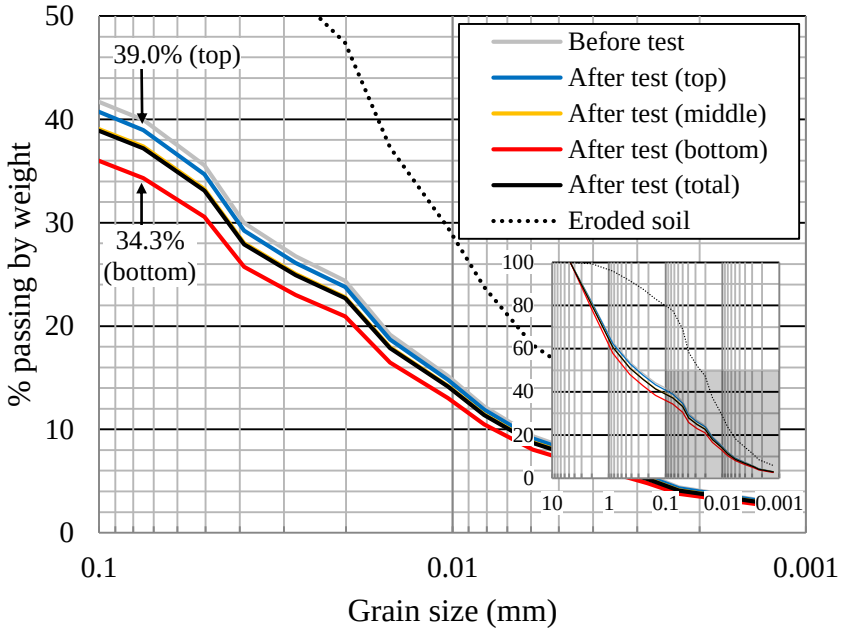

Figure 5-19 Particle size distribution of WG soil (D_r= 80%) at a hydraulic gradient of 120

5.4 Settlement

In the case of Gap soil, no noticeable settlement occurred during the test and *e* significantly increased from 0.57 to 0.82. However, the occurrence of internal instability was accompanied by the settlement in WG soil (Figure 5-20). For all test cases, the relationship between the amount of eroded soil and settlement showed a significant difference between internally stable and unstable soil. In internally stable soils, there is no clear relationship between the settlement and amount of eroded soil. However, in internally unstable soils, settlement increases as the amount of eroded soil increases. As demonstrated in Figure 5-21 and Figure 5-22, the patterns of settlement and accumulative eroded soil over time are very similar, indicating that the erosion of soil is accompanied by settlement. Therefore, it can be inferred that the erosion of WG soil occurs along with the deformation or collapse of the soil structure, unlike gap-graded soil. The deformation of the soil structure can be partially proved by the coarse particles within the eroded soil (the percentage of coarse particles larger than 0.075 mm in eroded soil ranges from 22 to 35%), which are the main elements of the soil structure (Figure 5-2). This results from the fact that during soil erosion, not only the fine particles but also the coarse particles flowed out, resulting in suffosion, in which the soil structure collapsed and the volume decreased.

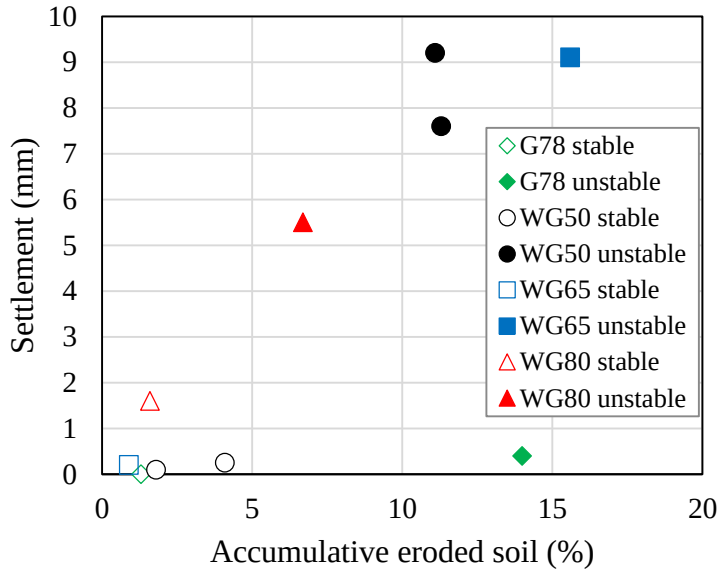

Figure 5-20 Accumulative eroded soil and settlement of test results

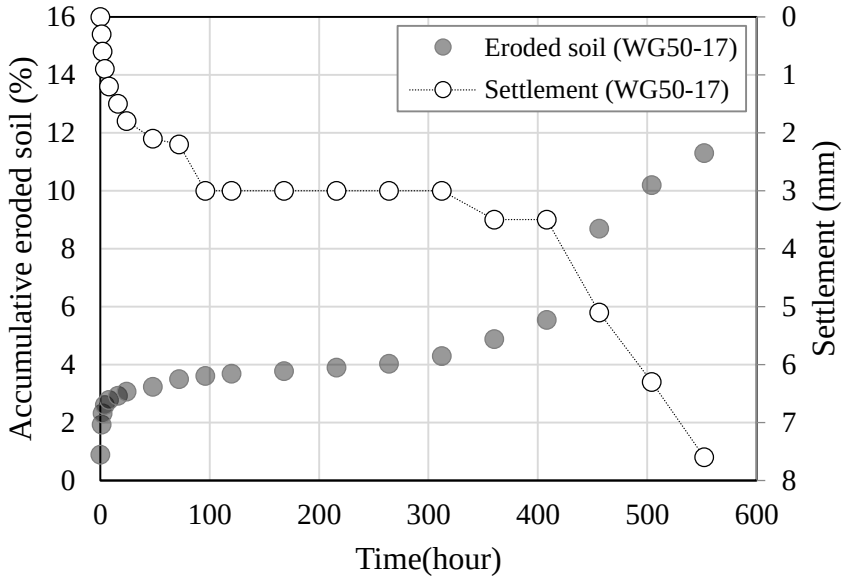

Figure 5-21 Accumulative eroded soil and settlement of WG soil (D_r= 50%) at a hydraulic gradient of 17

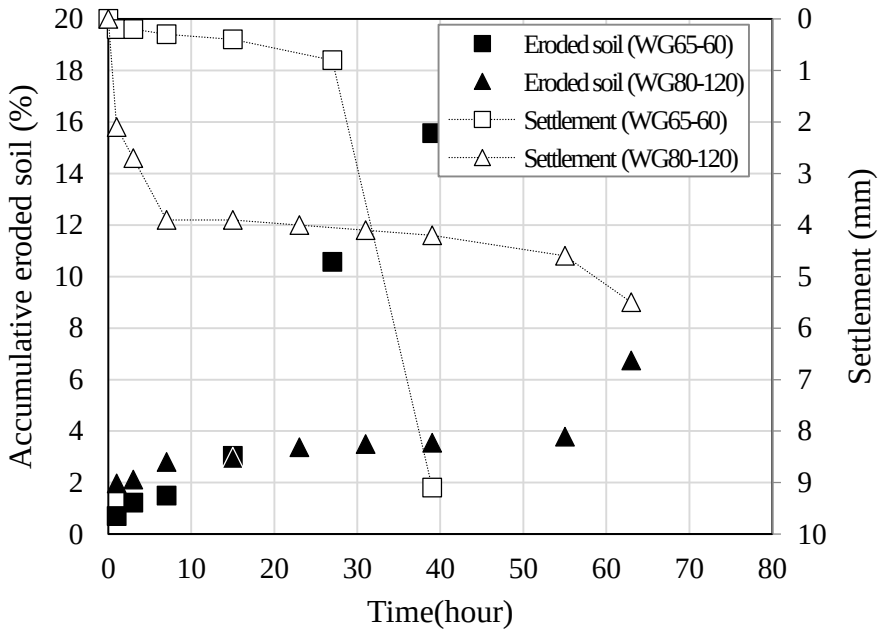

Figure 5-22 Accumulative eroded soil and settlement of WG soil (D_r= 65%) at a hydraulic gradient of 60 and WG soil (D_r= 80%) at a hydraulic gradient of 120

For internally unstable test results, the variation in *e* was calculated based on the volume change owing to the observed settlement and amount of eroded soil. For WG soil (D_r= 50%) at a hydraulic gradient of 17 and WG soil (D_r= 65%) at a hydraulic gradient of 60, *e* increased by 0.05 and 0.11, respectively, despite the settlement, resulting in an increase in *k* indicating that the influence of the eroded soil was more dominant (Figure 5-23 and Figure 5-24). However, in the case of WG soil (D_r= 80%) at a hydraulic gradient of 120, although 6.7% of the soil was discharged, a relatively higher settlement occurred, leading to an increase in *e* only by 0.01 (Figure 5-25).

In gap-graded soils, as fine particles can easily move through the constrictions between the coarse particles supporting the soil structure, suffusion can occur without changing the overall volume of the soil. However, in WG soils, fine particles may transfer the inter-particle effective stress. Therefore, when the fine particles are eroded by the seepage force, the structure of the soil collapses, inducing the migration of coarse particles, resulting in settlement. Moreover, as the relative density of WG soil increases, the finer particles are under higher effective stress, which will require a higher hydraulic gradient to cause internal instability. When the hydraulic gradient is high, the coarse particles can be rearranged and redeposited (Reddi et al., 2000b), resulting in great settlement. Consequently, when internal instability occurs within the soil, the higher the relative density, the greater the development of settlement.

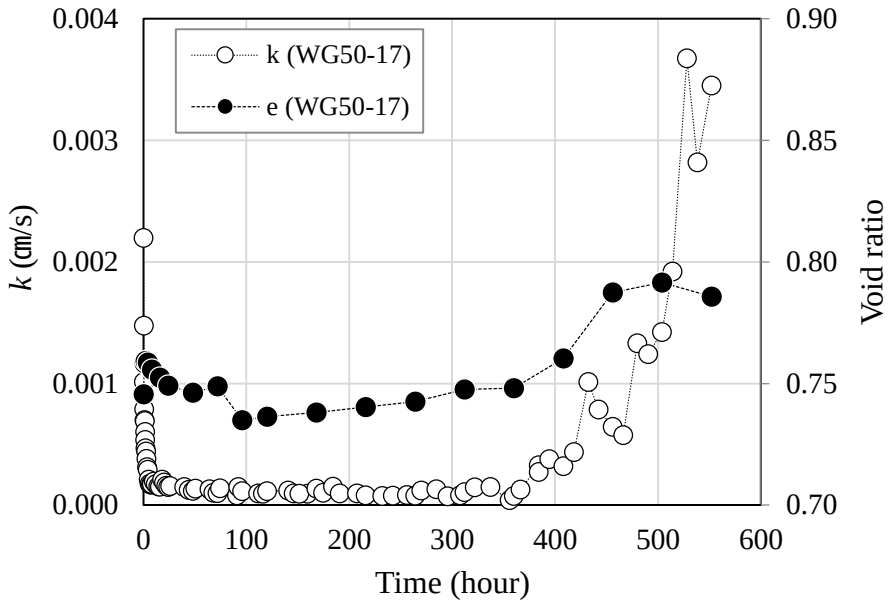

Figure 5-23 k and e of WG soil (D_r= 50%) at a hydraulic gradient of 17

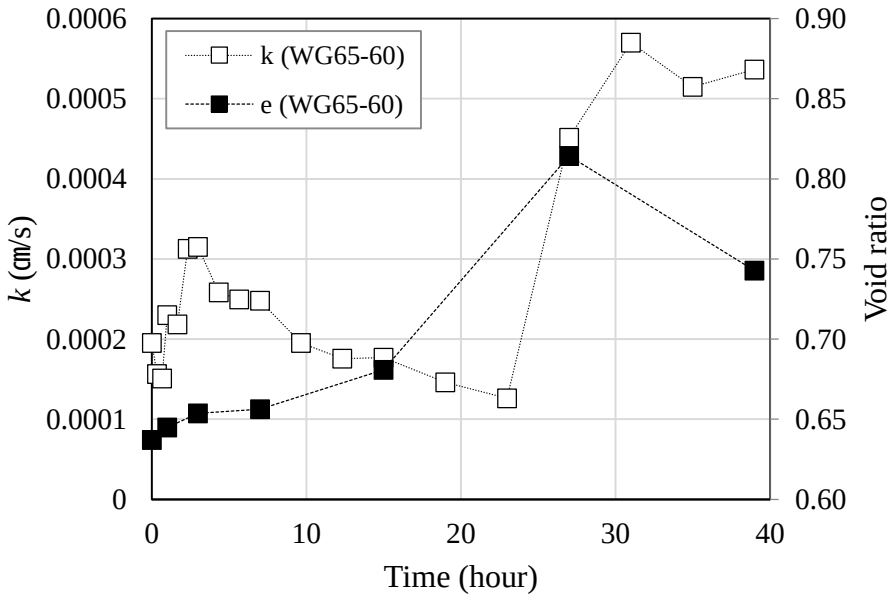

Figure 5-24 k and e of WG soil (D_r= 65%) at a hydraulic gradient of 60

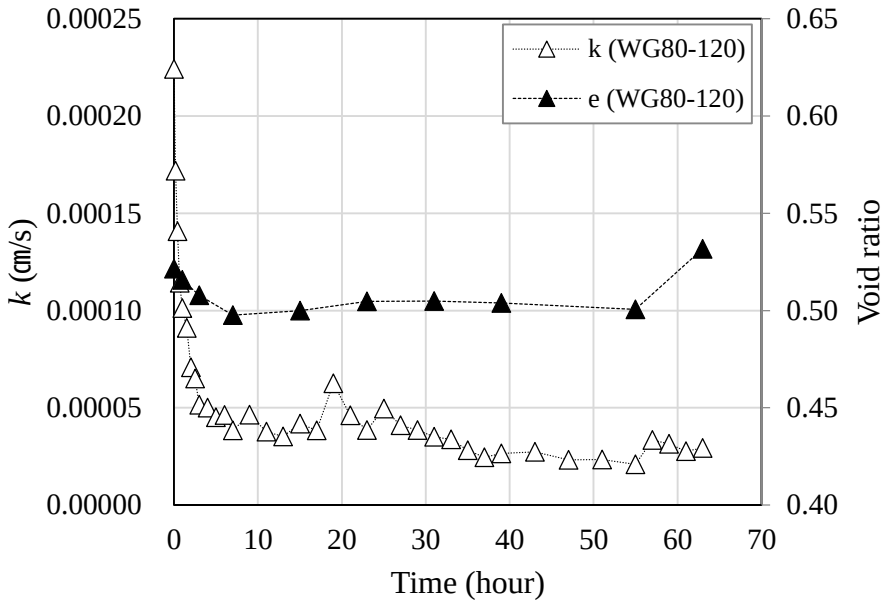

Figure 5-25 k and e of WG soil (D_r= 80%) at a hydraulic gradient of 120

5.5 Mechanism of internal instability

In the case of Gap soil, when the water flows, the fine particles move simultaneously from the top, the middle and the bottom and flow out even in the internally stable condition. The erosion of fine particles progressively increases D10 and *e*, resulting in an increase in *k*. In the internally unstable condition, most of the fine particles flow out and k increases significantly. Additionally, as the coarse particles that forms the structure of soil do not move, the overall volume of the soil does not change (Figure 5-26).

However, in the WG soil, different mechanism and progression of internal instability have been observed than those in the Gap soil. Based on the test results and analysis, the mechanism of internal instability and its progress in WG soil can be summarized as follows. The steps of internal instability were numbered in sequence and comprehensively compared with the test results (Figure 5-27).

At the beginning of the tests, some fine particles flowed out from the bottom part of the specimen, mainly due to gravity (Step 1). As a result, *k* exhibited small fluctuations within the range of less than k_0 (Figure 5-9 Figure 5-11). When the fine particles start to move due to the seepage force, some fine particles are clogged, resulting in a reduction in *k*, and some fine particles are discharged (Step 2). Consequently, *k* and amount of eroded soil gradually decreased, reaching the internally stable state (Figure 5-28). During this step, no significant settlement developed, and internal stability was maintained (Figure 5-20).

When sufficient seepage force was accumulated or a higher seepage force was applied, the clogging was removed, and the fine particles clogged at the bottom part of the specimen started to flow out together with the coarse particles (Step 3). As the effect of selective erosion of fines is more dominant during this process, D10, *e*, and *k* tend to increase (Figure 5-13 and Figure 5-14). In addition, because not only the fine particles but also the coarse particles flowed out, the soil structure collapsed and settlement occurred (Figure 5-20), leading to soil structure rearrangement (Step 4). Therefore, the internal instability of WG soil proceeds in the form of suffosion accompanied by changes in *k* and settlement (Figure 5-28).

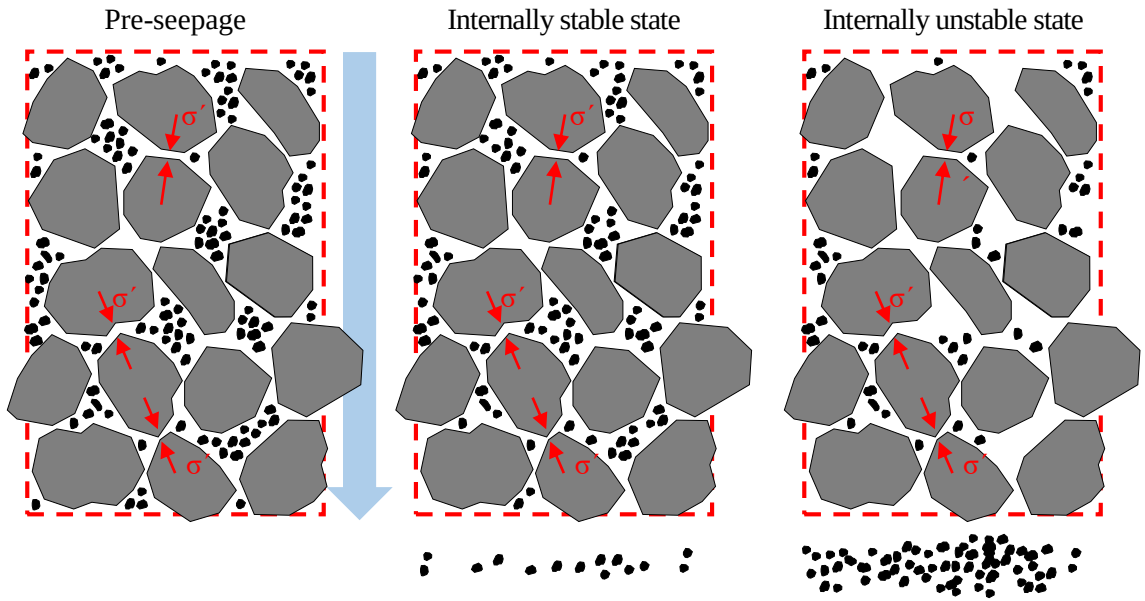

Figure 5-26 Schematic diagram of the progression of internal instability in Gap soil

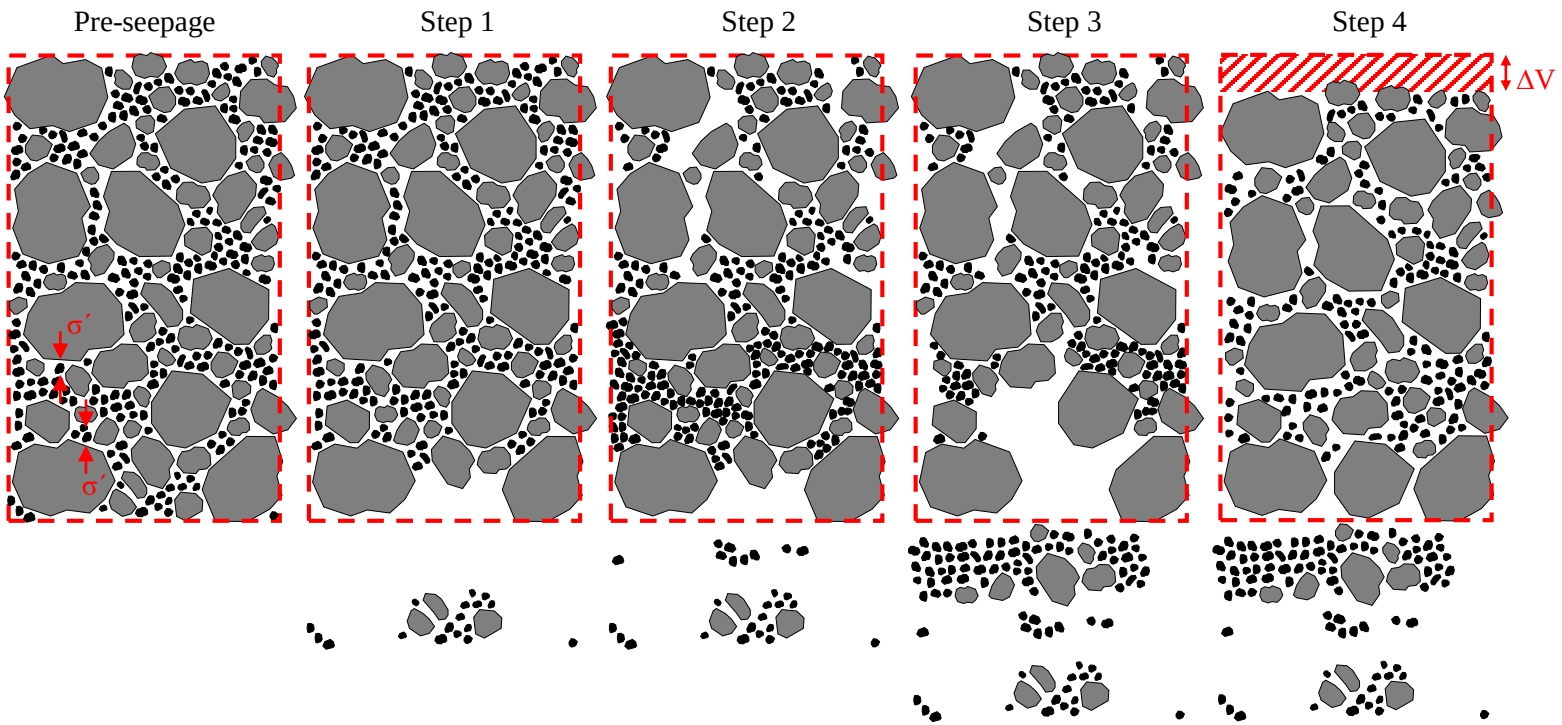

Figure 5-27 Schematic diagram of the progression of internal instability in WG soil

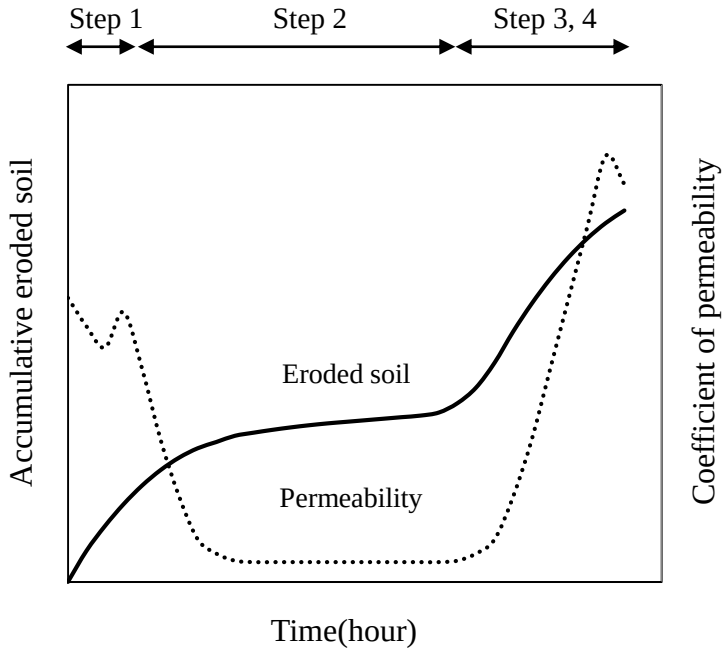

Figure 5-28 Schematic of internal instability behavior in WG soil

5.6 Summary

In the previous short-term test results in chapter 4, it has been proposed that the characteristics of the internal instability and development process of WG soil were different from those of the Gap soil. Therefore, in this chapter, long-term suffusion tests were conducted with various relative densities and constant hydraulic gradients to analyze the progress and cause of the internal instability of WG soil. Based on the test results, the specific findings of this study are summarized as follows:

1) In this research, long-term suffusion tests were conducted on Gap and WG soils under a hydraulic gradient relatively lower than the critical value determined in short-term tests. The results of long-term tests suggest that soil can be internally unstable at a lower hydraulic gradient. Furthermore, the lower the applied hydraulic gradient, the more time it took to reach the internal instability of the soils, and the Gap soil reached its internal instability faster at a lower hydraulic gradient than WG soil.
2) The higher the hydraulic gradient, the faster the erosion rate of the soil, owing to the greater seepage force acting on the soil. In addition, when the relative density of the WG soil increased, the amount of eroded soil decreased at the same hydraulic gradient. The fine particles in the WG soil may transfer inter-particle effective stress. Thus, the higher the relative density in the WG soils, the higher the effective stress that can

be applied to the fine particles, resulting in improved resistance to internal erosion.

3) The Gap soil showed clear manifestations of suffusion in both of internally stable condition and internally unstable condition. For the Gap soil, the constriction size of the coarse particles is larger than the size of the fine particles. Thus, the fine particles are under a small effective stress and can be easily moved by the seepage force.

4) In the internally stable condition, the WG soil showed a reduction in k and convergence to a constant value despite soil erosion. Based on the particle size distribution analysis, the fine particles in the top and middle parts moved downward and clogged in the bottom part of the specimen. Once the fine particles were clogged in the bottom part, D10 and e decreased, resulting in a reduction in the overall permeability. The flow rate decreased due to the decrease in k, and consequently, the amount of migration of fine particles and the amount of clogging decrease; thus, k converges.

5) WG soil, which was evaluated to be internally unstable, showed a reduction in k and erosion rate until the accumulative eroded soil reached approximately 4%. However, when the amount of accumulative eroded soil reached 4% or more, k and the erosion rate of soil increased rapidly with a reduction in the FS content in all parts of the specimen. From the test results, it can be concluded that D10 and e increase as clogging is released and fine particles are discharged, resulting in an increase in k.

6) In the case of the Gap soil, no noticeable settlement occurred during the test. However, in the internally unstable test results of WG soil, the settlement increased as the amount of eroded soil increased. The erosion of fine particles results in the collapse of the soil structure and migration of coarse particles, which leads to internal instability in the form of suffosion with a settlement. When internal instability occurs at low relative densities, k significantly increases because the effect of the selective erosion of fine particles is more dominant than that of the settlement. However, as the relative density of the soil increased, the effect of settlement increased, resulting in no significant change in k.
7) Based on the test results and analysis, the mechanism of internal instability and its progress in well-graded soils were proposed. In WG soil, internal instability proceeds in the form of suffosion accompanied by changes in k and settlement. This is a distinct difference from the suffusion mechanism commonly discovered in gap-graded soils.

Chapter 6. Test results with pore pressure transducer

6.1 Introduction

In the chapter 5, the mechanism of internal instability and its progress in well-graded soils were proposed. As shown in the long-term test results, D10 and *e* increased at the top and middle parts due to the migration of the fine particles, leading to a higher *k* and a lower hydraulic gradient. Meanwhile, in the bottom part, a reduction in *k* and an increase in hydraulic gradient were shown because the clogging of the fine particles reduced D10 and *e*. Therefore, when the fine particles are clogged in the bottom part, the pore water pressure in the bottom part will increase, and when the fine particles flow out, the pore water pressure will decrease. Moffat and Fannin (2006) and Moffat et al. (2011) also reported that the onset of internal instability was able to be detected by measuring water pressure along the length of the specimen. According to the previous studies, a suffusion test apparatus with pore pressure transducer was developed to verify the mechanism of the progress of internal instability in well-graded soil.

The tests were conducted for 30 and 60 minutes at a hydraulic gradient of 20 to obtain internally stable result and internally unstable result, respectively. The specimen was divided into four parts, a pore pressure transducer was installed, and the overall permeability and the pore pressure of each part were measured.

Then, the movement path of fine particles was analyzed by calculating the coefficient of permeability at each part using the pore pressure and overall permeability. In section 2, the permeability and the pore pressure of each part were presented over time. In section 3, based on the test results and analysis, the mechanism and progression of internal instability in well-graded soil were verified.

6.2 Hydraulic conductivity and pore water pressure

The height of the specimen was 100 mm, and pore water pressure transducers were installed at intervals of 25 mm. The pore water pressure transducers were numbered from the top to the bottom, and each division was identified according to the numbers and color of those (Figure 6-1). The differential pore water pressures acting on each parts were obtained from the measure pore water pressure. And, the differential total head (Δh) of each part can be calculated according to Bernoulli's equation (Eq. 6-1).

$$\Delta h = \mathrm{z} + \frac{\Delta u}{\gamma_w} \tag{6-1}$$

Where z, u, and γ_w is thickness of layer, pore water pressure, and unit weight of water, respectively. The coefficient of permeability of each part and the overall k were calculated using the differential head of each part and the flow rate.

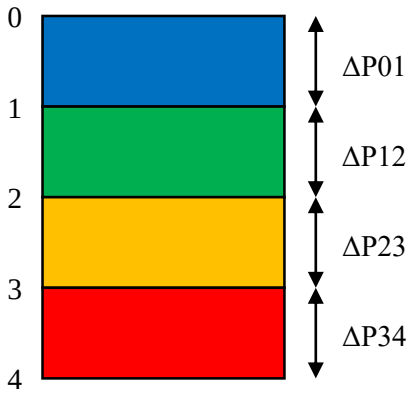

Figure 6-1 Schematic design of specimen and pore pressure transducer

6.2.1 Internally unstable result

Figure 6-2 shows the overall *k* and differential pore water pressure of each part at a relative density of 50% and a hydraulic gradient of 20 for 65 minutes. The overall *k* decreased for 40 minutes. At 45 minutes of experimental time, however, the overall *k* increased rapidly and then exhibited fluctuations within the range of more than initial *k*. The soil eroded quickly with the increase of the overall *k*, resulting in erosion of 3.9% of the total weight of the specimen.

When the overall *k* decreased, the differential pore water pressure in upper part (ΔP01 and ΔP12) did not demonstrate any significant changes and ΔP23 decreased, while the differential pore water pressure in the bottom (ΔP34) tended to increase. On the contrary, when the overall *k* rapidly increased, ΔP23 sharply increased, while ΔP34 abruptly decreased.

The fine particles in the top and middle moved downward and clogged in the bottom, resulting in increase of *k* at the top and middle and decrease of *k* at the

bottom. However, because the fine particles in the top moved rapidly, resulting in no head loss in the top (ΔP01 and ΔP12) from the beginning of the test, the reduction in the pore water pressure due to the movement of the fine particles at the top might not be evident.

The distributions of total head (h_T), elevation head (h_e), and pressure head (h_p) at the numbers shown in Figure 6-2 are demonstrated in Figure 6-3 and Figure 6-4. The *k* of each part was calculated using the differential head of each part overall permeability (Figure 6-5). When the overall *k* decreased, the *k* at the bottom (k34) decreased, while the *k* at other parts (k01, k12, k23) increased. And, the *k* gradually decreased toward the bottom. Afterwards, when the overall *k* increased, the *k* at the bottom (k34) sharply increased, resulting in the largest *k*, whereas the *k* at other parts decreased. In other words, the pattern of *k* at the bottom was similar to the overall *k*, and that at other parts showed the opposite tendency. The *k* at the bottom had a great influence on the overall *k*, and it was more evident in Figure 6-6, which showed normalized *k* over time.

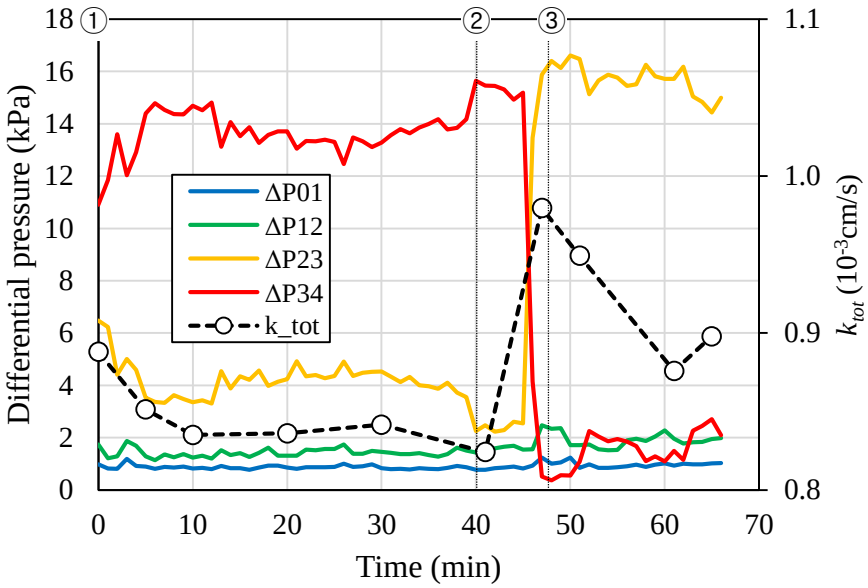

Figure 6-2 Overall k and differential pore water pressure in each part

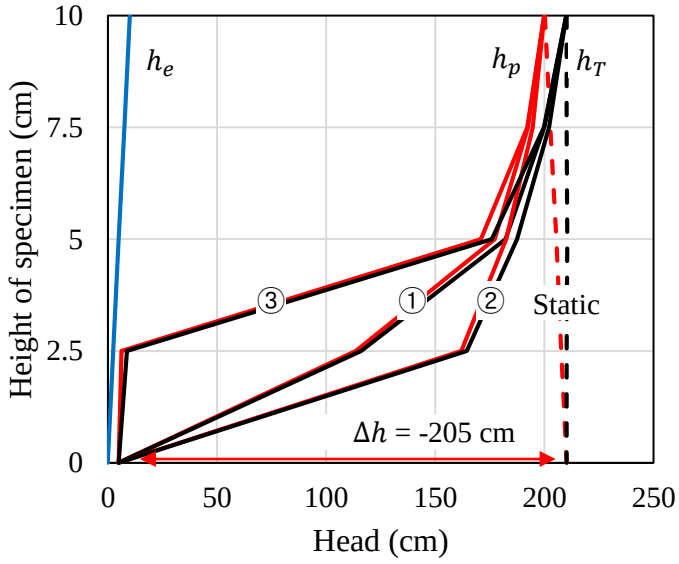

Figure 6-3 The distributions of total head (h_T), elevation head (h_e), and pressure head (h_p)

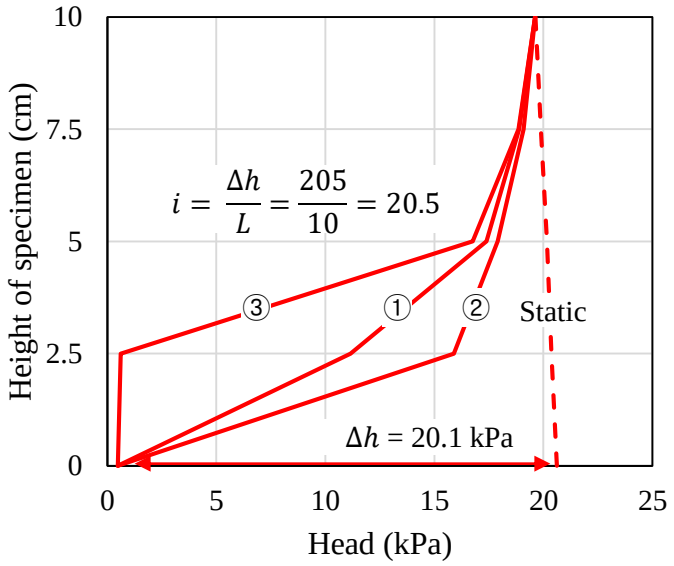

Figure 6-4 The distribution of pressure head

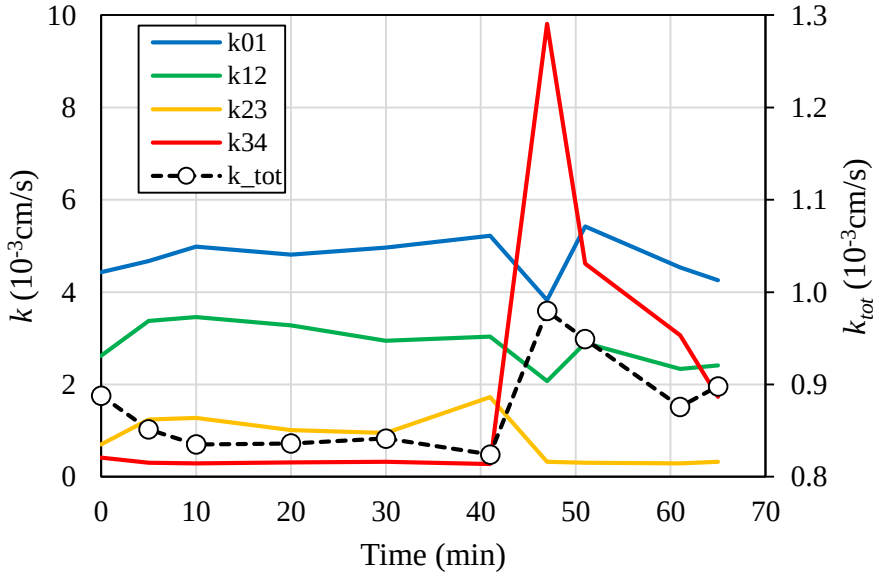

Figure 6-5 Overall *k* and *k* at each part

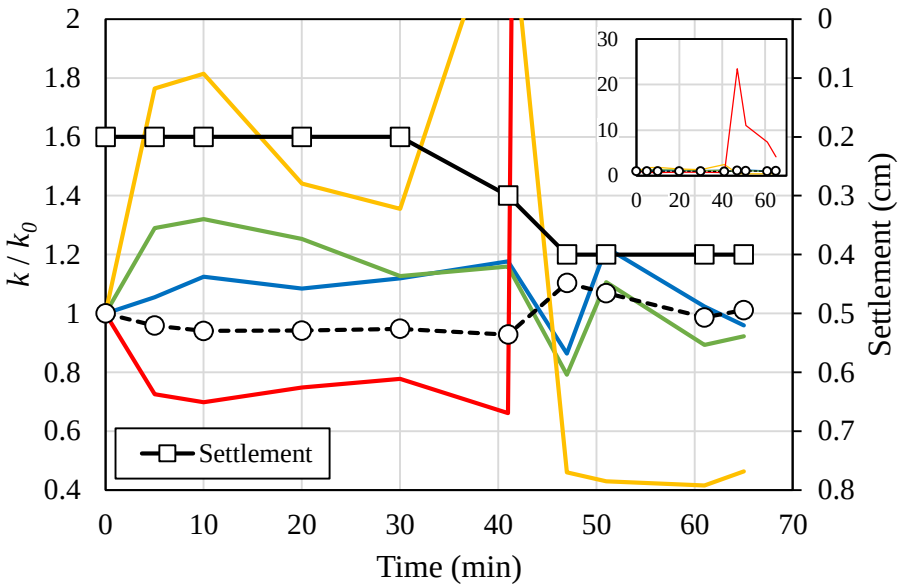

Figure 6-6 Normalized *k* and settlement

The particle size distribution analysis was performed by dividing the sample into four parts after the test to confirm the movement of fine particles. The FS content of each part was 37.1, 38.0, 37.0, and 35.3% in the 01 (top), 12, 23, and 34 (bottom) parts, respectively (Figure 6-7), indicating that fine particles were reduced in all parts when compared to the initial FS content (38.0%). The FS content in the bottom was the lowest, like the particle size distribution analysis result of internally unstable soil at a hydraulic gradient of 17 in Chapter 5.

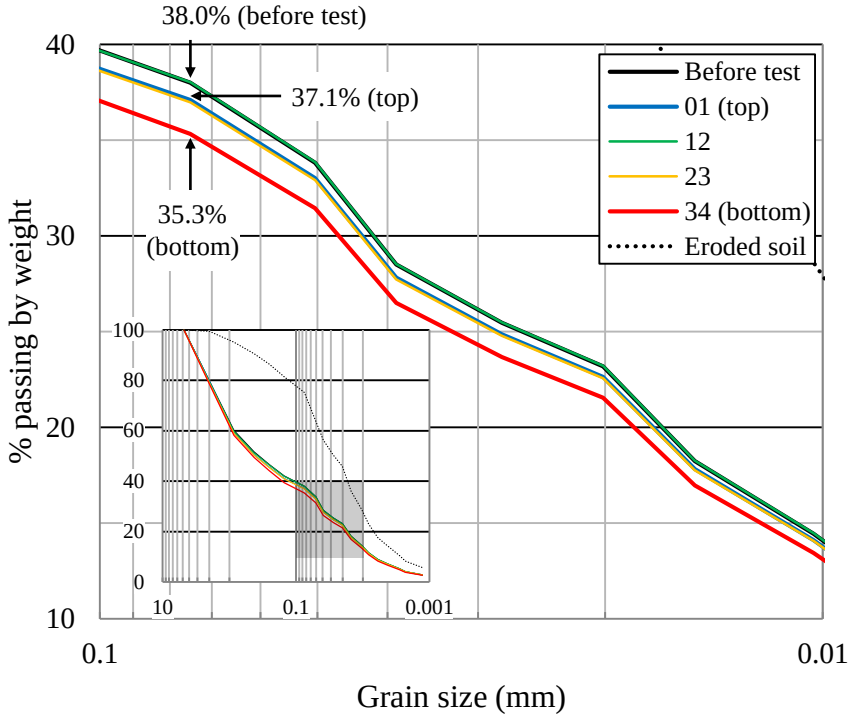

Figure 6-7 Particle size distribution of internally unstable result

6.2.2 Internally stable result

In order to investigate the specimen before onset of the internal instability, the test was conducted under the same conditions, a relative density of 50% and a hydraulic gradient of 20, and it was terminated after 30 minutes. The overall *k* and differential pore water pressure in each part were demonstrated in Figure 6-8. The overall *k* decreased during the test and the amount of eroded soil was

2.7% of total weight of specimen. At this time, the differential pore water pressure in the top (ΔP01) showed no significant change, while ΔP12 and ΔP23 decreased, and that of the bottom (ΔP34) increased. This result is quite similar to the previous test result.

The *k* in each part also showed a similar trend to the previous test result. When the overall *k* decreased, the *k* in bottom (k34) decreased, while the *k* in other parts (k01, k12, k23) increased (Figure 6-9 and Figure 6-10). Also, the *k* gradually decreased toward the bottom.

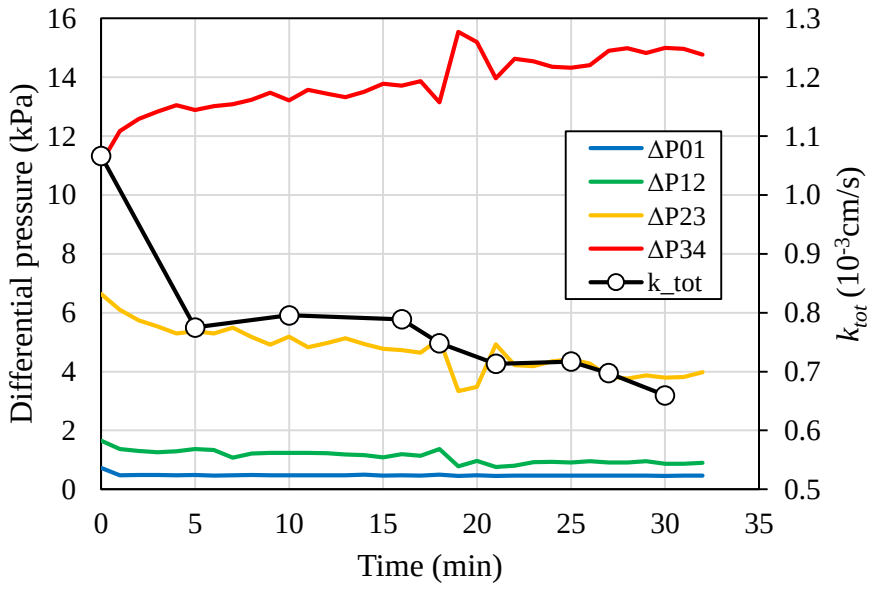

Figure 6-8 Overall *k* and differential pore water pressure in each part

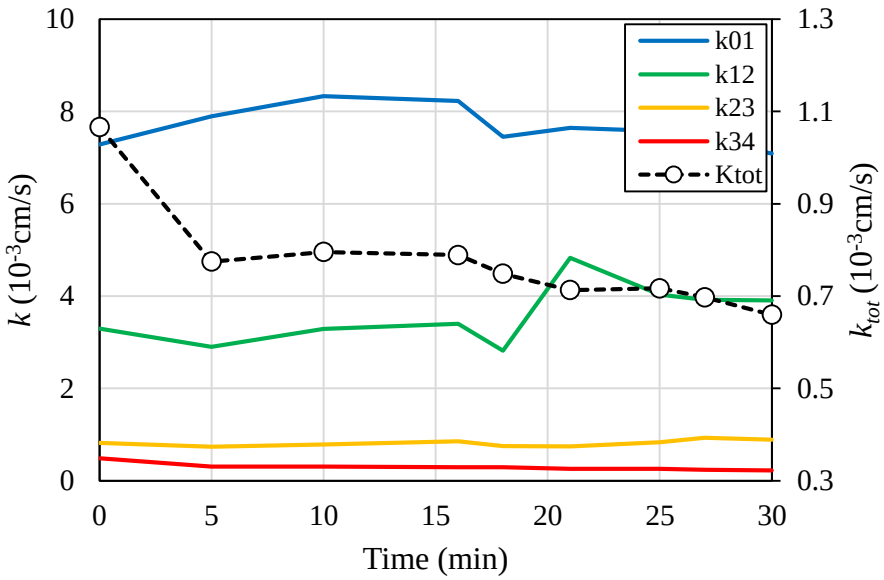

Figure 6-9 Overall *k* and *k* at each part

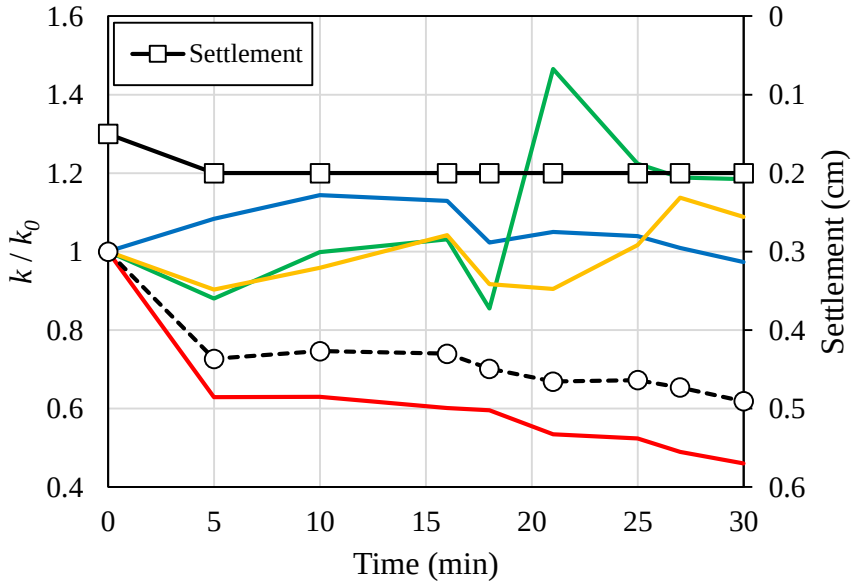

Figure 6-10 Normalized *k* and settlement

Particle size distribution analysis after the seepage experiment showed that the FS content of each part was 37.0, 38.0, 37.9, and 39.8% in the 01 (top), 12, 23, and 34 (bottom) parts, respectively (Figure 6-11). In contrast to the initial FS content (39.1%) of the soil, the FS content of the 01, 12, and 23 parts decreased, while that of the bottom increased, indicating that the fine particles in the top and middle moved downward and clogged in the bottom. This shows a similar trend to the particle size distribution analysis results of internally stable soil at a hydraulic gradient of 15 in Chapter 5.

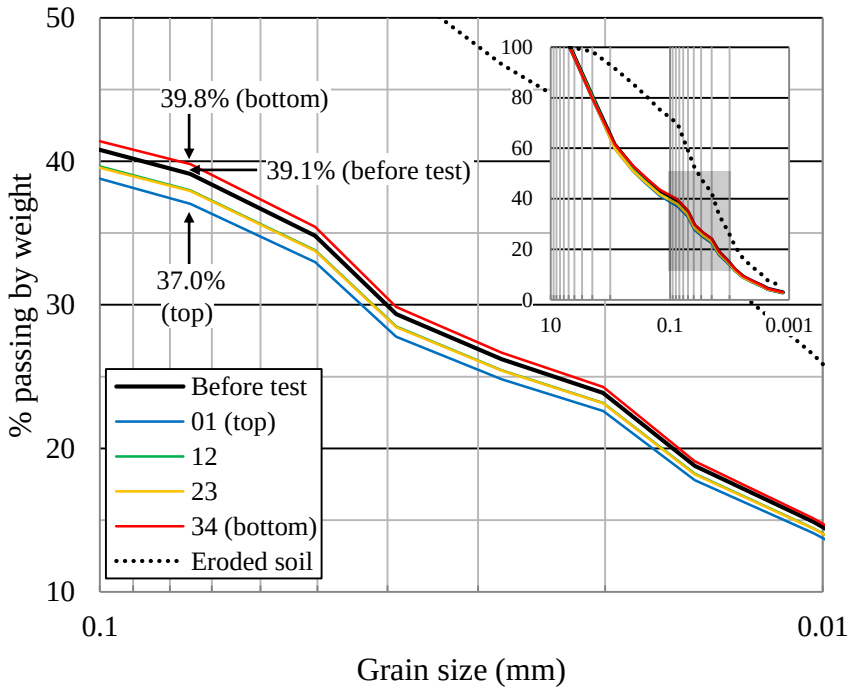

Figure 6-11 Particle size distribution of internally stable result

6.3 Verification of mechanism of internal instability in WG soil

As mentioned in Chapter 5, when water flowed downward through the soil, the fine particles in the top and middle moved downward and clogged in the bottom. Once the fine particles were clogged in the bottom part, D10 and *e* decreased, resulting in a reduction in *k* at the bottom, whereas it increased in the top and middle owing to the erosion of fine particles. Although the D10 and *e* of the entire specimen increased, the overall *k* decreased due to decrease in *k* at the bottom. Consequently, the pore water pressure in the bottom increased and that in the top and middle decreased (Figure 6-12 Step 2).

As the pore water pressure in the bottom increases, the seepage force acting on the soil in the bottom increases while the effective stress decreases. When sufficient seepage force was accumulated, the clogging was removed, and the fine particles clogged at the bottom of the specimen flowed out, resulting in the increase of *k* at the bottom and overall *k*. At the same time, a rapid decrease in pore water pressure at the bottom increased pore water pressure at the top and middle, resulting in the decrease of *k* at the top and middle. Therefore, the *k* at the top and middle decreased due to an increase in pore water pressure, not due to the movement of particles (Figure 6-12 Step 3).

In the test result, when the pore water pressure acting on the bottom was about 16 kPa, the erosion rate of soil and the permeability increased rapidly. The hydraulic gradient acting at this time was about 65, which is higher than the critical hydraulic gradient of 40 investigated in the short-term test, and it

can be enough to break clogging.

The clogging and breakage of it occurred locally and instantaneously. Therefore, the breakage of clogging and erosion of fine particles may result in an abrupt change in the k.

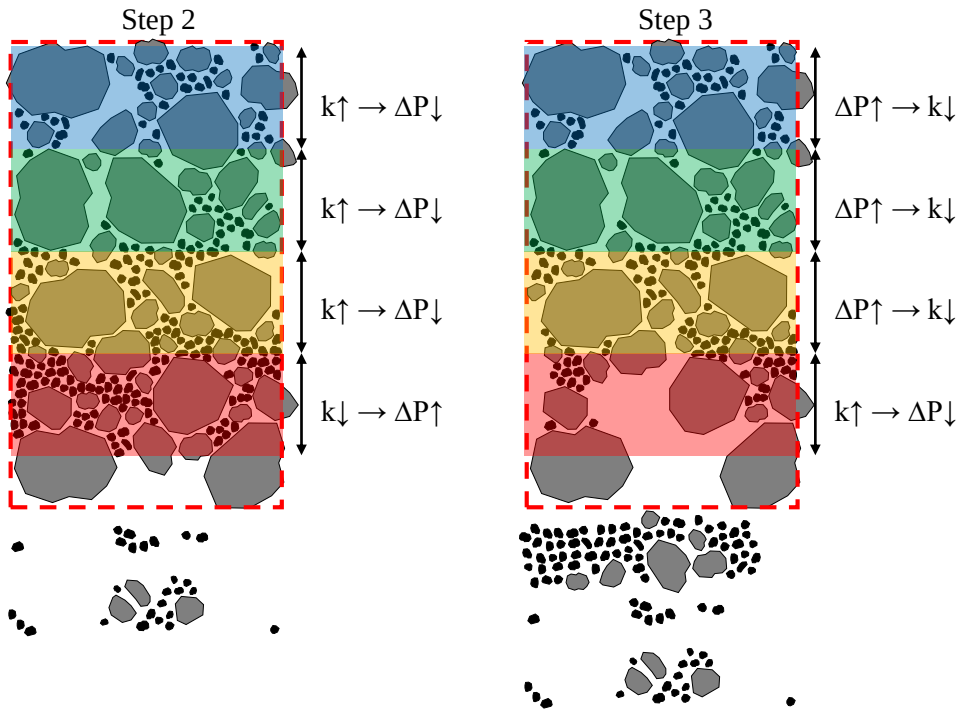

Figure 6-12 Schematic diagram of the progression of internal instability in WG soil

6.4 Summary

In the previous long-term test results in Chapter 5, the mechanism of internal instability and its progress in well-graded soils were proposed. In this Chapter, the tests were conducted to verify the mechanism using developed apparatus with pore water pressure transducer. Based on the test results, the specific findings of this study are summarized as follows:

1) The fine particles in the top and middle moved downward and clogged in the bottom, resulting in increase of k at the top and middle and decrease of k at the bottom. The overall k decreased due to decrease in k at the bottom. Consequently, the pore water pressure in the bottom increased and that in the top and middle decreased.
2) When sufficient seepage force was accumulated, the clogging was removed, and the fine particles clogged at the bottom of the specimen flowed out, resulting in the increase of k at the bottom and the decrease of pore water pressure.
3) The local hydraulic gradient breaking the clogging should be higher than the critical hydraulic gradient in the short-term test.
4) The breakage of clogging may result in an abrupt change in the k due to its local and instantaneous characteristic.

Chapter 7. Conclusions and Recommendations

7.1 Conclusions

This dissertation assessed the internal instability of well-graded soils, which have a particle size distribution that represents fill dam materials in South Korea, and investigated its mechanism and progression. Short- and long-term experiments were carried out on both gap-graded and well-graded soils at various relative densities and hydraulic gradients. For the experiment, a new suffusion test apparatus was designed, and can measure the amount of eroded soil and water without disassembly during the test. In the short-term tests, the internal instability of the soils was evaluated according to indicators of previous studies. Additionally, the occurrence and characteristics of internal instability of the well-graded soils were investigated. In the long-term tests, the internal instability over time was assessed, and its progress and causes were studied. Based on the test results, the mechanism of internal instability on well-graded soil was proposed. Then, seepage tests with pore pressure transducer verified the mechanism and progress of internal instability in well-graded soils. The main conclusions drawn from the experiments are summarized below.

Characteristic of internal instability

- The Gap soil showed clear manifestations of suffusion in both internally stable and unstable conditions of short- and long-term tests. The constriction size of the coarse particles is larger than the size of fine particles. Thus, the fine particles are subject to a small effective stress and can be easily moved by seepage force.
- In short-term test, the WG soil exhibited similar suffusion results to Gap soil, such as erosion of fine particles and increases in k and e. However, sudden increases in k and soil discharge occurred at the onset of internal instability, which followed the reduction in k, thereby exhibiting an internal erosion process that differ from that of Gap soil. Additionally, fine particles and coarse particles flowed out, resulting in settlement.
- In long-term tests, the WG soil in the internally stable condition showed a reduction in k and convergence to a constant value despite soil erosion. In addition, the WG soil, which was evaluated to be internally unstable, showed a reduction in k and erosion rate until the accumulative eroded soil reached approximately 4%. However, when the amount of accumulative eroded soil reached 4% or more, k and the erosion rate of soil increased rapidly.
- The breakage of clogging may result in an abrupt change in k due to its local and instantaneous characteristics.

Effects of hydraulic gradient and relative density

- As the hydraulic gradient increased, the erosion rate became faster, owing to the greater seepage force acting on the soil.
- The hydraulic gradient at which internal instability occurs was higher for WG soil than for Gap soil.
- The WG soil showed higher resistance to internal erosion when compacted to a greater relative density. An increase in the degree of compaction not only increased the critical hydraulic gradient, but also reduced the amount of eroded soil at the same hydraulic gradient. The fine particles in the WG soil may transfer inter-particle effective stress. Thus, as the relative density in the WG soils increased, the effective stress that could be applied to the fine particles also increased, resulting in improved resistance to internal erosion.

Hydraulic conductivity

- The Gap soil showed progressively increase in k with soil erosion in both of internally stable and unstable conditions.
- In the internally stable condition, the WG soil showed a reduction in k and convergence to a constant value despite soil erosion. Based on the particle size distribution analysis, the fine particles in the top and middle parts moved downward and clogged in the bottom part of the specimen. At this point, D10 and e decreased, resulting in a reduced overall

permeability. The flow rate also decreased due to the decrease in k, and consequently, the amounts of migration of fine particles and of clogging decreased; thus, k converged.

- WG soil, which was evaluated to be internally unstable, showed a reduction in k due to clogging. Then, D10 and e increased as clogging was released and fine particles were discharged, resulting in an increase in k.
- The seepage tests with pore pressure transducer verified that the fine particles in the top and middle parts moved downward and clogged in the bottom, resulting in increase of k at the top and middle and decrease of k at the bottom, which caused the reduced overall k.
- When the clogging was removed, and the fine particles clogged at the bottom of the specimen flowed out, the k at the bottom increased, resulting in the increase of overall k.

Settlement

- In the Gap soil, no noticeable settlement occurred during the test.
- In the internally unstable test results of WG soil, the settlement increased as the amount of eroded soil increased. The erosion of fine particles resulted in the collapse of the soil structure and migration of coarse particles, which led to internal instability in the form of suffosion with a settlement.
- When internal instability occurred at low relative densities, k

significantly increased because the effect of the selective erosion of fine particles was more dominant than that of the settlement. However, as the relative density of the soil increased, the effect of settlement also increased, resulting in no significant change in *k*.

Mechanism of internal instability

- Based on the test results and analysis, the mechanism of internal instability and its progress in well-graded soils were proposed. In WG soil, internal instability proceeded in the form of suffosion accompanied by changes in *k* and settlement. This mechanism showed a distinct difference from the suffusion that is commonly discovered in gap-graded soils.
- In the Gap soil, when the water flowed, the fine particles moved simultaneously from the top to the bottom and flow out. The erosion of fine particles progressively increased D10 and *e*, thereby *k* increased. In addition, as the coarse particles that forms the soil structure do not move, the overall volume of the soil did not change.
- In WG soil, at the beginning of the tests or at a low hydraulic gradient, some fine particles flowed out from the bottom part of the specimen, mainly due to gravity. When the fine particles started to move due to the seepage force, some fine particles in the top and middle moved downward and clogged in the bottom while other fine particles flowed out. The erosion of fine particles increased *k* at the top and middle.

However, the clogging of fine particles decreased k at the bottom, which reduced the overall k. Consequently, the pore water pressure in the bottom increased and those in the top and middle decreased.

- When sufficient seepage force accumulated due to the increase of pore water pressure in the bottom or due to applied higher seepage force, clogging is removed, and the fine particles clogged at the bottom part of the specimen flowed out together with the coarse particles. The increase of k at the bottom increased the overall k. In addition, because not only the fine particles but also the coarse particles flowed out, the soil structure collapsed and settlement occurred, leading to soil rearrangement.

Evaluation of internal instability

- The tests using different identification methods (fraction loss of soils and change in k) showed inconsistent results. Therefore, considering both the fraction loss of soils and the change in k was more appropriate for evaluating the internal stability of well-graded soils.
- In this study, long-term suffusion tests were carried out on Gap and WG soils under a hydraulic gradient that is relatively lower than the critical value determined in short-term tests. The results of long-term tests showed that soil can be internally unstable at a lower hydraulic gradient.
- When the local hydraulic gradient was higher than the critical

hydraulic gradient in the short-term test, the clogging could be broken.

- Furthermore, the lower the applied hydraulic gradient, the more time was needed to reach the internal instability of the soils. The Gap soil reached its internal instability faster at a lower hydraulic gradient than WG soil.

Application

- The short-term tests were conducted while gradually increasing the hydraulic gradient, and the long-term tests were performed at constant hydraulic gradients. Therefore, in the short-term test, the specimen experienced relatively lower hydraulic gradient than the target amount, and in the long-term test, the specimen was subjected to the target hydraulic gradient at the initiation of the test. No significant difference was observed at a relatively low hydraulic gradient. However, as the hydraulic gradient increased, the amount of eroded soil during the same period of time was greater in the latter (long-term test) than the former (short-term test). Gradual increases in hydraulic gradient could stabilize soils at low hydraulic gradient, resulting in high resistance to internal instability. Therefore, after the construction of the dam, the rapid rise of water level must be avoided when the water is stored.
- The movement path of fine particles and onset of internal instability were detected by measuring pore water pressure. In well-graded soils, internal instability started near the filter material. Therefore, internal

instability can be investigated in advance by monitoring the pore water pressure.

7.2 Recommendations for further researches

The experimental studies presented in this dissertation contribute to the understanding of the characteristics and development of internal instability in well-graded soils. The findings can be used as important data to deepen the understanding of development of internal instability in well-graded soils. Additionally, the test confirms that the movement path of fine particles and onset of internal instability can be detected by measuring pore water pressure. However, in this study, given that the applied hydraulic gradients are higher than in field condition, to predict the potential of internal instability in hydraulic earth structures remains difficult. Extending the prediction of internal instability requires further researches on the following topics:

- Whether internal instability can occur under the hydraulic gradient applying in field condition needs to be confirmed and predicted. Investigation of the change in pore water pressure with time and the pore water pressure that initiates the internal instability will make those possible.
- Research on the amount of eroded soil, strength of soil, and strain (settlement) is also needed. In this study, k rapidly increased and significant settlement occurred at 4% of accumulative eroded soil. Thus, the possible causes of such scenarios merit exploration.

List of References

ASTM (2016a) Standard test methods for maximum index density and unit weight of soils using a vibratory table. D4253−16, West Conshohocken, PA

ASTM (2016b) Standard test methods for minimum index density and unit weight of soils and calculation of relative density. D4254−16, West Conshohocken, PA

Bendahmane F, Marot D, Alexis A (2008) Experimental parametric study of suffusion and backward erosion. J. Geotech. Geoenviron. Eng. 134(1):57–67. https://doi.org/10.1061/(ASCE)1090-0241(2008)134:1(57)

Burenkova VV (1993) Assessment of suffosion in non-cohesive and graded soils. In: Proceedings of Filters in Geotechnical and Hydraulic Engineering. Karlsruhe, Germany.

Chang DS, Zhang LM (2013a) Critical hydraulic gradients of internal erosion under complex stress states. J. Geotech. Geoenviron. Eng. 139(9):1454–1467. https://doi.org/10.1061/(ASCE)GT.1943-5606.0000871

Chang DS, Zhang LM, (2013b) Extended internal stability criteria for soils under seepage. Soils Found. 53(4):569–583. https://doi.org/10.1016/j.sandf.2013.06.008

Chapuis RP (2015) Predicting the saturated hydraulic conductivity of soils: a review. Bulletin of Engineering Geology and the Environment. 71:401-434.

Chung C, Lee H, Kwak T, Apparatus and method for suffusion test. Patent number 10-1855633, South Korea.

Farzalizadeh R, Hasheminezhad A, Bahadori H (2021) Shaking table tests on wall-type gravel and rubber drains as a liquefaction countermeasure in silty sand. Geotext. Geomembr. https://doi.org/10.1016/j.geotexmem.2021.06.002

Fell R, Wan CF, Cyganiewicz J, Foster M (2003) Time for development of internal erosion and piping in embankment dams. J. Geotech. Geoenviron. Eng. 129(4), https://doi.org/10.1061/(ASCE)1090-0241(2003)129:4(307)

Fell R, MacGregor P, Stapledon D, Bell G, Foster M (2015) Geotechnical Engineering of Dams, 2nd edition. Taylor & Francis Group, London, UK

Foster M, Fell R, Spannagle M (2000) The statistics of embankment dam failures and accidents. Can. Geotech. J. 37:1000–1024. https://doi.org/10.1139/t00-030

Ghadr S, Samadzadeh A, Bahadori H, Assadi-Langroudi A (2020) Liquefaction resistance of fibre-reinforced silty sands under cyclic loading. Geotext. Geomembr. 48(6):812-827, https://doi.org/10.1016/j.geotexmem.2020.07.002

ICOLD (2017) Internal erosion of existing dams, levees and dikes, and their foundations. International Commission on Large Dams, Paris, France

Istomina VS (1957) Filtration Stability of Soils. Gostroizdat, Moscow, Russia.

Israr J, Indraratna B (2019) Study of critical hydraulic gradients for seepage-induced failures in granular soils. J. Geotech. Geoenviron. Eng. 145(7) 04019025. https://doi.org/10.1061/(ASCE)GT.1943-5606.0002062

Israr J, Zhang G (2021) Geometrical assessment of internal instability potential of granular soils based on grading entropy. Acta Geotech. 16:1961-1970, https://doi.org/10.1007/s11440-020-01118-0

Kaoser S, Barrington S, Elektorowicz M, Ayadat T (2006) The influence of hydraulic gradient and rate of erosion on hydraulic conductivity of sand-bentonite mixtures. Soil. Sediment. Contam. 15:481-496, https://doi.org/10.1080/15320380600847815

Ke L, Takahashi A (2014) Experimental investigations on suffusion characteristics and its mechanical consequences on saturated cohesionless soil. Soils Found. 54(4):713–730. https://doi.org/10.1016/j.sandf.2014.06.024

Kenney TC, Chahal R, Chiu E, Ofoegbu GI, Omange GN, Ume CA (1985) Controlling constriction sizes of granular filters. Can. Geotech. J. 22(1):32–43. https://cdnsciencepub.com/doi/10.1139/t85-005

Kenney TC, Lau D (1985) Internal stability of granular filters. Can. Geotech. J. 22(2):215–225. https://cdnsciencepub.com/doi/10.1139/t85-029

Kezdi A (1979) Soil physics. Elsevier, Budapest, Hungary.

Kim I (2019) Suffusion sensitivity of earth-fill dam soils in Korea through seepage tests.

MSc Thesis, Seoul National Univ. Seoul, Korea

Li M (2008) Seepage induced instability in widely graded soils. Ph.D. Thesis, The University of British Columbia, Vancouver, Canada

Liu J (2005) Seepage control of earth-rock dams: theoretical basis, engineering experiences and lessons. China Waterpower Press, Beijing, China

Liu K, Qiu R, Su Q, Ni P, Liu B, Gao J, Wang T (2021) Suffusion response of well graded gravels in roadbed of non-ballasted high speed railway. Constr. Build. Mater. 284:122848. https://doi.org/10.1016/j.conbuildmat.2021.122848.

Locke MR (2001) Analytical and laboratory modelling of granular filters for embankment dams. PhD Thesis, Univ. Wollongong Wollongong, Australia

Luo Y, Qiao L, Liu X, Zhan M, Sheng J (2013) Hydro-mechanical experiments on suffusion under long-term large hydraulic heads. Nat. Hazards. 65:1361–1377. https://doi.org/10.1007/s11069-012-0415-y

Moffat RA, Fannin RJ (2006) A Large permeameter for study of internal stability in cohesionless soils. Geotech. Test. J. 29 (4). https://doi.org/10.1520/GTJ100021

Moffat R, Fannin RJ, Garner SJ (2011) Spatial and temporal progression of internal erosion in cohesionless soil. Can. Geotech. J. 48(3):399–412. https://cdnsciencepub.com/doi/10.1139/T10-071

NDMR (2013) Report on the Sandae Embankment Dam Failure in Gyeongju. National Disaster Management Research Institute, Ulsan, Korea

Reclamation and USACE (2019) Best Practices in Dam and Levee Safety Risk Analysis. United States Department of the Interior, Bureau of Reclamation and U.S. Army Corps of Engineers, Washington District of Columbia, USA

Reddi LN, Ming X, Hajra MG, Lee IM (2000a) Permeability reduction of soil filters due to physical clogging. J. Geotech. Geoenviron. Eng. 126(3):236–246, https://doi.org/10.1061/(ASCE)1090-0241(2000)126:3(236)

Reddi LN, Lee I, Bonala MV (2000b) Comparison of internal and surface erosion using flow pump tests on a sand-kaolinite mixture. Geotech. Test. J. 23(1):116–122. https://doi.org/10.1520/GTJ11129J

Skempton AW, Brogan JM (1994) Experiments on piping in sandy gravels. Géotechnique 44(3):449–460. https://doi.org/10.1680/geot.1994.44.3.449

Sterpi D (2003) Effects of the erosion and transport of fine particles due to seepage flow. Int. J. Geomech. 3(1):111-122. https://doi.org/10.1061/(ASCE)1532-3641(2003)3:1(111)

Sun BC (1989) Internal stability of clayey to silty sands. PhD Thesis, University of Michigan, Ann Arbor, USA

Taylor H (2016) Assessing the potential for suffusion in sands using x-ray micro-CT images. PhD Thesis, Imperial College London, London, United Kingdom

Terzaghi K (1922) Failuare of dam foundations by piping and means for preventing it (in German), Die Wasserkraft, Special Forchheimer Issue, 17, pp. 445-449

Terzaghi, K. (1939) Soil mechanics: a new chapter in engineering science. J. Instn. Civ. Engrs, 12: 106-141.

Terzaghi, K., Peck, R.B. and Mesri, G. (1996) Soil mechanics in engineering practice, 3rd edition, NY: John Wiley and Sons, New York.

USACE (1953) Filter Experiments and Design Criteria. U.S. Army Engineer Waterways Experiment Station Corps of Engineers, Vicksburg, USA

Vaughan, P.R., 1994. Criteria for the use of Weak and Weathered Rock for Embankment Fill and its Compaction Control. In: 13th ICSMFE. New Delhi, India.

Wan CF (2006) Experimental investigation of piping erosion and suffusion of soils in embankment dams and their foundations. Ph.D. Thesis, The University of New South Wales, Sydney, Australia

Wan CF, Fell R (2008) Assessing the potential of internal instability and suffusion in embankment dams and their foundations. J. Geotech. Geoenviron. Eng. 134(3):401–407. https://doi.org/10.1061/(ASCE)1090-0241(2008)134:3(401)

초 록

내부 침식은 성토댐의 안정성에 영향을 미치는 중요한 원인 중 하나이며, 내부불안정성으로 알려진 suffusion과 suffosion은 내부 침식의 한 형태이다. Suffusion은 부피 변화없이 침투압에 의해서 세립질이 조립질 사이를 이동하여, 선택적으로 침식되는 것으로 정의하고, Suffosion은 suffusion과 같은 메커니즘으로 발생한, 부피변화를 동반한다고 정의하고 있다. 내부불안정성이 발생하면 세립질이 유출되어 간극비가 증가하고, 이로 인해 투수계수가 증가하며, 흙의 전단강도가 감소할 수 있다. 또한, 후방침식, 침하, 사면붕괴의 원인이 될 수도 있다고 알려져 있다.

Gap-graded soil은 양극화된 세립질과 조립질로 이루어진 흙으로, 일반적으로 내부불안정성에 취약하며, 세립질의 유출과 투수계수, 간극비의 증가와 같은 명확한 내부불안정성을 보인다. 따라서, 주로 gap-graded soil을 이용하여 내부불안정성에 대한 연구를 수행하였다. 그러나 국내 흙댐 제체재료와 같이 여러가지 입도분포가 혼합되어 있는 well-graded soil에 대한 연구는 제한적으로 수행되었으며, 내부불안정성 발생 여부 및 형태, 원인에 대한 분석이 부족한 실정이다.

따라서, 본 논문에서는 새로 개발한 내부불안정성 실험 장치를 이용하여, gap-graded soil과 well-graded soil에 대하여 다양한 상대밀도와 동수경사에서 침투실험을 실시하였다. 단기실험에서는 동수경사를 단계적으로 증가시키며 실험을 수행하고, 흙의 유출량과 투수계수를 기준으로 내부불안정성의 발생을 분석하였다. 실험 결과, well-

graded soil은 gap-graded soil과는 달리 내부불안정성이 시작되기 전에 투수계수가 감소하다 내부불안정성이 시작될 때 급격하게 투수계수와 흙의 유출속도가 증가하는 경향을 보였다. 또한, 상대밀도가 증가할수록 내부불안정성이 발생하는 동수경사가 증가하였다.

장기실험은 내부불안정성의 진행과정과 원인을 분석하기 위하여 동수경사를 일정하게 유지하면서 수행하였다. 내부적으로 안정한 조건에서 well-graded soil은 하부에 세립분들이 막히면서 전체 투수계수를 감소시켰고, 내부적으로 불안정한 조건에서는 투수계수가 감소하다가 흙의 유출량과 투수계수가 갑자기 증가하는 경향을 보였다. 또한, 조립질과 세립질이 같이 유출되며 침하가 발생하는 suffosion의 형태로 내부불안정성이 진행되었다. 실험결과를 바탕으로 well-graded soil의 내부불안정성의 진행 메커니즘을 제안하였다.

제안된 내부불안정성 메커니즘을 검증하기 위하여 간극수압계를 설치한 침투실험을 실시하였다. 세립질이 유출되는 부분은 투수계수가 증가하고, 간극수압이 감소한 반면, 세립질이 쌓이는 부분은 투수계수가 감소하고, 간극수압이 증가하였다. 따라서, 간극수압을 측정하여 세립질의 이동을 조사하고 메커니즘을 검증하였다.

본 연구에서는 well-graded soil의 내부불안정성의 특성 및 진행과정이 gap-graded soil과 다름을 확인하였고, 그 원인에 대하여 분석하였다. 이 연구 결과는 well-graded soil에서 내부불안정성의 진행과정을 이해하고, 안정성을 평가하는 참고자료로 사용될 수 있을 것이다.

주요어: 내부침식, 내부불안정성, 침투실험, 막힘, 제체재료
학 번: 2017-34915

감사의 글

회사를 그만두고 대학원에 들어온 지가 엊그제 같은데, 벌써 졸업할 시기가 되었습니다. 대학원에 들어와 결혼을 하였고, 두 아들을 얻었으며, 이제는 학위까지 받게 되었습니다. 이곳에서 제 인생의 가장 중요한 일들을 모두 이룬 것 같습니다. 늦은 나이에 다시 학교로 돌아왔을 때, 어떻게든 빨리 졸업을 하려고 생각하였으나, 막상 나갈 때가 가까워 오니 아쉬움이 밀려옵니다. 부족한 논문이 완성되기까지 지도해 주신 교수님들과 도와주신 선·후배님들께 진심으로 감사드립니다.

회사를 다니면서 가슴 한 곳에 공부를 더 하지 못한 것에 대한 아쉬움이 계속 남아있었으나, 다시 공부할 수 있는 기회를 주시고, 여기까지 이끌어 주신 정충기 선생님께 먼저 감사의 말씀을 드립니다. 앞으로도 부끄럽지 않은 제자가 되도록 노력하겠습니다. 그리고 바쁘신 와중에도 논문을 심사해주시고 지도해 주신 김성렬 교수님, 박준범 교수님, 정영훈 교수님, 김태식 교수님께 감사드립니다.

나이 많은 선배의 연구실 생활과 학업을 도와준 후배님들에게도 진심으로 감사드립니다. 백성하, 곽태영, 이승환, 신규범, 조범희, 구교영, 유병수, 김인현, 송영우, 정택규, 김기연, 이민호, 임철민, 홍성호, Tran, Rahim, 김경선, 김재규, 한정우, 홍승완, 황병윤, 조기안, 한재인 모두에게 감사드립니다.

항상 아들의 앞날을 걱정하시며 잘 되길 기도하시던 아버지, 어머니 감사하고 사랑합니다. 언제나 응원해주시고 손자들 돌보느라

고생하신 장인, 장모님 감사드립니다. 앞으로 가야할 길과 해야할 일에 대해서 많은 조언을 해준 우리 형 고마워. 옆에서 응원해 주신 형수님, 윤로, 나로, 형님, 아주머님, 시연이도 고맙습니다. 마지막으로 언제나 내편인 은하와 우리 두 아들 은로와 서로에게 이 논문을 드립니다.